Biochemical investigations of two polyketide synthase subclasses – highly reducing/non-reducing pairs, and polyketide synthase non-ribosomal peptide synthetases.

by

Rachel V. K. Cochrane

A thesis submitted in partial fulfillment of the requirements for the degree of

Doctor of Philosophy

Department of Chemistry,
University of Alberta

Abstract

Cladosporin is a polyketide metabolite that is biosynthesized by a highly reducing (HR)/non-reducing (NR) polyketide synthase (PKS) pair, wherein they catalyse head-to-tail condensation of acetyl and malonyl CoA units with subsequent β-keto modification. Cladosporin has recently been reported as a potent anti-malarial, acting as a nanomolar inhibitor of the *Plasmodium falciparum* lysyl tRNA synthetase. Sequencing of the genome of the producer organism, *Cladosporium cladosporioides*, allowed for identification of the cladosporin gene cluster. The HR and NR PKSs encoded therein, Cla2 and Cla3 respectively, were heterologously expressed. A series of substrate analogues were then synthesized and used in enzyme assays with Cla2. These studies showed that Cla2 could produce cladosporin from the advanced pentaketide intermediate. Cla2 also accepts analogues that contain the "unnatural" configuration at the key β-hydroxy group in the molecule, but does not recognize intermediates in which this β-hydroxy group is absent. Furthermore, Cla2 accepts analogues with shorter carbon chains, but not longer than is naturally present, suggesting a hydrophobic pocket of restricted size in the enzyme.

The polyketide 10,11-dehydrocurvularin (DHC) is also biosynthesized by a HR/NR PKS pair. The genome of the producer organism, *Alternaria cinerariae*, was sequenced, and the DHC PKSs expressed heterologously in yeast. Availability of similar DHC-producing PKSs from *Aspergillus terreus* allowed us to compare biosynthetic machinery for the same metabolite in different organisms. Bioinformatic analyses suggest

that sequence differences between the two sets of proteins are concentrated in specific domains, where they can be found mainly on the outer surface and specific faces of the protein.

Lovastatin belongs to a group of therapeutics known as the statins, which are widely prescribed in patients with elevated levels of cholesterol. Lovastatin production is mediated by a HR PKS, LovB, in conjunction with an enoyl reductase partner, LovC, in *Aspergillus terreus*. During the biosynthesis of lovastatin, an interesting enzyme catalysed Diels-Alder reaction is proposed to occur in order to generate the correct stereochemistry of the decalin core. LovB contains an unusual truncated non-ribosomal peptide synthetase (NRPS) portion at its C terminus, which includes a condensation (C) domain that is thought to catalyse this reaction. In order to test this hypothesis, a series of linear hexaketide analogues, which are unable to undergo cyclization, were synthesized. These intermediates were sent to our collaborators for co-crystallization with the LovB CON domain. A ^{13}C labeled tetraketide intermediate was also synthesized for feeding studies with LovB, to confirm its intermediacy in the biosynthesis.

Chaetoglobosin A and cytochalasin E belong to a group of polyketides collectively known as the cytochalasins. This group of molecules is made by PKS-NRPS enzymes, which synthesize the polyketide backbone using their PKS domains and then add an amino acid using the NRPS portion. The polyketide-amino acid intermediate is proposed to undergo reductive release from the enzyme, followed by cyclizations and oxidation to afford the final metabolites. The exact process by which these post-PKS modifications occur is still unknown. With hopes of studying these mechanisms in more detail, synthesis of an advanced polyketide intermediate was initiated. Further elaboration

of the synthesized compounds will afford the mature polyketide chain which will be sent to our collaborators in UCLA for enzymatic assays with the respective PKS-NRPS.

Preface

Most of chapter 2 has been published - Rachel V. K. Cochrane, Randy Sanichar, Gareth R. Lambkin, Béla Reiz, Wei Xu, Yi Tang, John C. Vederas. Production of New Cladosporin Analogues by Reconstitution of the Polyketide Synthases Responsible for the Biosynthesis of this Antimalarial Agent. *Angew. Chem. Int. Ed. Engl*, **2015**, DOI: 10.1002/ange.201509345.

Most of chapter 3 has been published – Rachel V. K. Cochrane, Zhizeng Gao, Gareth R. Lambkin, Wei Xu, Jaclyn M. Winter, Sandra L. Marcus, Yi Tang, John C. Vederas. Comparison of 10,11-dehydrocurvularin polyketide synthases from *Alternaria cinerariae* and *Aspergillus terreus* highlights key structural motifs. *ChemBioChem*, **2015**, *17*, 2479-2483.

Acknowledgements

"*There is no such thing as a 'self-made' man. We are made up of thousands of others. Everyone who has ever done a kind deed for us, or spoken one word of encouragement to us, has entered into the make-up of our character and of our thoughts, as well as our success.*"

- George Matthew Adams

I would like to start by thanking the entire mass spectral, NMR and analytical services staff for their contributions toward my thesis work – I couldn't have done it without you.

Thanks also to Vederas group members both past and present, for making my experience here unforgettable. In particular, Shaun McKinnie, Justin Thuss and Stephen Cochrane – I am extremely grateful to have had you three by my side over the last five years. To my BFF in the lab, Kaitlyn Towle, thank you for the hours of laughter both in and out of work. You are a wonderful mother, and an incredibly strong woman. To the infamous David Dietrich – you have influenced so many; I am incredibly grateful to know you. You are truly one-in-a-million. Randy, my thanks to you not only for proofreading my thesis, but also for being such a pleasure to work with. I am honored to have my name alongside yours in-print. I would also like to gratefully acknowledge Dr. Marco van Belkum for proof-reading this thesis.

It would be amiss if I did not thank Mr. Gareth Lambkin of Biological Services. Gareth, thank you for invaluable advice, and for letting me talk your ear off. It's been a pleasure.

For my husband, Stephen, the reason I get out of bed in the morning, I have no words emphatic enough to communicate my thanks. Without you I could not make it through the tumultuous journey of parenthood. You are the yin to my yang, and my best friend. And to my beautiful son Caleb, thank you for continually making me a better person.

Of course, thanks to the man who made this all possible, Professor John C. Vederas, a man whose talents and interests lie far beyond the area of science. Thank you for being a mentor and a friend.

Table of Contents

List of Figures

List of Schemes

List of Tables

List of Abbreviations

[α]	Specific rotation
6-MSA	6-methylsalicylic acid
A	Adenylation domain
Å	Angstrom
ACN	Acetonitrile
ACP	Acyl carrier protein domain
AMP	Adenosine monophosphate
ARO	Aromatase
AT	Acyl transferase domain
ATP	Adenosine triphosphate
bp	Base pairs
BVMO	Baeyer-Villiger monooxygenase
c	Concentration in g 100 mL^{-1} (specific rotation)
CON	Condensation domain
cDNA	Complementary deoxyribonucleic acid
CHS	Chalcone synthase
CoA	Coenzyme A
CYC	Cyclase
δ	Chemical shift in ppm (for NMR)
d	Doublet

DAL	Dihydroxyphenylacetic acid
DCM	Dichloromethane
DEBS	6-deoxyerythronolide B synthase
DH	Dehydratase domain
DHC	Dehydrocurvularin
DHZ	Dehydrozearalenol
DIBAL-H	Diisobutylaluminium hydride
DIPEA	*N,N*-diisopropylethylamine
DMAP	4-(dimethylamino)pyridine
DMF	Dimethylformamide
DML	Dihydromonacolin L
DMSO	Dimethyl sulfoxide
DNA	Deoxyribonucleic acid
EDC	1-Ethyl-3-(3-dimethylaminopropyl)carbodiimide
EDTA	Ethylenediaminetetraacetic acid
EI	Electron impact
eq	Equivalents
ER	Enoyl reductase domain
ES	Electrospray
FAS	Fatty acid synthase
HMG-CoA	3-hydroxy-3-methylglutaryl-coenzyme A
HMM	Hidden Markov model
HMPA	Hexamethylphosphoramide

HPLC	High performance liquid chromatography
HR PKS	Highly reducing polyketide synthase
HWE	Horner-Wadsworth Emmons
IR	Infrared
J	Coupling constant in Hertz
kb	Kilobase
kDa	Kilodaltons
KR	Ketoreductase domain
KRS1	Lysyl transfer ribonucleic acid
KS	Ketosynthase domain
KSα	Ketosynthase domain alpha
KSβ	Ketosynthase domain beta
LB	Lysogeny broth
LC-ESI-MS	Liquid chromatography-electrospray ionization-mass spectrometry
LNKS	Lovastatin nonaketide synthase
m	Multiplet
m/z	Mass to charge ratio
MAT	Malonyl-CoA:acyl transferase domain
Mb	Megabase
MSAS	6-methylsalicylic acid synthase
MT	Methyl transferase domain
NADPH	Nicotinamide adenine dinucleotide phosphate

NaHMDS	Sodium hexamethyldisilazide
NMR	Nuclear magnetic resonance
NR PKS	Non-reducing polyketide synthase
NRPS	Non-ribosomal peptide synthetase
PDB	Protein Data Bank
PCR	Polymerase chain reaction
Ph	Phenyl
PKS	Polyketide synthase
PKS-NRPS	Polyketide synthase-non-ribosomal peptide synthetase
PMB	*Para*-methoxybenzyl
Ppant	Phosphopantetheine
ppm	Parts per million
Pptase	Phosphopantetheinyl transferase
PR PKS	Partially reducing polyketide synthase
PT	Product template domain
PyBOP	Benzotriazol-1-yl-oxytripyrrolidinophosphonium hexafluorophosphate
q	Quartet
quant.	Quantitative yield
R	Reductase domain
RAL	Resorcylic acid lactone
RP-HPLC	Reverse phase high performance liquid chromatogaphy
rpm	Revolutions per minute

SAM	*S*-adenosyl methionine
SAT	Starter acyl transferase domain
SNAC	*N*-acetyl cysteamine
T	Thiolation domain
TAR	Transformation associated recombination
TBAI	Tetrabutylammonium iodide
TBDMS	*Tert*-butyldimethylsilyl
TCEP	*Tris*(2-carboxyethyl)phosphine
TE	Thioesterase domain
TFA	Trifluoroacetic acid
THF	Tetrahydrofuran
THP	Tetrahydropyran
TLC	Thin later chromatography
TrCl	Trityl chloride
tRNA	Transfer ribonucleic acid
UV-vis	Ultraviolet-visible spectroscopy
ΨER	Pseudo enoyl reductase domain
ΨKR	Pseudo ketoreductase domain
ΨMT	Pseudo methyltransferase domain

1 Introduction

Polyketides are a group of secondary metabolite natural products that are produced by several classes of organism, including bacteria, plants, and fungi.[1-6] These compounds often have potent biological activities and thus have proven to be of particular use in the pharmaceutical industry. Polyketides have been shown to have cholesterol lowering,[7, 8] anticancer,[9, 10] antibiotic,[11] and HIV-inhibitor activities,[12] figure 1-1.

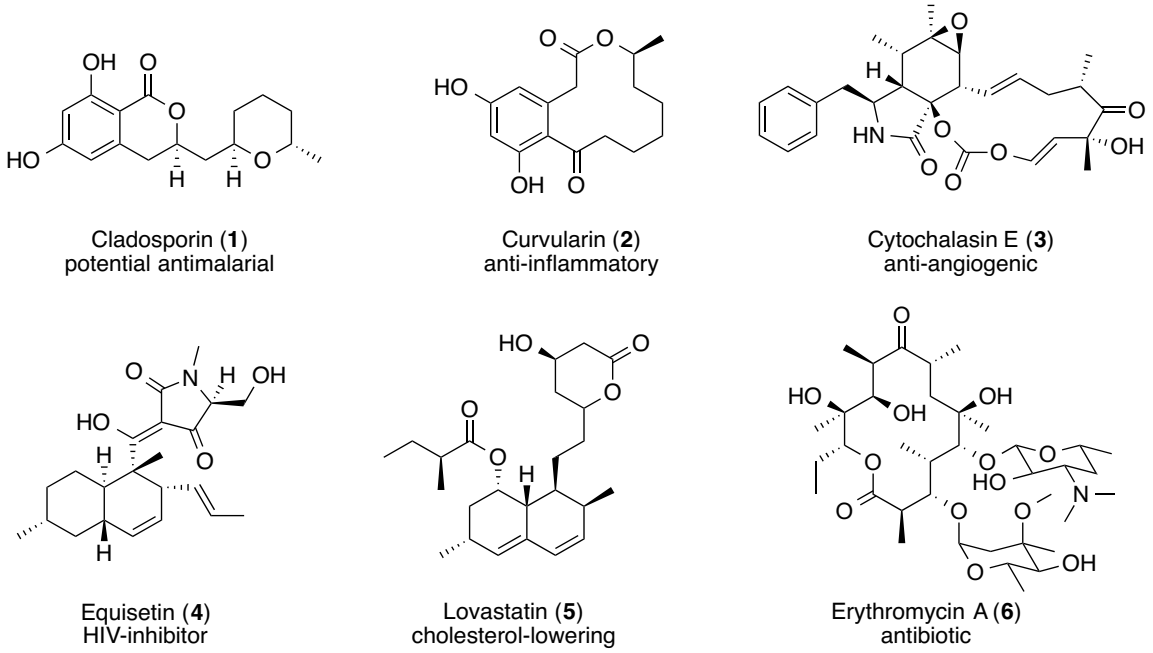

Figure 1-1. Select examples of polyketides used as therapeutics.

Their complex structure makes them an interesting avenue of research for synthetic chemists and natural product chemists alike, with research ranging from elegant syntheses to investigation of complex biosynthetic pathways and enzymology. The ultimate goal remains the same – to understand and harness the potential of these astounding natural products.

1.1 Polyketide and fatty acid biosynthetic assembly

In nature, polyketides are assembled by head-to-tail condensation of simple carboxylic acid derivatives (eg. acetyl-CoA, malonyl-CoA and methylmalonyl-CoA) catalysed by polyketide synthases (PKS). This is conducted in a similar fashion to their primary metabolite cousins, fatty acids, which are assembled by condensation of acetyl-CoA units by fatty acid synthases (FAS), as shown in figure 1-2.[13]

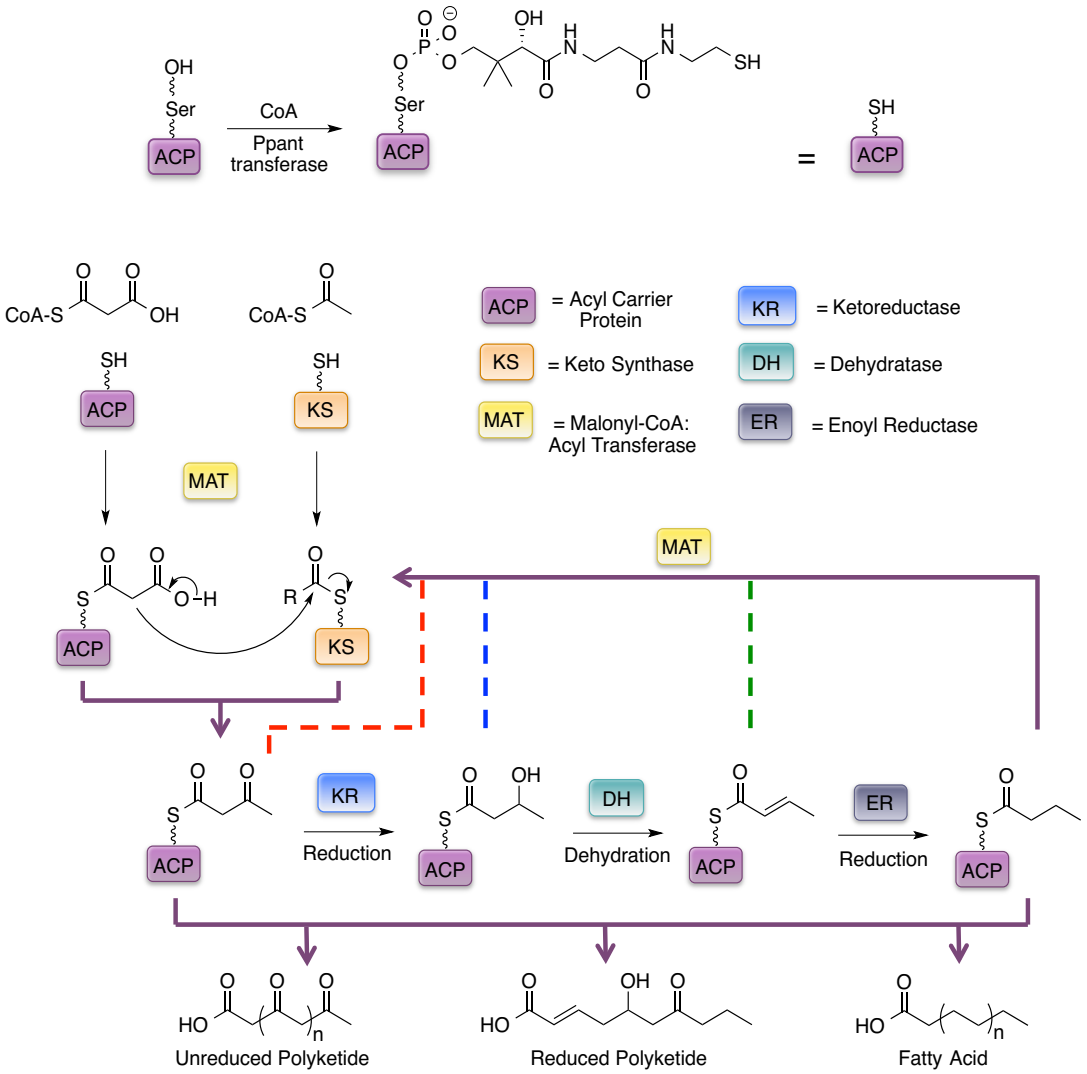

Figure 1-2. Biosynthetic assembly of polyketides and fatty acids.

Before the biosynthesis can begin, activation of the apo-ACP to the active holo form must occur. This involves addition of a phosphopantetheinyl (Ppant) moiety from CoA to an active site serine of the ACP, catalysed by a Ppant transferase (Pptase).[14] This Ppant arm is roughly 18Å long and allows the growing acyl chain to reach the active sites of other domains in the PKS enzyme.

The biosynthesis of these natural products begins with loading of malonyl-CoA onto the ACP free thiol of Ppant, catalysed by the MAT domain. Concurrent to this, the MAT domain also catalyses loading of the KS domain active site cysteine with either acetyl-CoA or the acyl intermediate. The KS domain then catalyses a decarboxylative Claisen condensation of the malonate onto the acyl intermediate, thereby extending the acyl chain by an additional two carbons, or "ketide" unit, to form a β-keto intermediate. This β-keto intermediate can then undergo a variety of modifications, such as reduction of the ketone by the KR domain, dehydration by the DH domain, and finally reduction of the double bond catalysed by the ER domain. During fatty acid biosynthesis, the acyl intermediate undergoes all of these modification steps successively, with subsequent chain extensions, to furnish the fully reduced carbon chain. In contrast, during polyketide biosynthesis, the acyl chain can be transferred back to the KS domain where it will undergo another round of chain extension and subsequent modifications. The exact nature of this enzymatic "programming" is still unknown. To understand how these cryptic enzymes work would not only further our knowledge of enzymology as a whole, but also potentially allow us to manipulate the outcome of their specific biochemical modifications in order to furnish novel polyketides and therapeutics of our design.

1.2 Types of PKSs

Domain names that are commonly encountered in these enzymatic systems and that will be used hereafter are listed in table 1-1 for reference.

Abbreviation	Domain name
ACP	Acyl carrier protein
KS	Ketosynthase
MAT	Malonyl-CoA:acyl transferase
KR	Ketoreductase
DH	Dehydratase
ER	Enoyl reductase
TE	Thioesterase
SAT	Starter-unit acyl transferase
PT	Product template
MT	Methyl transferase
CON	Condensation
A	Adenylation
T	Thiolation
R	Reductase
E	Epimerase

Table 1-1. List of domain abbreviations.

There are three main types of PKS, as laid out in figure 1-3, with type I PKSs being subcategorized into modular and iterative. Further to this, iterative type I PKSs can then be further divided into groups based on the processing domains they each contain.

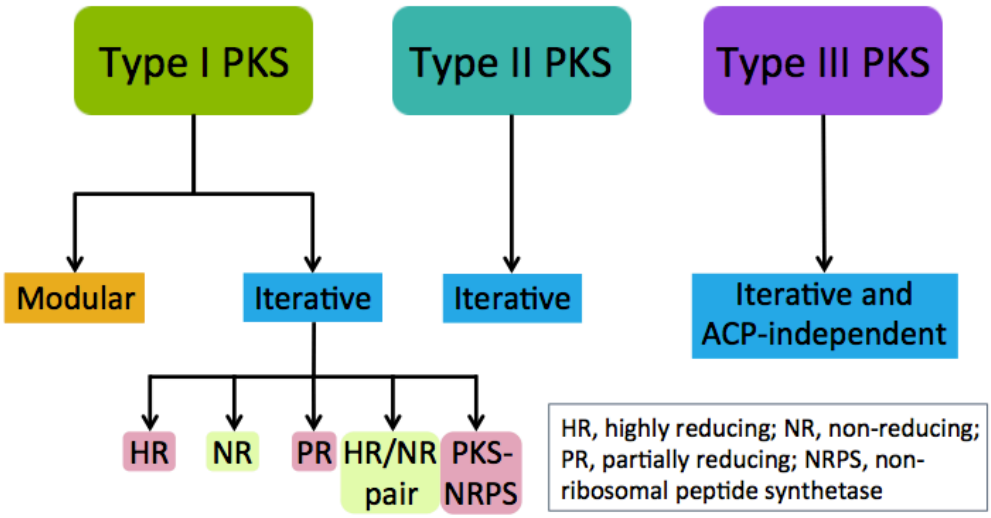

Figure 1-3. Types of PKS and their classification.

1.2.1 Type I PKSs

1.2.1.1 Modular type I PKSs

Type I modular PKSs, which are most often isolated from bacteria, are large multifunctional proteins that are organized into modules.[1, 2, 15, 16] Each module contains a distinct set of domains and is responsible for addition of one ketide unit. Each domain acts only once in an "assembly line" fashion, with initial loading of the starter unit onto the ACP, followed by β-keto modification according to the processing domains contained within the module.

Such enzymes are exemplified by the well-studied 6-deoxyerythronolide B synthase (DEBS) from *Saccharopolyspora erythraea*, which is responsible for production of the macrocyclic core of the antibiotic erythromycin (**6**), figure 1-4.[17-21]

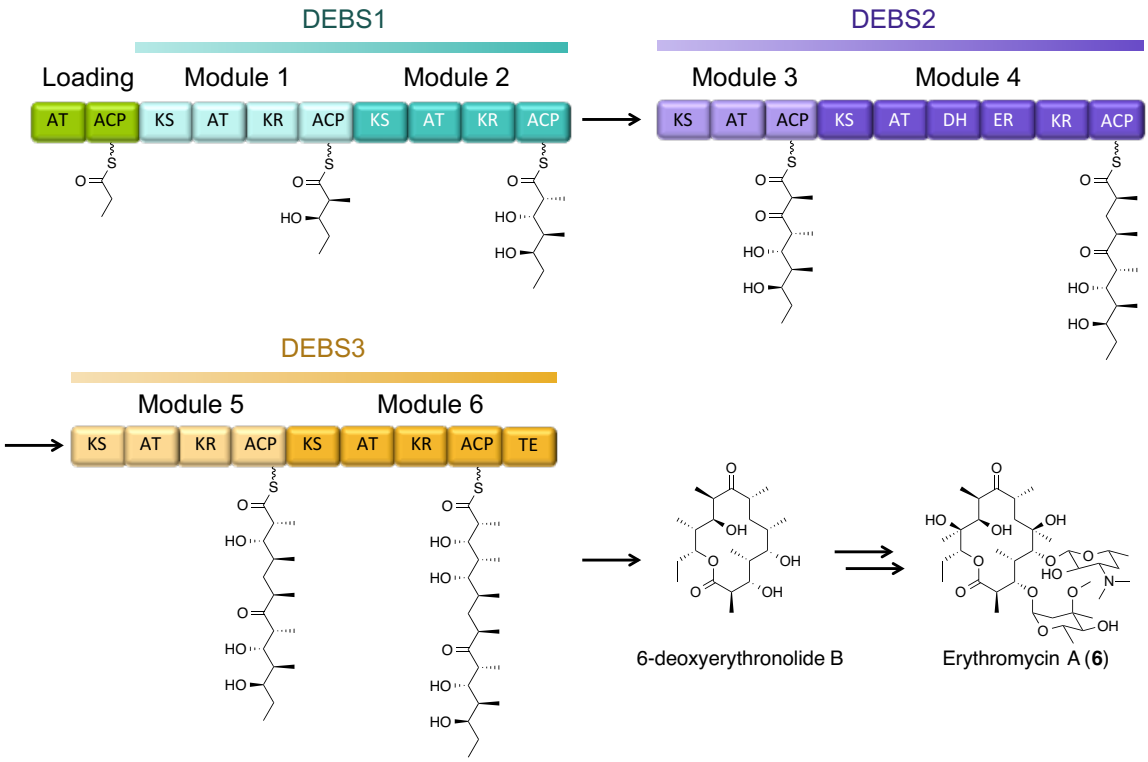

Figure 1-4. Biosynthesis of 6-deoxyerythronolide B by the type I modular PKS, DEBS, *en route* to erythromycin A in *Saccharopolyspora erythraea*.[17-21]

1.2.1.2 Iterative type I PKSs

Iterative type I PKSs, which are most commonly isolated from fungi, are similar to modular type I PKSs in that they consist of one large multifunctional protein.[22-24] However, iterative type I PKSs contain only one copy of each domain, and use them iteratively in order to furnish their final product. This group of PKSs can be further subcategorized based on the modifying domains they contain, figure 1-5.

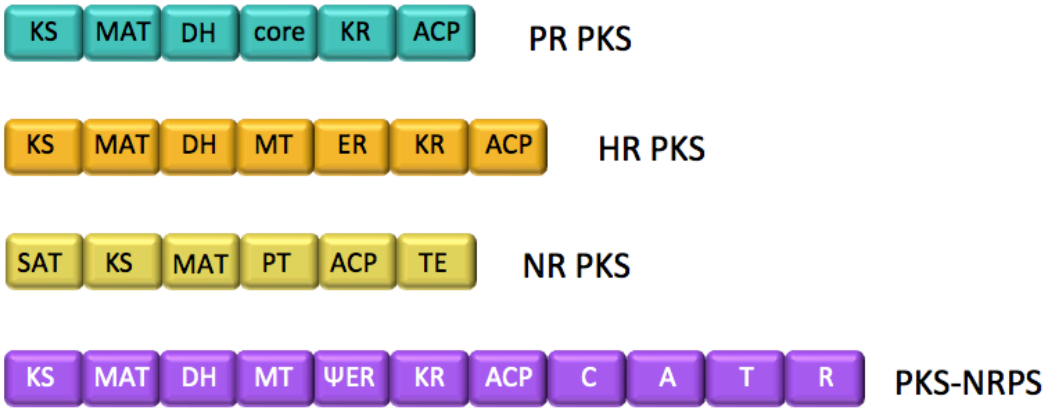

Figure 1-5. Representative examples of domain architecture of several subcategories of iterative type I PKSs.

A highly reducing (HR) PKS generally contains all modifying domains (KR, DH, ER) as well as the standard ACP, MAT and KS. A representative example is that of the lovastatin nonaketide synthase (LNKS), LovB. As is often the case for HR PKSs, LovB contains an inactive ER domain, and so requires the cooperation of LovC,[25] an ER partner also encoded in the lovastatin gene cluster in *Aspergillus terreus*. Together, LovB and LovC synthesize the main nonaketide backbone (dihydromonacolin L, **7**) of the cholesterol lowering drug lovastatin.[26-28] The biosynthesis of this metabolite has been the subject of extensive isotopic labeling, genetic and biochemical studies, and will be discussed in further detail in chapter 4.

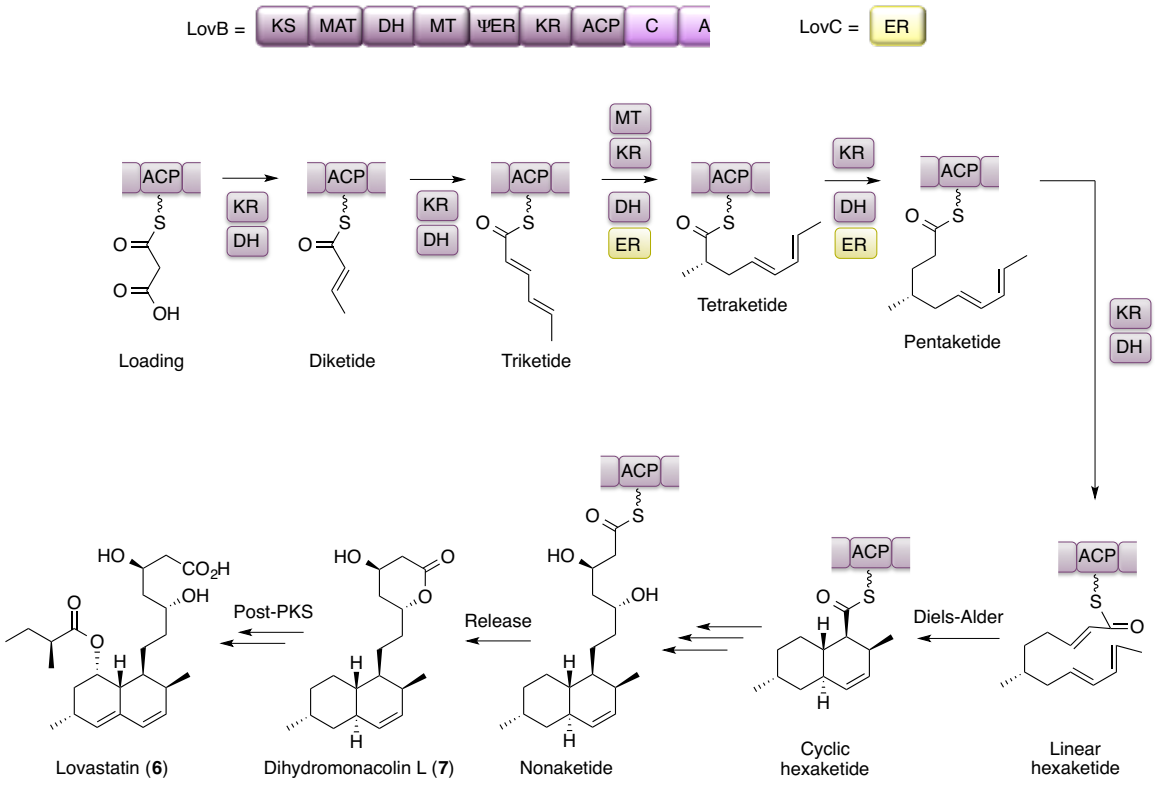

Figure 1-6. Biosynthesis of lovastatin by the HR PKS LovB and the ER LovC in *Aspergillus terreus*.

Non-reducing (NR) PKSs contain the necessary loading and extension domains and a starter-unit acyl transferase (SAT) domain, as well as a product template (PT) domain and thioesterase domain (TE), but do not contain any of the modifying domains present in an HR PKS. As such, these enzymes produce non-reduced, aromatic compounds like the anthraquinone, norsolorinic acid. The NR PKS PksA synthesizes norsolorinic acid *en route* to the potent hepatocarcinogen aflatoxin B_1 (**8**) in *Aspergillus parasiticus*.[29] Here, it catalyses seven successive condensation reactions starting from hexanoate, followed by two cyclization events and an aromatization. TE-catalysed release

of this bicyclic intermediate, followed by oxidation furnishes norsolorinic acid, which undergoes further post-PKS modification to produce (**8**).

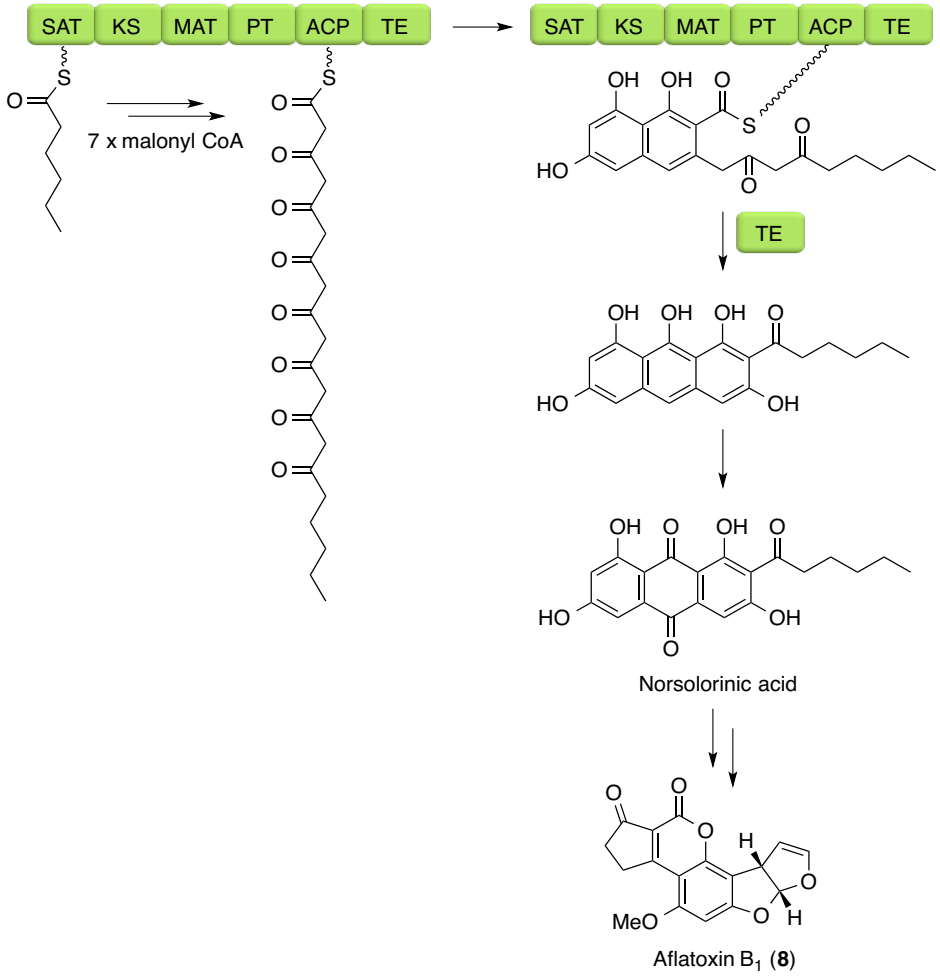

Figure 1-7. Biosynthesis of norsolorinic acid by PksA in *Aspergillus parasiticus*.

One of the smallest iterative type I PKSs is the partially reducing (PR) PKS 6-methylsalicylate synthase (MSAS), first isolated from *Penicillium patulum* in 1970.[30] MSAS has an N-terminal KS domain, followed by MAT, DH, a "core" domain, and a KR and ACP, with no TE domain for product release.[31, 32] It was recently shown that the

"core" domain is essential for subunit-subunit interactions in the homotetrameric MSAS, and that the DH domain may also by capable of catalyzing thioester hydrolysis to release 6-methylsalicylate from the enzyme.[33]

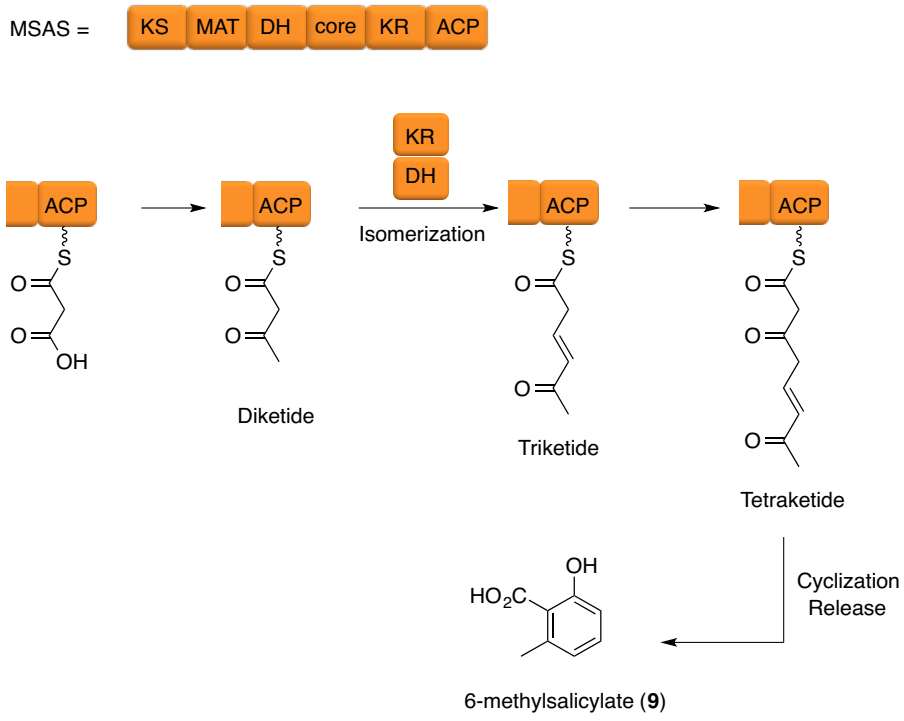

Figure 1-8. Biosynthesis of 6-methylsalicylate by a PR PKS, MSAS, in *Penicillium patulum*.

When examining the polyketide produced by a HR/NR PKS pair it is evident from the structure that a high level of reduction occurs early in the biosynthesis with no reduction during the latter chain extensions. HR/NR PKS pairs will be discussed in more detail in chapters 2 and 3, but for now a representative example is shown in figure 1-9 – the HR (Hpm8) and NR (Hpm3) PKSs responsible for production of nonaketide backbone (dehydrozearalenol, **10**) of hypothemycin (**11**) in *Hypomyces subiculosis*.[34-36]

Hpm8 first synthesizes the hexaketide chain, which is then passed to Hpm3 for three subsequent rounds of chain extension. Tautomerization and cyclizations followed by TE-catalysed off-loading affords dehydrozearalenol (DHZ, **10**), which is elaborated into (**11**) by post-PKS tailoring enzymes.

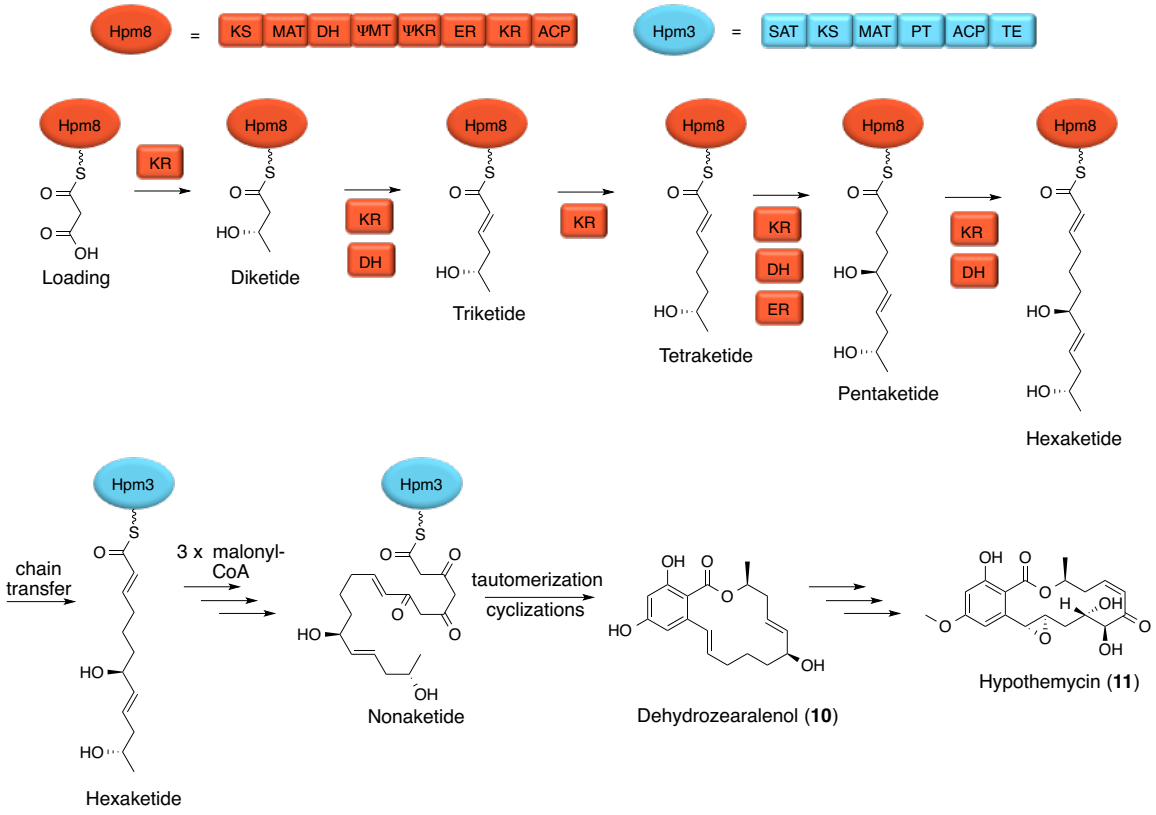

Figure 1-9. Biosynthesis of dehydrozearalenol by a HR/NR PKS pair in *Hypomyces subiculosis*.

The final category of iterative type I PKSs is the PKS-nonribosomal peptide synthetase (NRPS) hybrid. NRPSs are large multimodular proteins that catalyze the consecutive condensation of multiple amino acids to furnish peptide products,

independent of the ribosome (figure 1-10).[37] The adenylation (A) domain is first responsible for activating the amino acid using ATP to form the amino acid-AMP ester, which is then passed to the thiolation (T) domain where the condensation (CON) domain is responsible for addition of the next amino acid to the growing peptide chain. A fourth domain present in the NRPS system is the thioesterase (TE) domain, which catalyzes offloading of the peptide by either hydrolysis or macrocyclization. This TE-mediated release of the product is the best understood, and generally considered the most canonical, method of metabolite release from both NRPS and PKS systems.[38] However, the TE domain may also catalyze Claisen-like cyclization, as is the case for PksA, figure 1-7. Furthermore, there have been an increasing number of examples is which reductase (R) domains (that show sequence homology to the short-chain dehydrogenase/reductase superfamily) catalyze NAD(P)H-dependent reductive release or Dieckmann condensation to release the product.[39-44]

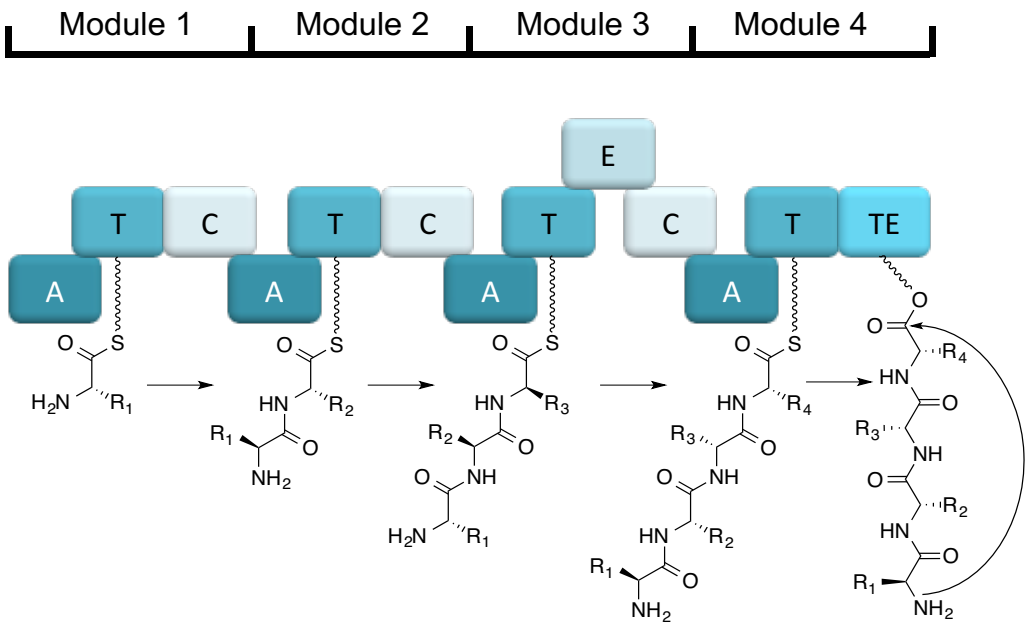

Figure 1-10. Basic mechanism of an NRPS. Each arrow represents addition of an amino acid that has been activated by the A domain using ATP.

The domain architecture of a PKS-NRPS is similar to that of the previously mentioned lovastatin, however, a true PKS-NRPS contains a fully intact NRPS portion. A representative example of a PKS-NRPS is that of CheA, which is responsible for the production of chaetoglobosin A in *Penicillium expansum* (figure 1-11). Once the HR PKS portion of the enzyme has synthesized the nonaketide backbone, the intermediate is passed to the T domain. Here, the CON domain catalyzes addition of a tryptophan residue, which has been pre-activated by the A domain, to the polyketide chain. Following this, it is postulated that the C-terminal reductase (R) domain catalyzes reductive offloading to furnish the aldehyde intermediate shown in figure 1-11. This intermediate is then thought to undergo a series of cyclizations and post-PKS oxidations to furnish the final product, chaetoglobosin A (**12**).

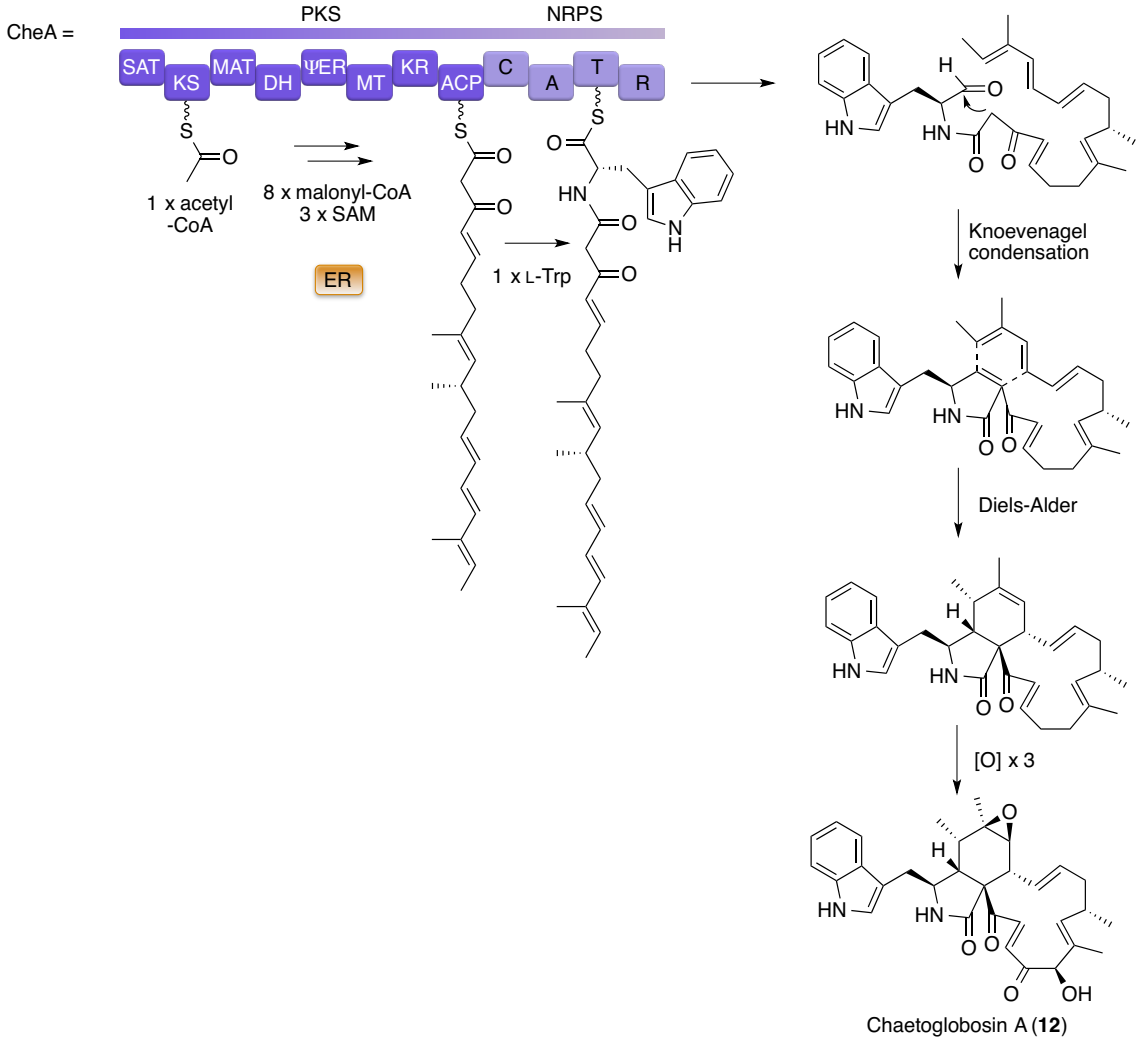

Figure 1-11. Biosynthesis of chaetoglobosin A by the PKS-NRPS, CheA.

As previously mentioned, several methods of metabolite offloading exist. For example, it was recently shown by Schmidt and co-workers that EqiS, the PKS-NRPS responsible for production of the metabolite equisetin (**4**) in *Fusarium heterosporum*, contains an R domain that is capable of catalyzing a Dieckmann condensation to yield the tetramic acid moiety, figure 1-12.[45]

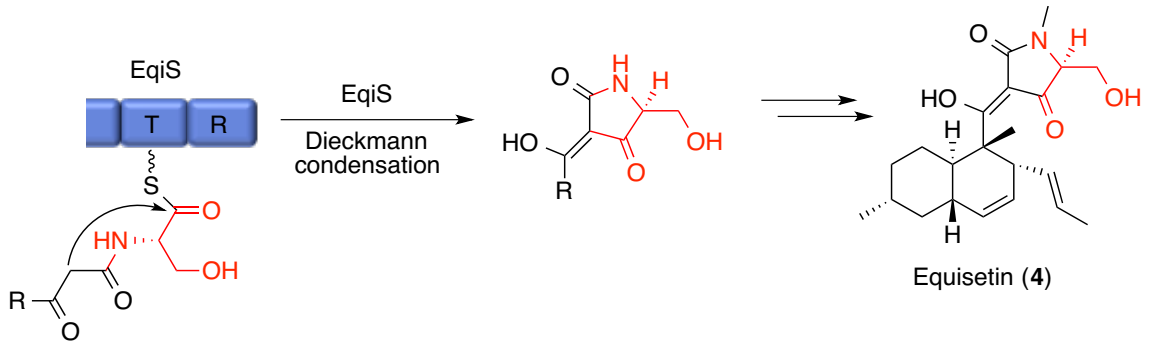

Figure 1-12. Formation of the tetramic acid group in equisetin by EqiS, catalysed by the R domain. The R group represents the polyketide chain, with the amino acid-derived portion of the molecule highlighted in red. Timing of the *N*-methylation is thought to be after tetramic acid formation.

The mechanism by which the R domain catalyzes chain release is far less understood than the typical TE-mediated release. It remains unclear how these R domains can catalyze both NAD(P)H-dependent reduction and non-redox Dieckmann condensation reactions.

1.2.2 Type II PKSs

This category of PKSs can be found mainly in bacteria, and is comprised of freely dissociable, iteratively acting enzymes.[46, 47] These enzymes often produce large polyaromatic compounds, and do so by using a so-called "minimal" set of PKS domains – typically KS_{α}, KS_{β}, and ACP, figure 1-13. The mechanism by which the minimal PKS initially loads malonyl CoA is still a topic of debate, but it is known that the KS_{α} first

catalyses decarboxylative Claisen condensation of malonyl CoA onto the acyl intermediate. This process may then undergo several iterations to generate the polyketide of desired chain length. KS_{β}, which lacks the necessary active site cysteine in order to be catalytically active, is thought to in part determine overall chain length formed. This minimal PKS complex may also recruit additional auxiliary enzymes such as cyclases (CYC) or aromatases (ARO) as necessary to furnish the aromatic polyketide. Furthermore, this aromatic polyketide may then be further elaborated by methyl transferases or glycosyl transferases. All necessary PKS and post-PKS modifying enzymes are often found clustered together in the genome where they are each encoded by a separate gene, in contrast to type I PKSs.

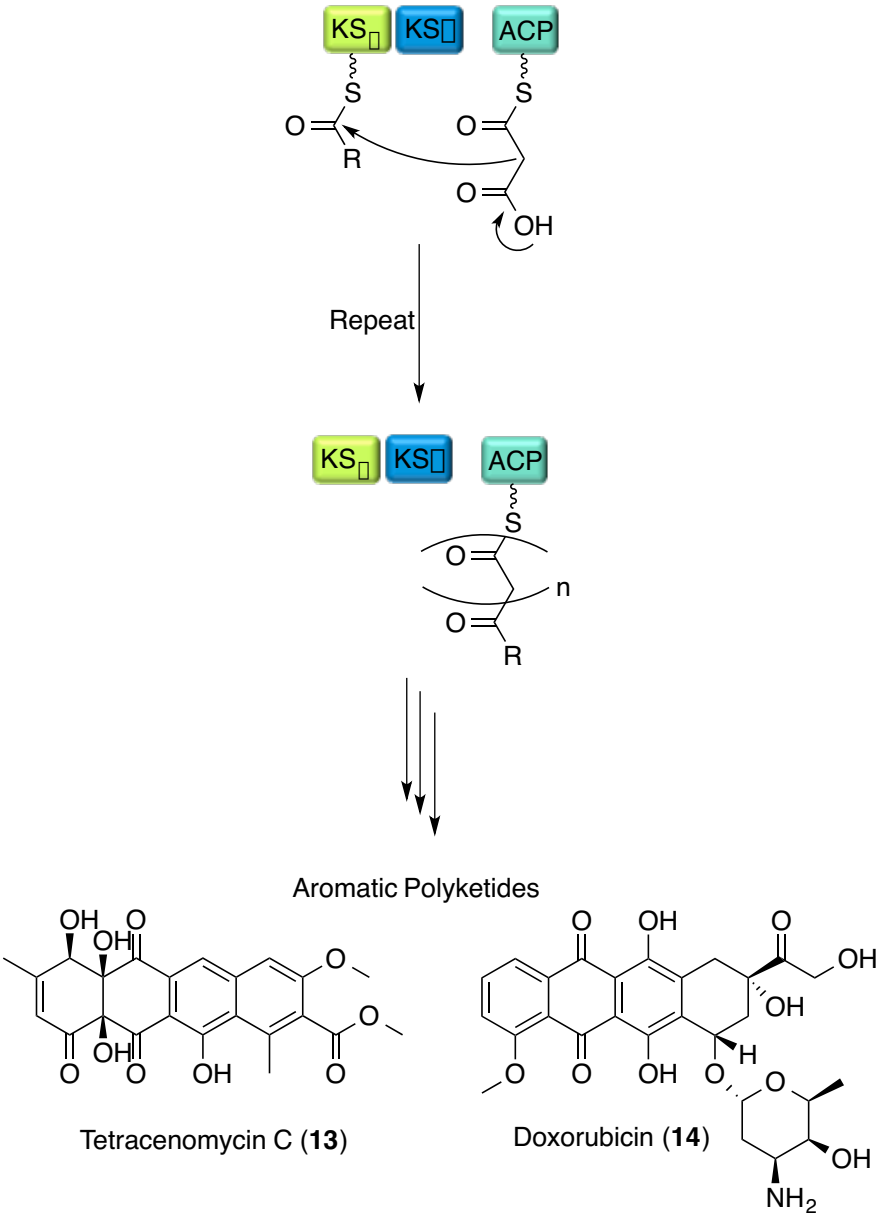

Figure 1-13. Basic mechanism of a type II PKS. The two examples shown are biosynthesis of tetracenomycin C by *Streptomyces glaucescens* and the anticancer agent doxorubicin in *Streptomyces peucetius*.

1.2.3 Type III PKSs

The final type of PKS enzymes is the type III PKS, which encompasses the well-known chalcone synthases (CHSs).[48-50] These enzymes can be found predominantly in plants, where they synthesize the starting materials for a diverse set of metabolites known as the phenylpropanoids. In contrast to both type I and type II PKSs, the type III PKS is independent of ACP, instead using CoA thioesters directly. A typical example of this category of enzymes is the biosynthesis of chalcone (**15**) by CHS, figure 1-14. CHS catalyses three successive condensations of malonyl CoA, starting from *p*-coumaroyl CoA to synthesize chalcones. What is perhaps most interesting about this homodimeric subset of PKSs, is that they catalyse all necessary loading, decarboxylation and cyclization reactions in just one active site.

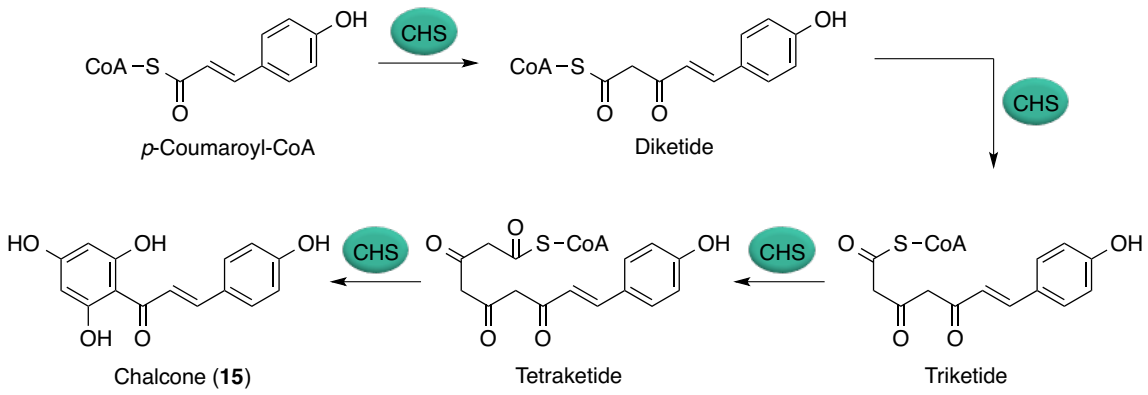

Figure 1-14. Biosynthetic reactions of chalcone synthase (CHS).

1.3 Conclusion

Although significant strides have been made in our understanding of these enigmatic enzymes, the rules governing iterative programming remain a mystery. In order to elucidate the biosynthetic mechanisms by which iterative type I PKSs function, I have studied five metabolites in this thesis: cladosporin; 10,11-dehydrocurvularin (DHC); lovastatin; chaetoglobosin A; and cytochalasin E. Recent advances in heterologous expression of fungal PKSs in *Saccharomyces cerevisiae* allowed me to successfully express the cladosporin PKSs (Cla2 and Cla3) from *Cladosporium cladosporioides*, and the DHC PKSs (Dhc3 and Dhc5) from *Alternaria cinerariae*. Using these purified enzymes I was able to conduct advanced intermediate analogue feeding assays, thus furthering our knowledge of enzyme promiscuity. Bioinformatic analyses also enhanced our understanding of key protein-protein interactions in relation to metabolite formation.

In the case of lovastatin, chaetoglobosin A and cytochalasin E, synthesis of proposed biosynthetic intermediates will allow investigation of cryptic enzyme catalysed reactions during formation of these metabolites, such as the elusive Diels-Alderase activity. Furthermore, recognition and incorporation of these advanced intermediates will bring us one step closer in understanding each biosynthetic step that these amazing enzymes catalyse.

2 Cladosporin

Cladosporin (**1**, figure 2-1) (also known as asperentin) is a tricyclic octaketide that was first isolated from *Cladosporium cladosporioides* in 1971,[51] and shortly thereafter in 1972 from *Aspergillus flavus*.[52] It is also produced by several other fungal species including *Chaetomium*,[53] *Penicillium,*[54] and *Eurotium*.[55, 56] Cladosporin exhibits some interesting bioactivity, including antifungal,[57] antibiotic,[55, 58] and plant growth inhibitory properties,[59] as well as anti-inflammatory effects in mouse lung tissue.[60] Most recently, cladosporin has been shown to be a potent, nanomolar, inhibitor of *Plasmodium falciparum* blood and liver-stage proliferation.[61] Although many antimalarial agents currently exist, endoperoxides represent the only class of molecules for which resistance has not significantly developed, and even these do not inhibit the asymptotic liver stage infection. The discovery of cladosporin's antimalarial activity represents a promising lead for treatment of the disease, and crystal structures of cladosporin in complex with both human, and *P. falciparum* lysyl tRNA synthetases have been published.[62-64]

The absolute configuration of cladosporin was confirmed by our group in 1989,[65, 66] with a substantial gap before the stereochemistry of its diastereomer isocladosporin was confirmed.[67, 68] Since then, several reports of the total synthesis of cladosporin, and isocladosporin have appeared in the literature.[69]

The biosynthetic machinery responsible for production of cladosporin in any organism has not been reported. To better understand cladosporin assembly, and to enable design and synthesis of better analogues, we sought to identify the cladosporin PKSs, heterologously express these enzymes, and reconstitute cladosporin production *in vivo* and *in vitro*.

2.1 Cladosporin biosynthesis

Cladosporin was previously believed to be biosynthesized by two type I iterative PKSs – a HR and NR pair, in a similar fashion to related metabolites previously studied in our group.[34, 70-74] Due to the necessary reduction of the C3 position of cladosporin we had hypothesized that the HR PKS must be responsible for biosynthesis up until the pentaketide stage, including formation of the THP ring.[66] The acyl intermediate would then be passed to the NR partner for three subsequent rounds of chain extension, followed by off-loading to release cladosporin from the enzyme.

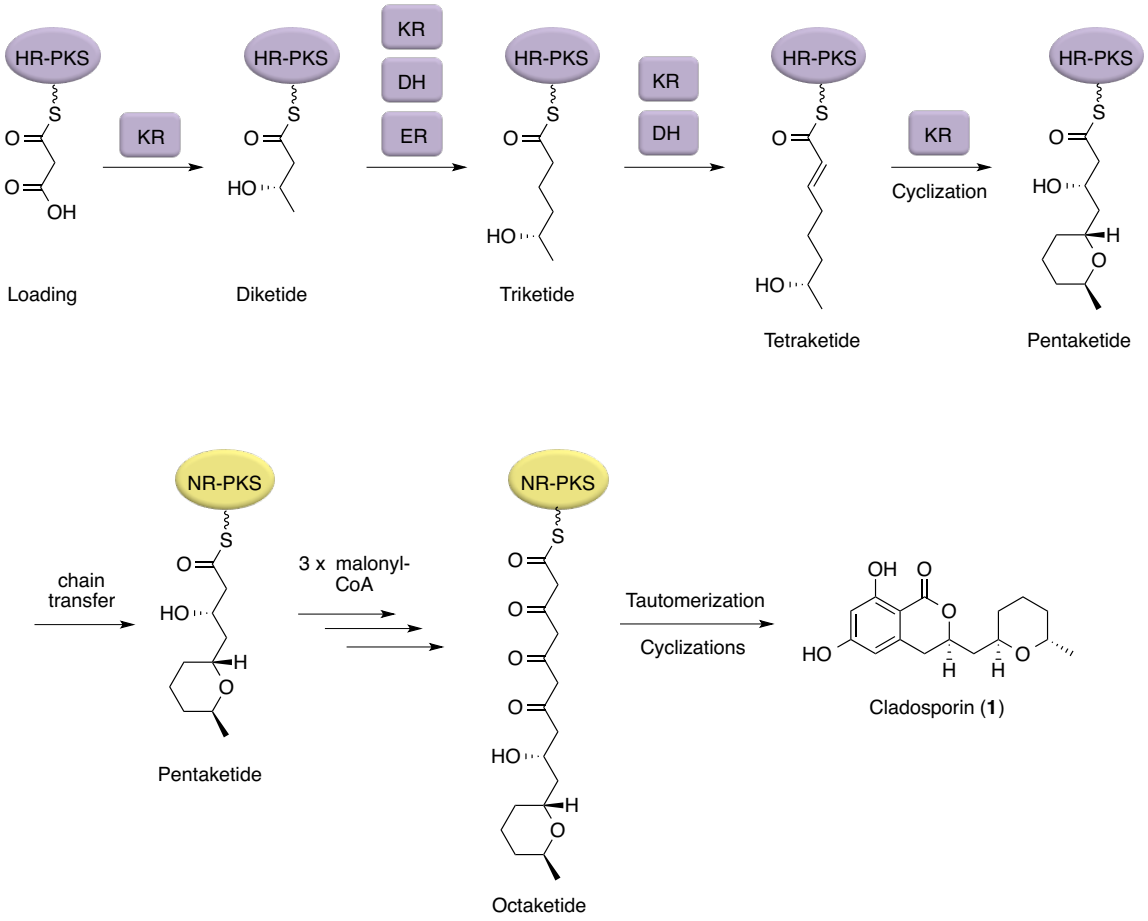

Figure 2-1. Proposed biosynthesis of cladosporin. The exact timing of tetrahydropyran (THP) ring formation is still unknown.

2.2 Results and discussion

2.2.1 Genome mining

In order to efficiently screen the genome of *Cladosporium cladosporioides* using a probe homologous to the appropriate PKS sequences, a fosmid library of genomic DNA was

prepared using the CopyControl™ Fosmid Library Production Kit from Epicentre, figure 2-2.

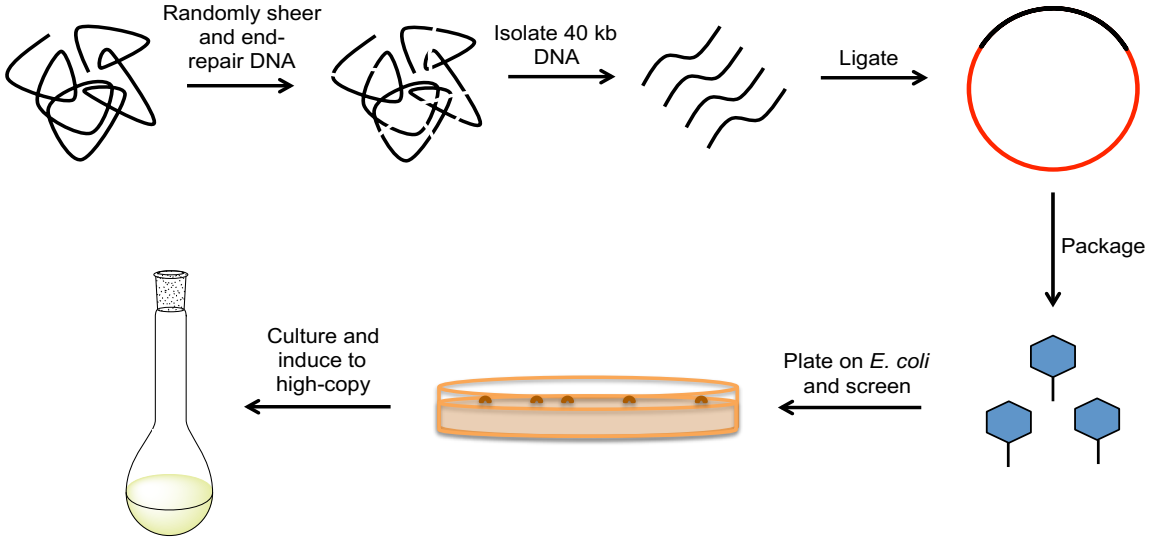

Figure 2-2. Preparation of the CopyControl™ Fosmid Library with subsequent screening and induction of the clones to high-copy number.

DNA was isolated from a 7 day culture of *Cladosporium cladosporioides* UAMH 5063 and fragments of roughly size 40 kb ligated into the pCC1FOS vector (figure 2-3). The clones were packaged using MaxPlax lambda packaging extracts contained within the kit, and then used to infect EPI300-T1R *E. coli* cells.

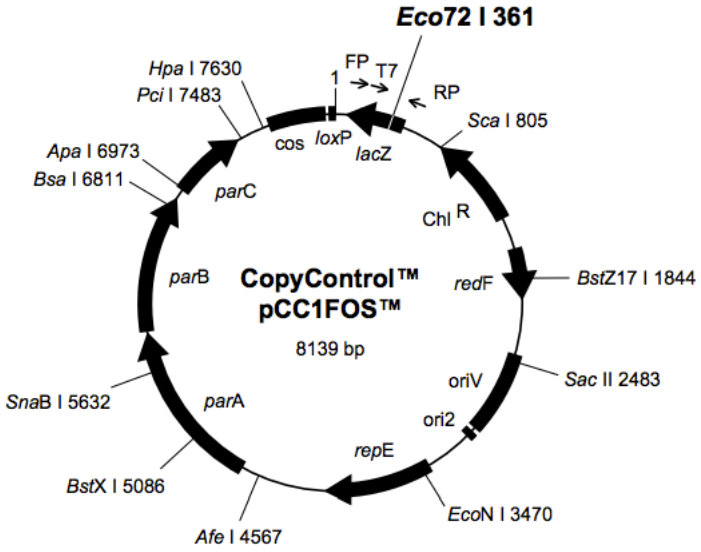

Figure 2-3. Vector map for pCC1FOS. The vector contains an *Eco*72 I blunt-end restriction site, the inducible high-copy origin of replication, oriV, and a cos site for DNA recognition during packaging.

The clones were then screened using dot-blot hybridization with a homologous KS probe containing DNA from PKS13, the NR PKS responsible for biosynthesis of zearalenone in *Gibberella zeae*. The probe had been labeled with alkaline phosphatase using the AlkPhos Direct Labelling and Detection System, figure 2-4. The membranes were imaged to check for chemiluminescense, which would indicate the presence of complimentary DNA.

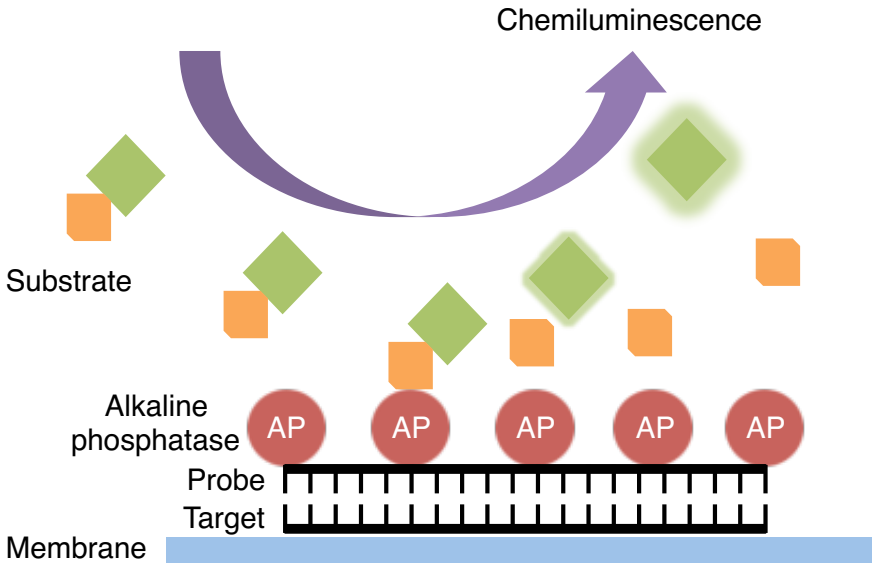

Figure 2-4. The Amersham AlkPhos Direct system that was used for labelling and detection of PKS DNA.

Unfortunately, after several rounds of infection and detection, no PKS DNA had been found using this method. The entire process was repeated, different hybridization conditions were used, such as raising and lowering the temperature during the hybridization stage. We also tried using an AT probe instead of a KS probe, and although all our positive controls worked, no PKS DNA could be found. We reasoned that perhaps the genome of *C. cladosporioides* was too large for any reasonable chance of finding a single gene cluster of interest, and so we decided to have the genome sequenced.

2.2.2 Genome sequencing and gene cluster analysis

With the decreasing price of whole genome sequencing, it became reasonable to have the genome of *C. cladosporioides* UAMH 5063 sequenced. The genomic DNA was isolated from a 7-day culture of the organism, and sent to Ambry Genetics for sequencing using their Illumina HiSeq 2000 capabilities. This resulted in 30 Mb of genomic information over a total of 764 contigs. The genomic data was annotated using Antibiotics & Secondary Metabolite Analysis Shell (antiSMASH v2.0),[75] which identified 50 putative secondary metabolite gene clusters, seven of which encode type I iterative PKSs. One gene cluster in particular possessed high sequence homology with the PKSs responsible for production of hypothemycin and zearalenone. Gene sequences contained within this gene cluster were identified and spliced using HMM-based software FGENESH (Softberry).[76] The model organism used for this prediction software was *Penicillium notatum*. The HR PKS was predicted to contain 6 exons, and had a total length of 7107 bp, the NR PKS has 5 introns, with 6222 bp after intron removal. The intron-less sequences were then analyzed using BLAST (NCBI).

Encoded in the gene cluster are six genes, numbered Cla1 through Cla6. The HR, Cla2, and NR PKS, Cla3, encoded in the gene cluster contain all domains necessary for production of cladosporin *in vivo,* figure 2-5. Cla2 contains a "core" domain that is comprised of a pseudo KR domain (ΨKR, or structural KR subdomain) and a pseudo MT domain (ΨMT). The ΨKR contains a truncated Rossmann fold and acts to stabilize the catalytic KR subdomain, while the ΨMT is thought to be an evolutionary relic from

FASs.[15] Also contained within the gene cluster is a putative lysyl tRNA synthetase, perhaps alluding to cladosporins proposed mode of action in *P. falciparum*.[61] This putative lysyl tRNA synthetase, Cla4, will be discussed in greater detail in chapter 2.2.6. Furthermore, the gene cluster contains genes encoding a hypothetical transposase (*cla1*), a hypothetical ankyrin-containing protein (*cla5*), and a putative glycoside hydrolase (*cla6*).

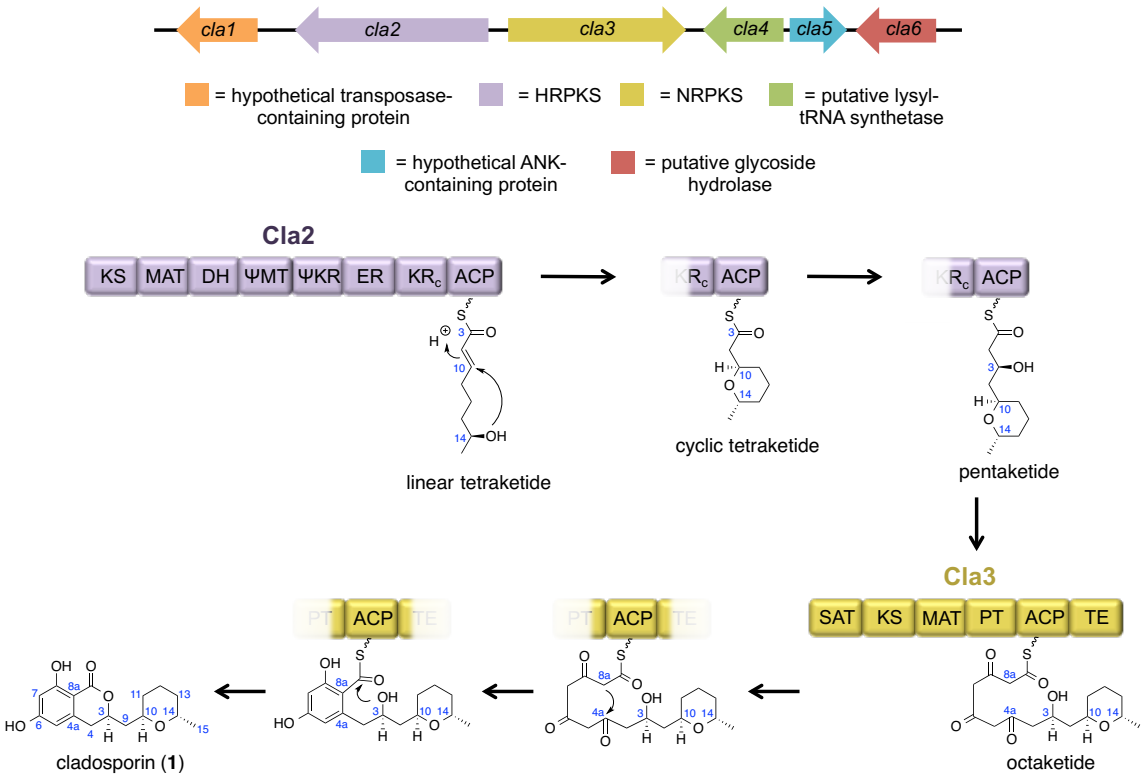

Figure 2-5. Cladosporin gene cluster in *C. cladosporioides* and putative biosynthesis by the HR PKS Cla2 and NR PKS Cla3.

2.2.3 Heterologous expression

In order to further study the biosynthesis of cladosporin, Cla2 and Cla3 were cloned into auxotrophic expression vectors pKOS518-120A and pXK30, figure 2-6. These 2μ-based yeast-*E. coli* shuttle vectors, were acquired from our collaborators in the Yi Tang lab at UCLA. Cla2 was cloned into pKOS518-120A, and contains a TRP1 auxotrophic marker along with NdeI-EcoRI restriction sites, figure 2-6. Cla3 was cloned into pXK30, which contains a URA3 auxotrophic marker and NdeI-PmlI restriction sites, figure 2-6. Both plasmids were cloned using a technique known as transformation-associated recombination (TAR), which is widely employed for cloning of large genes.[77] To use TAR, ~35 bp overlaps that are homologous to the ends of the linearized vector, must be added to the gene of interest using PCR. Both this gene and the linearized vector are then transformed into *S. cerevisiae* where they undergo recombination to yield the circular plasmid containing the gene.

The use of two expression vectors with different auxotrophic markers allowed for co-transformation of the two genes into *Saccharomyces cerevisiae* BJ5464-NpgA. This yeast strain has been specially engineered for such purposes: it has several gene knockouts that render it auxotrophic for the genes present in these plasmids; it is highly deficient in vacuolar proteases; and it contains an integrated copy of the *Aspergillus nidulans* phosphopantetheinyl transferase NpgA.

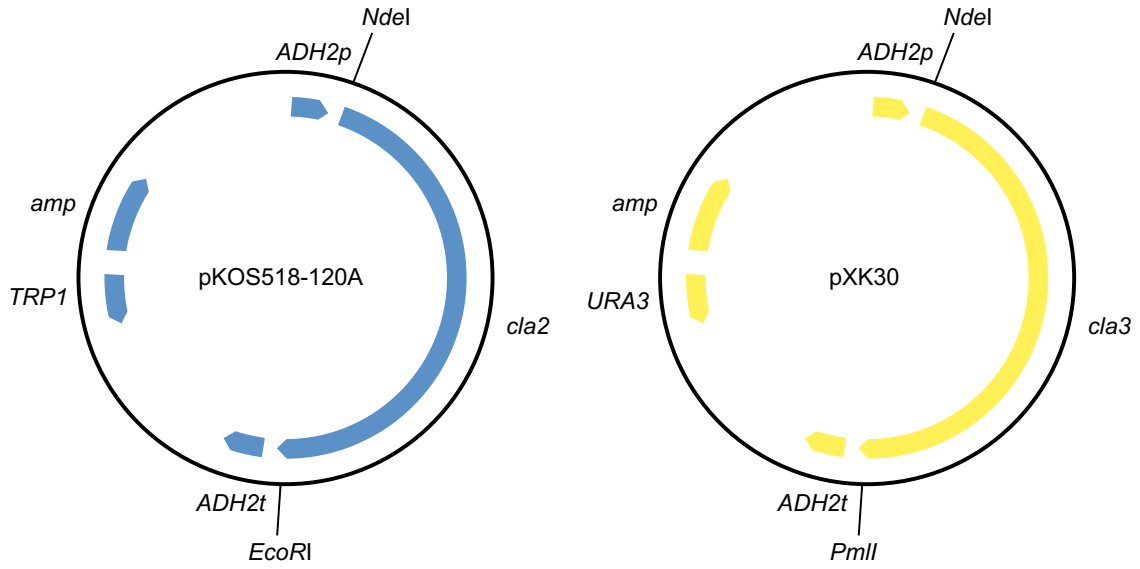

Figure 2-6. Yeast expression plasmids pKOS518-120A with cla2 and pXK30 with cla3 cloned. ADH2p is the alcohol dehydrogenase promoter sequence, ADH2t in the terminator sequence, and amp is an ampicillin resistance gene.

Both His-tagged proteins were successfully expressed and isolated from single transformants (figure 2-7), and cladosporin was extracted and purified from double transformants (figure 2-8). Interestingly, addition of 1 % NaOAc and 0.5 % cyclopentanone boosted metabolite production from 300 μg/L to a titer of 10 mg/L after RP-HPLC purification, figure 2-8. This was based on previous research that had identified cyclopentanone as an efficient inducer of the ADH2 promoter.[78] We reason that NaOAc provides additional starting material for metabolite biosynthesis.

Identity of cladosporin was confirmed by LC-ESI-MS using combined retention time matching with accurate mass matching, and NMR analysis. This confirmed our identification of the cladosporin gene cluster in *C. cladosporioides*. Further study of Cla2

was hampered by low-expression, and so we chose to focus our efforts on the study of Cla3.

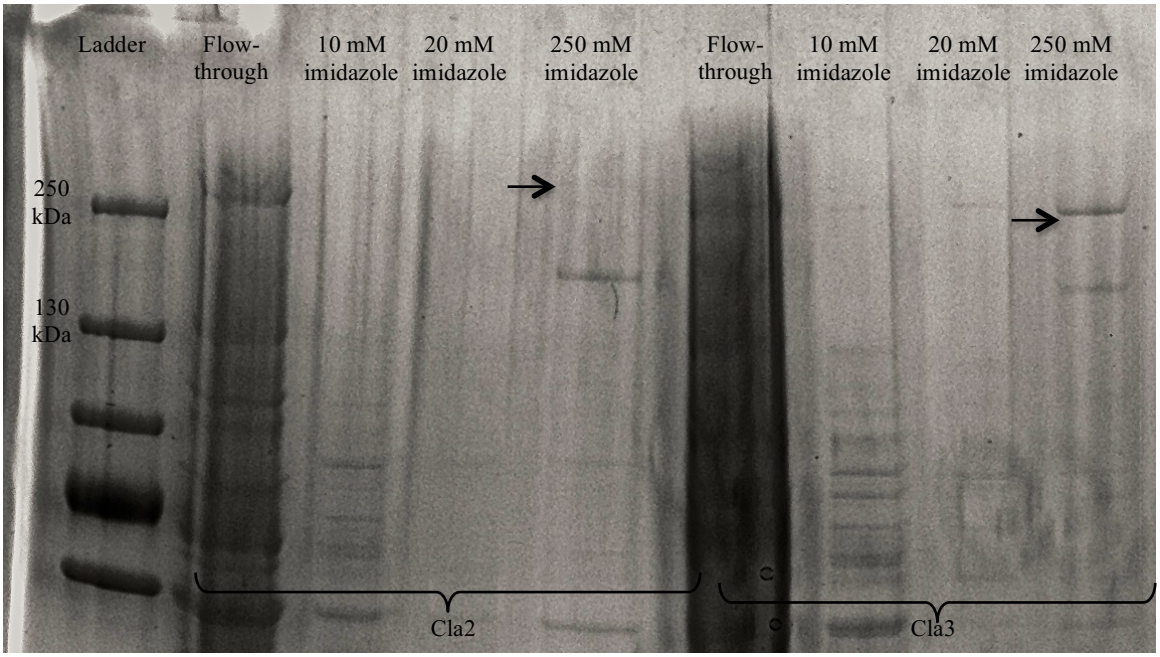

Figure 2-7. SDS-PAGE gel of single yeast transformants. Protein was isolated by nickel column chromatography with several gradients of imidazole-containing buffer. The arrows indicate the band for the HR PKS Cla2, and NR PKS Cla3. The lower molecular weight bands were confirmed by trypsin-MS/MS to be truncated protein.

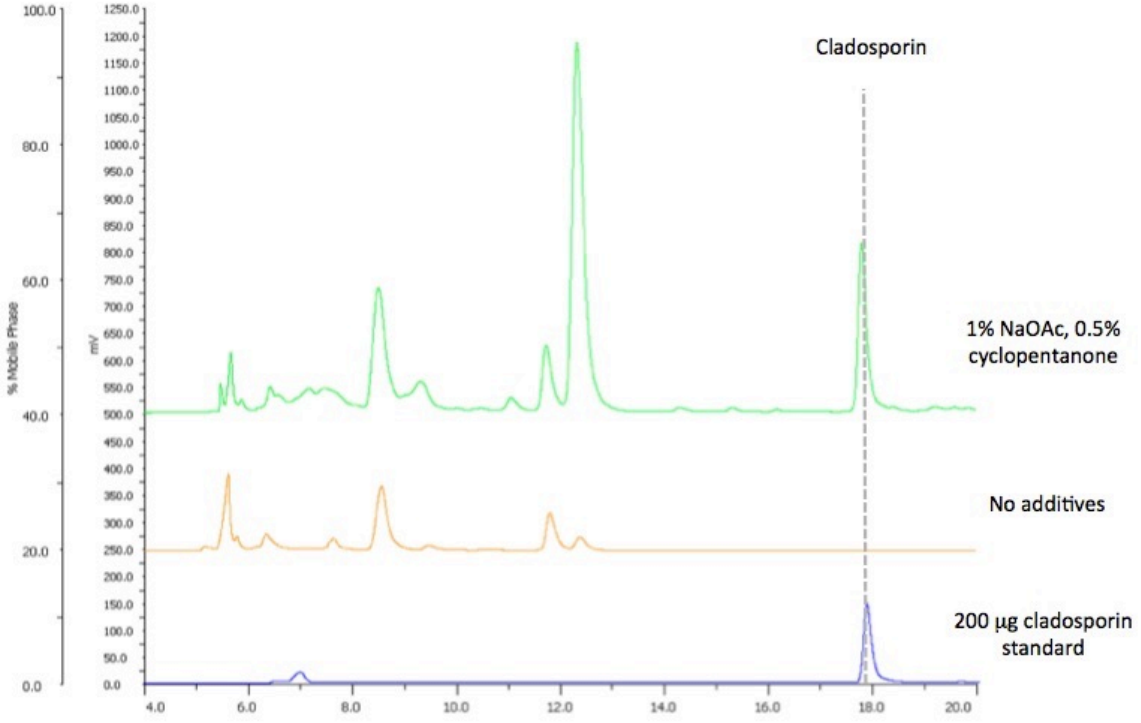

Figure 2-8. HPLC trace of double transformant extract with and without addition of NaOAc and cyclopentanone.

2.2.4 Advanced intermediate assays

To further probe the biosynthesis of cladosporin *in vivo*, we conducted advanced precursor feeding studies. The necessary reduction of the C3 position of cladosporin led us to believe that the HR PKS, Cla2, is responsible for biosynthesis up to the pentaketide stage, inclusive of the tetrahydropyran (THP) ring, whereas the three subsequent ketide extensions with no reduction are catalyzed by Cla3.

Consistent with observations on other NR PKSs that require an HR PKS partner,[34] when Cla3 was provided with malonyl-CoA, it is not able to load and produce

cladosporin on its own. Based on our proposed biosynthetic route, the proposed pentaketide intermediate was synthesized as a *N*-acetylcysteamine (SNAC) thioester (**16**) by another graduate student, Mr. Randy Sanichar. The pentaketide intermediate was fed to purified Cla3, along with malonyl-CoA and after 24-hour incubation at room temperature, metabolites were extracted and analyzed by LC-ESI-MS. Presence of cladosporin in the extract was confirmed using combined retention time matching with accurate mass matching, thus confirming that the pentaketide intermediate analogue is recognized by Cla3, figure 2-9.

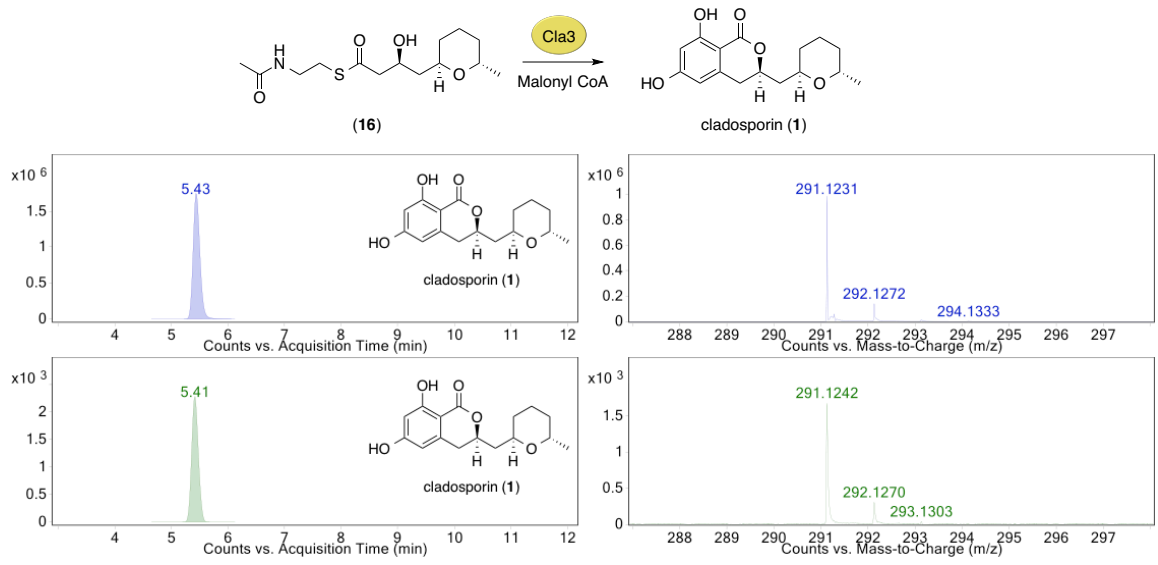

Figure 2-9. EIC and mass spectrum of extract from pentaketide feeding assay. Synthetic standard traces are shown in blue.

It is likely that the final product of the HR PKS Cla2 remains covalently bound as a thioester, until transfer to the SAT domain of the NR PKS Cla3. This "5+3" ketide assembly of cladosporin represents the first example of its type, with other DAL- and

RAL-type polyketides assembled in a "4+4" (dehydrocurvularin)[72-74] "6+3" (hypothemycin, zearalenone)[34, 79] and "5+4" (radicicol)[70, 80] fashion. Thus THP ring formation appears to be catalysed by Cla2, where oxa-Michael type cyclization on an unsaturated thioester intermediate at the tetraketide stage would be highly favoured, figure 2-10.

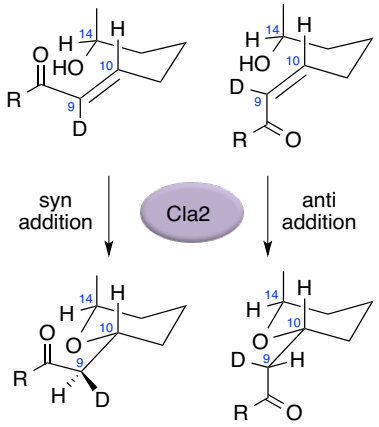

Figure 2-10. Proposed modes of oxa-conjugate addition catalysed by Cla2, both of which are consistent with the stereochemistry observed in the natural product.[66]

Knowing that Cla3 could function in the absence of Cla2, and having active enzyme in hand, we were interested in exploring the substrate scope of Cla3. Mr. Randy Sanichar synthesized the pentaketide analogues shown in figure 2-11.

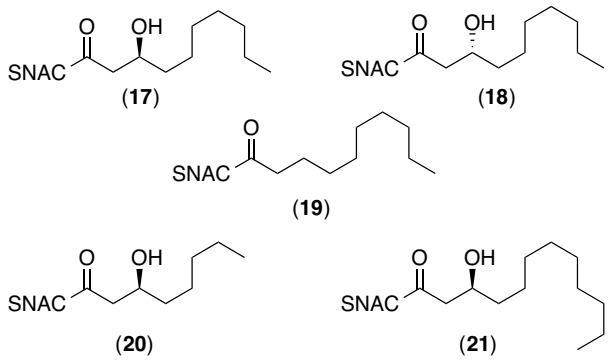

Figure 2-11. SNAC thioester analogues to probe substrate scope of Cla3

The pentaketide analogues were designed so as to investigate several criteria for substrate recognition: necessity of the THP ring; "correct" stereochemistry of the hydroxy group; presence of hydroxy group; and tolerance of chain length. The advanced intermediates were fed to purified Cla3, along with malonyl-CoA and after 24-hour incubation at room temperature, metabolites were extracted and analyzed by LC-ESI-MS. Synthetic product standards were also synthesized by Mr. Randy Sanichar, and these were used to confirm presence or absence of the expected product in the extract using combined retention time matching with accurate mass matching.

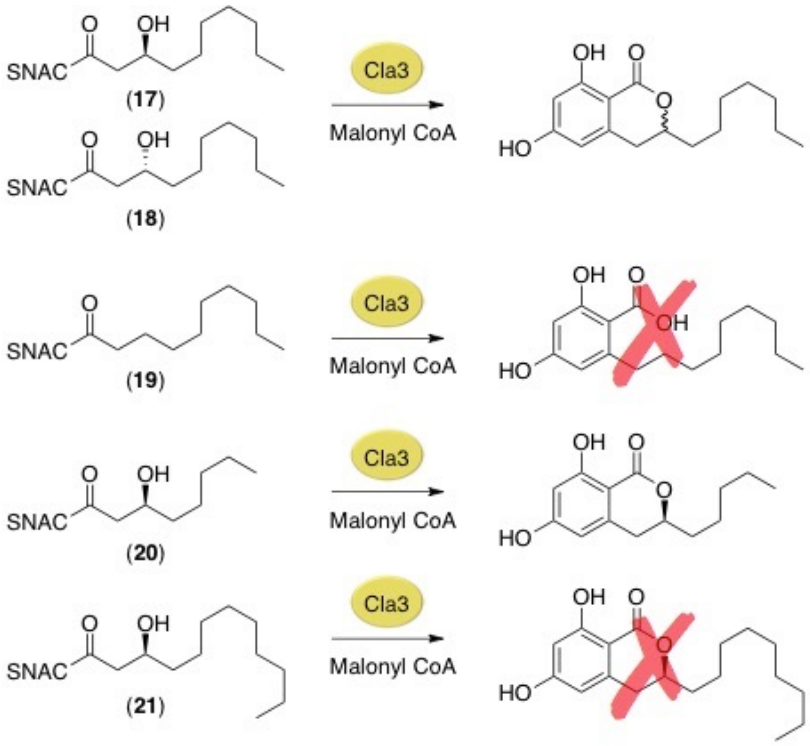

Figure 2-12. Substrate incorporation by Cla3.

Based on the results from the feeding studies with unnatural analogues, it was observed that Cla3 accepts several unnatural substrate analogues (**17**, **18** and **20**) that do not contain the THP ring, perhaps indicating that this moiety is not necessary for recognition by the enzyme. Cla3 recognized and incorporated compound **18**, with the "unnatural" β-hydroxy stereochemistry, but in contrast, did not produce any of the expected product from compound **19**. The presence of a β-hydroxy group therefore appears vital, but its stereochemical configuration seems unimportant for recognition. Lastly, the fact that Cla3 does not accept carbon chains longer than ten carbons, suggests a hydrophobic binding pocket of limited size in the enzyme.

2.2.5 Modeling studies

Having confirmed production of cladosporin from SNAC-pentaketide and conducted feeding studies with pentaketide analogues, we sought to further investigate cladosporin biosynthesis by Cla3. We conducted homology modeling on the PT domain of Cla3. The PT domain is proposed to stabilize reactive polyketide intermediates, guiding correct folding and cyclization events.[81]

In an effort to better understand how the THP ring of the natural substrate fits in the active site, we generated a homology model of $Cla3_{PT}$ using the I-TASSER online modeling server.[82-84] The model was generated using the crystal structure of the PT domain from PksA, the NR PKS responsible for biosynthesis of aflatoxin B_1 in *Aspergillus parasiticus* (PDB ID 3HRQ),[29] as the top threading template. Energy minimised structures of the penta- through octaketide natural intermediates were created in Avogadro,[85] and docked into the active site of $Cla3_{PT}$ using AutodockVina, figure 2-13.[86]

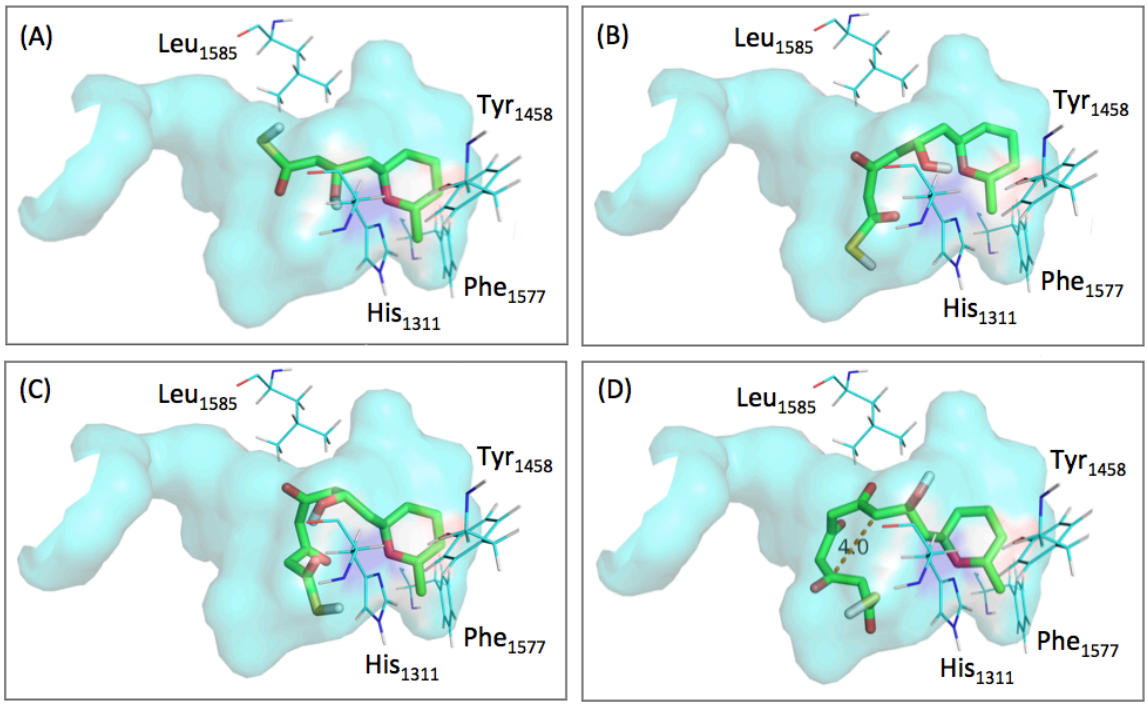

Figure 2-13. Cla3$_{PT}$ homology model with penta- through octaketide thioacid analogues (A-D, respectively) docked in the active site. Conserved residues are highlighted.

Our homology model indicates that the THP ring can be readily accommodated in the PT active site. Furthermore, it can be seen that the pentaketide analog is relatively linear in the active site with the hexaketide starting to form a bent conformation. The heptaketide analogue forms a looped structure, leading to the highly constricted uncyclised octaketide in which C8a is now only 4Å away from C4a. Presumably, the linear octaketide would then cyclise and the resulting aromatized intermediate could then be transferred to the TE domain, where hydrolysis and/or lactone formation could occur to produce cladosporin.

2.2.6 Potential resistance mechanism

As previously mentioned, a putative lysyl tRNA synthetase was discovered in the cladosporin gene cluster in *C. cladosporioides*. Resistance genes can often be found close to the biosynthetic machinery of the natural product, as is the case for lovastatin (**5**), a polyketide that will be discussed in greater detail in chapter 4. Lovastatin inhibits 3-hydroxy-3-methylglutaryl-coenzyme A (HMG-CoA) reductase in the mevalonate pathway, thereby preventing biosynthesis of cholesterol. Contained within the lovastatin gene cluster is a gene, *lvrA*, which encodes an enzyme very similar to the hydroxymethyl glutaryl coenzyme A reductase. This "self-resistance" gene imparts resistance to lovastatin when introduced to the lovastatin-sensitive organism *Aspergillus nidulans*.[26]

In light of the recent interest in cladosporin's antimalarial properties due to inhibition of *P. falciparum* lysyl tRNA synthetase (KRS1), we chose to investigate this apparent "resistance gene" in greater detail.

Through a series of elegant experiments conducted by Hoepfner et al. in 2012,[61] the authors identified two key residues in the active site of their *S. cerevisiae* KRS1 homology model that conferred cladosporin resistance to the organism: Gln324 and Thr340. When glutamine is replaced with a less polar valine residue, and threonine replaced with a slightly less sterically demanding serine residue, as is the case in *P. falciparum* KRS1, the lysyl tRNA synthetase is inhibited by cladosporin and the organism becomes sensitive to it, as highlighted in table 2-1.

Organism		Cladosporin inhibition (uM)	Key active site residues	
Plasmodium falciparum		0.04 – 0.08	Val	Ser
Homo sapiens		>10	Gln	Thr
Saccharomyces cerevisiae		30 – 110	Gln	Thr
Cladosporium	Cla4	N/A	Gln	Thr
cladosporioides	Lys2	N/A	Ile	Thr
	Lys3	N/A	Val	Leu

Table 2-1. Cladosporin activities based on key active site residues. Table modified from Hoepfner *et al.*[61]

Interestingly, the lysyl tRNA synthetase contained within the cladosporin gene cluster, Cla4, contains the Gln-Thr pair at positions analogous to 324 and 340 of yeast KRS1. Furthermore, two other lysyl tRNA synthetases, Lys2 and Lys3, can be found elsewhere in the *C. cladosporioides* genome, neither of which contain the Gln-Thr pair thought to be necessary for resistance to cladosporin, table 2-1. This may indicate that Cla4 is under the same regulation as the PKSs Cla2 and Cla3, and that when biosynthesis of cladosporin is switched on, transcription of *cla4* will be necessary for continued protein biosynthesis in the fungus.

Further to this we generated a homology model of Cla4, with hopes of further elucidating cladosporins mode of action. I-TASSER selected the crystal structure of human KRS1 (PDB ID: 3BJU) as its top threading template.[87] Based on the recently

published co-crystal structure of *P. falciparum* KRS1 with cladosporin bound (PDB ID: 4PG3),[63] we superimposed cladosporin into the active site of our Cla4 homology model. Cla4 has a narrower active site cavity in comparison to *P. falciparum* KRS1, with Gln318 and Thr334 preventing binding of cladosporin: specifically, the methyl group of Thr334 has a steric clash with the methyl substituent of cladosporin. Moreover, AutodockVina was unable to dock cladosporin in the active site of Cla4, but when the natural substrate ATP was docked into the active site we can see that the polar Gln318 preferentially forms H-bonds with the phosphate groups of ATP. ATP also forms electrostatic interactions with the side chains of Arg320 and Arg548, as well as several other backbone interactions.

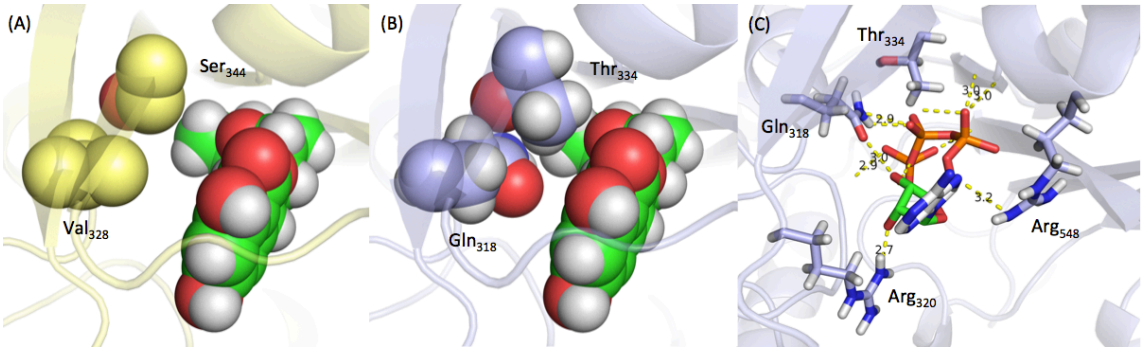

Figure 2-14. (A) Crystal structure of *P. falciparum* KRS1 with cladosporin (green) bound in the active site (B) Space filling model of Cla4 homology model with cladosporin superimposed in the active site (C) Active site of Cla4 with ATP docked.

2.3 Conclusions and outlook

Prior to our recent work on cladosporin the absolute configuration of cladosporin and its diastereomer isocladosporin had been elucidated, along with a putative biosynthesis of cladosporin proposed. The present work consists of identification of the cladosporin gene cluster in *C. cladosporioides* along with complete reconstitution of the PKS biosynthetic machinery in *S. cerevisiae*. Given that *S. cerevisiae* is such an extensively studied organism for heterologous production of other natural products such as artemisinic acid and lovastatin, this result constitutes a significant step toward large-scale production of cladosporin. Furthermore, the promiscuity of Cla3, highlighted through incorporation of advanced intermediate analogues, could allow for the semi-synthesis of new antimalarial analogs. Additional advanced intermediate feeding studies, to include analogues of the THP ring, could help uncover the extent of this substrate scope.

Our discovery of the cladosporin gene cluster also highlighted a probable self-resistance mechanism in *C. cladosporioides*. Bioinformatic analysis of Cla4, the lysyl tRNA synthetase encoded in the cladosporin gene cluster, indicate that Cla4 contains two key active site residues that likely render cladosporin incapable of binding. We hypothesize that transcription of Cla4 is tied to transcription of Cla2 and Cla3, allowing for *C. cladosporioides* to be resistant to inhibition by its own secondary metabolite. We plan to crystallize Cla4, in hopes of gleaning further structural information about the ATP binding pocket, aiding in the design of more potent antimalarial therapeutics.

3 Dehydrocurvularin

Curvularins are a group of phytotoxic polyketide natural products produced by several fungal species including *Alternaria*,[88-91] *Nectria*, *Curvularia*,[92, 93] *Penicillium*,[94] *Aspergillus*,[95, 96] and *Eupenicillium*.[97] Curvularins contain a 12-membered dihydroxyphenylacetic acid lactone (DAL) ring, similar to the better-known 14-membered resorcylic acid lactone (RAL) ring found in polyketides such as zearalenone (**24**),[79] hypothemycin (**11**) [34] and radicicol (**25**),[70] figure 3-1.

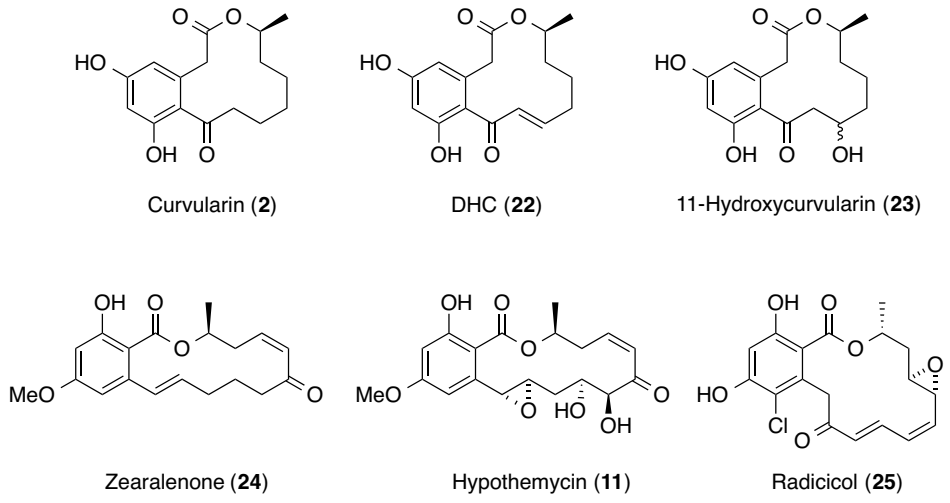

Figure 3-1. Dihydroxyphenylacetic acid lactone (DAL) and resorcylic acid lactone (RAL) polyketides.

The curvularins possess some interesting biological activities. They inhibit the inducible nitric oxide synthase (iNOS) in mammals, thus modulating the

proinflammatory immune response.[94] 10,11-Dehydrocurvularin (DHC, **22**) itself induces overexpression of heat shock factor 1 (HSF1) and various other chaperone proteins, thereby activating the heat shock response, a conserved evolutionary mechanism by which cells maintain protein homeostasis.[98]Also, both DHC and curvularin (**2**) inhibit the TGF-β signalling pathway, which is upregulated during tumor progression.[99] Through these two mechanisms, DHC acts as a broad-spectrum inhibitor of several cancer cell lines *in vitro*, with potential for development as a new cancer therapeutic.[96] In light of these interesting biological activities, several chemical syntheses of (**2**) and its derivatives have been reported.[100-107]

After initial structural elucidation of DHC by Arthur Birch and colleagues,[108] our group confirmed the origin of all constituent atoms and successfully incorporated advanced isotopically labeled intermediates into (**22**) using cultures of *Alternaria cinerariae*.[71-74] In order to fully understand biosynthetic assembly of DHC, the goal of this project was to identify and heterologously express the PKSs responsible for DHC production in *Alternaria cinerariae*.

3.1 DHC biosynthesis

During the course of this study, the heterologous expression of two PKSs (CurS1 and CurS2) responsible for DHC production in *Aspergillus terreus* was reported by Molnar and co-workers.[109] They showed that in *A. terreus*, DHC is biosynthesized in a "4+4" fashion by cooperation of two type I iterative polyketide synthases (PKSs)[3, 22, 110]

- a highly reducing (HR) PKS and a non-reducing (NR) PKS - in a similar fashion to RALs. They also re-engineered the product template (PT) domain of the NR PKS CurS2, allowing it to make RALs instead of the DAL dehydrocurvularin.[111]

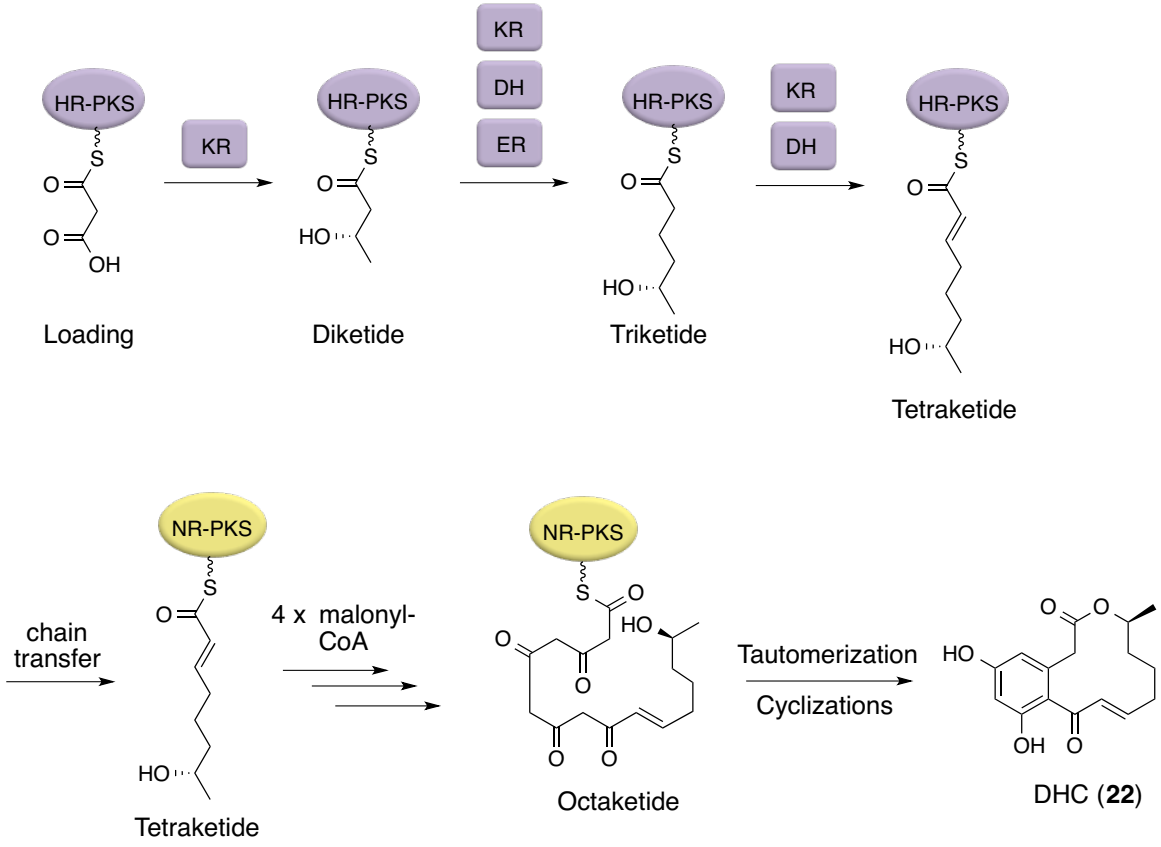

Figure 3-2. Biochemical steps *en route* to DHC in *Aspergillus terreus*.

Formation of the same secondary metabolite, DHC, by two quite different fungal classes, namely Dothideomycetes (*Alternaria*) and Eurotiomycetes (*Aspergillus*) afforded us a unique opportunity to compare biosynthetic machinery for its production.

3.2 Results and discussion

3.2.1 Sequencing and heterologous expression

Previous work conducted in our group by Dr. Zhizeng Gao, Dr. Jesse Li and Dr. Sandra Marcus had identified the PKSs responsible for DHC production in *Alternaria cinerariae* ATCC 11784 using a degenerate PCR primers approach. High sequence similarity in the KS domain of DAL and RAL polyketides was exploited to design a primer pair based on the gene sequence of the KS domain from the HR PKS ZEA2 from *Gibberella zeae*.[112, 113] These primers were used to amplify complimentary regions of DNA from an *A. cinerariae* cDNA library. This KS DNA was sequenced, and new PCR primers designed to amplify the corresponding KS sequence from *A. cinerariae* genomic DNA. A fosmid library of *A. cinerariae* DNA was created, and the KS DNA used as a probe to identify the PKSs contained therein. Using this approach, a HR and NR PKS were detected and subsequently sequenced by primer walking by Dr. Jesse Li and Dr. Sandra Marcus.

In order to fully elucidate the DHC gene cluster, and eliminate the need for extensive primer walking, we sent *A. cinerariae* ATCC 11784 for genome sequencing by Ambry genetics, using their Illumina HiSeq 2000 facilities. This resulted in a total of 34 Mb of genomic information, obtained over a total of 907 contigs. The genome was annotated using Antibiotics & Secondary Metabolite Analysis Shell (antiSMASH v. 2.0),[75] which identified 39 secondary metabolite gene clusters, 8 of which are for type I iterative PKSs. One gene cluster in particular closely resembles the gene clusters of

hypothemycin and radicicol. Hidden Markov model (HMM)-based gene sequences contained within this gene cluster were predicted using FGENESH (Softberry),[76, 114] and the resulting sequences analyzed using BLAST (NCBI). Five genes potentially related to DHC biosynthesis were identified (figure 3-3) using this approach, by Dr. Zhizeng Gao.

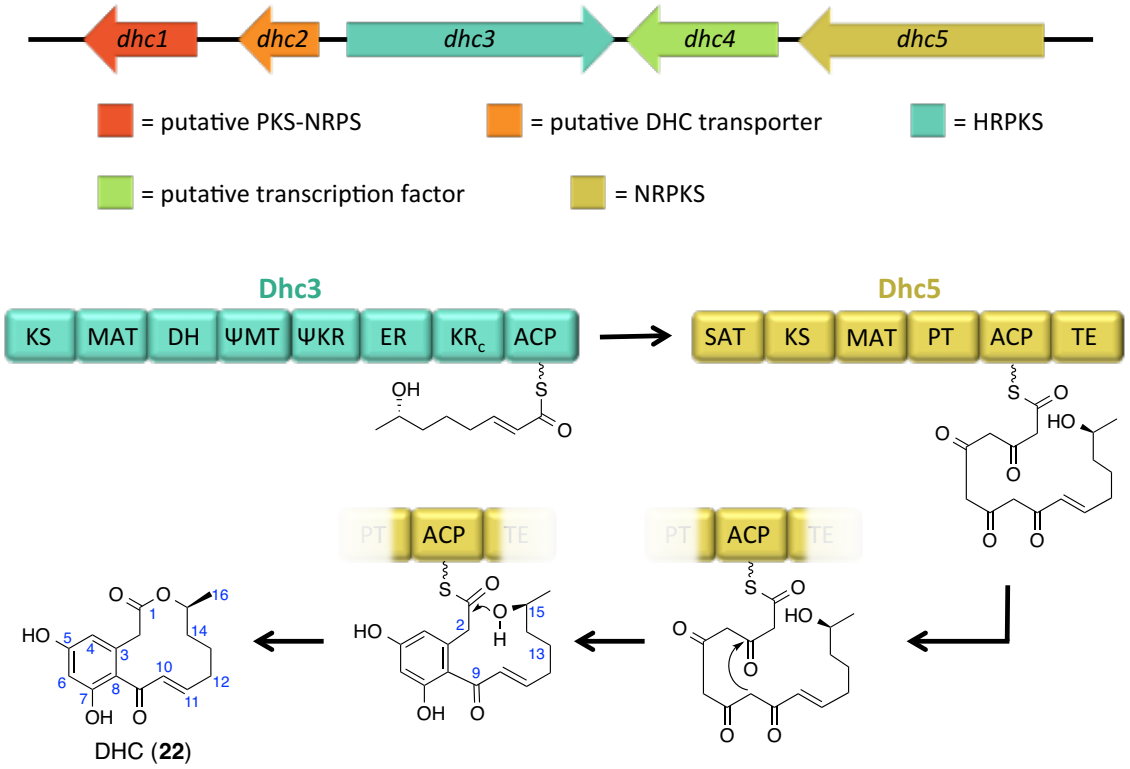

Figure 3-3. DHC gene cluster and proposed biosynthesis in *Alternaria cinerariae*.

The gene cluster encodes a HR and NR PKS, *dhc3* and *dhc5* respectively, with all domains necessary for biosynthesis of (**22**). Also contained within the gene cluster is a putative PKS-NRPS of unknown function (*dhc1*), a putative DHC transporter (*dhc2*), and a putative transcription factor (*dhc4*). Both intron-free *dhc3* (7.1 kb) and *dhc5* (6.2 kb) were cloned by Dr. Zhizeng Gao into auxotrophic expression vectors pKOS518-120A

and pXK30 for expression in the protease deficient *S. cerevisiae* strain BJ5464-NpgA. Unfortunately, Dr. Gao was unable to get DHC production. Therefore, my work continued on in the form of single and double transformations using the plasmids Dr. Gao had cloned. Both Dhc3 and Dhc5 could be isolated from single transformants (figure 3-4) in hopes of conducting advanced intermediate studies. Double transformation yielded on average 11 mg/L of DHC after RP-HPLC purification. Addition of 1 % NaOAc and 0.5 % cyclopentanone boosted metabolite production from 500 μg/L to a titer of 11 mg/L after RP-HPLC purification, figure 3-5.

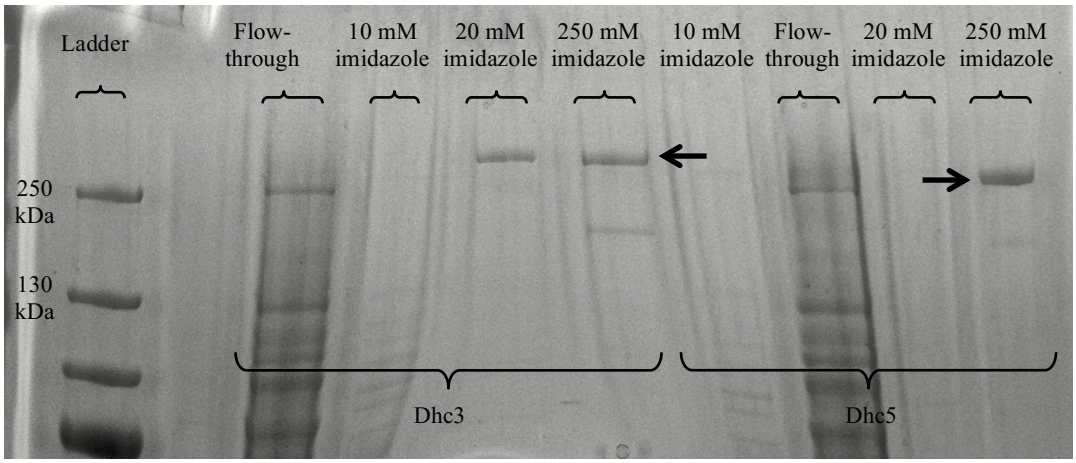

Figure 3-4. Dhc3 and Dhc5 isolated from single transformations. Proteins were isolated using nickel column chromatography with several concentrations of imidazole-containing buffer. Arrows indicate Dhc3 and Dhc5 protein bands.

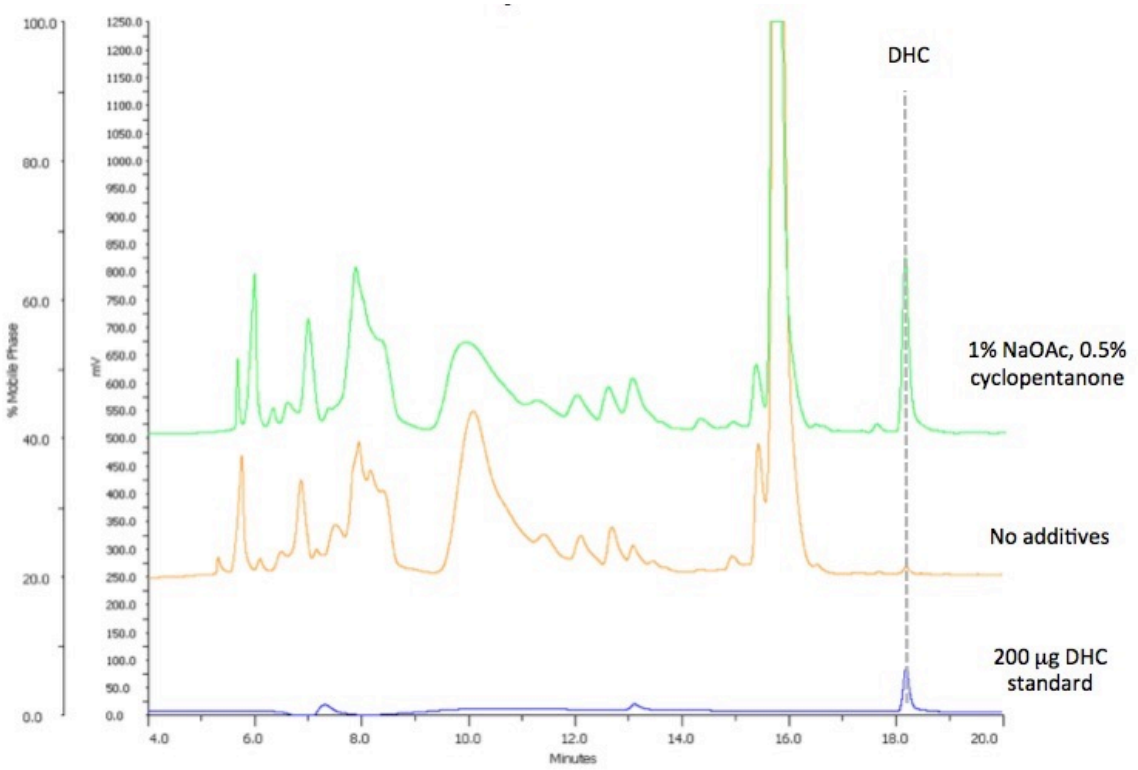

Figure 3-5. HPLC traces of extracts from double transformations with and without addition of NaOAc and cyclopentanone.

The identity of DHC was confirmed by NMR, and by LC-ESI-MS, confirming that Dhc3 and Dhc5 are responsible for DHC biosynthesis in *A. cinerariae*. As previously mentioned, Molnar and co-workers reported the expression of DHC PKSs, CurS1 and CurS2, from *Aspergillus terreus*, wherein they conducted advanced intermediate incorporation experiments.[109] Instead, with the aim of comparing the production of DHC in different organisms, we embarked on structural studies of Dhc3 and Dhc5.

3.2.2 Phylogenetic and bioinformatic analysis

Comparison of the DHC gene clusters from the two different organisms highlighted some quite evident differences. In particular, the *A. cinerariae* gene cluster possesses a putative PKS-NRPS that the *A. terreus* gene cluster does not.

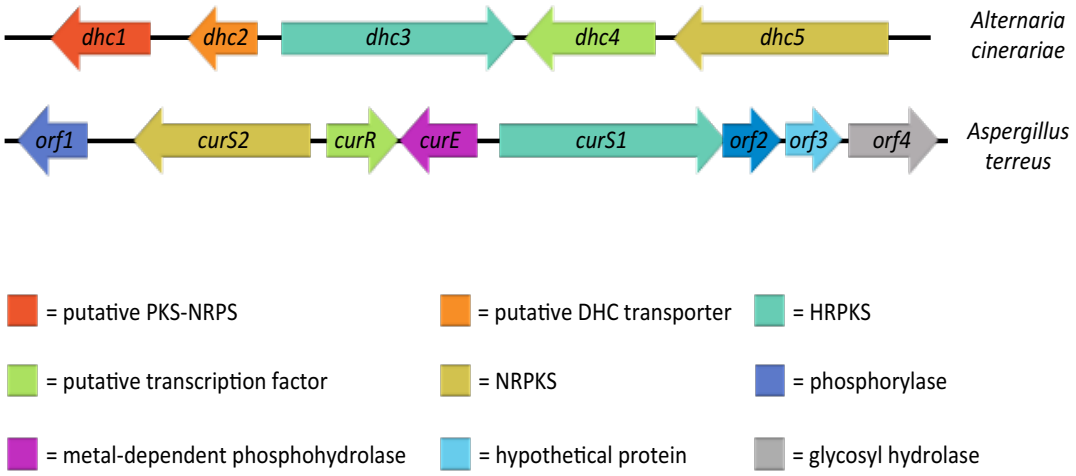

Figure 3-6. Comparison of DHC gene clusters from *A. cinerariae* and *A. terreus*.

We specifically compared sequences of Dhc3 and Dhc5 to the DHC PKS homologs from *A. terreus*, CurS1 and CurS2.[109] Dhc3 and Dhc5 share 75% and 77% sequence identity with CurS1 and CurS2, respectively, however the differences appear to be clustered in specific areas, table 3-1.

Protein	Domain	% Identity (homology)
Dhc3	KS	87 (94)
	AT	78 (87)
	DH	77 (86)
	core	52 (70)
	ER	86 (91)
	KR	83 (91)
	ACP	83 (86)
Dhc5	SAT	71 (83)
	KS	93 (96)
	AT	76 (88)
	PT	78 (89)
	ACP	83 (93)
	TE	85 (90)

Table 3-1. Direct sequence comparison of Dhc3 and Dhc5 with CurS1 and CurS2, respectively.

The ΨKR domain (or structural KR subdomain) contained within the "core" domain of the HR PKSs acts to stabilize the catalytic subdomain and the ΨMT subdomain also contained within the core unit is thought to be an evolutionary relic from FASs. When Dhc3 is compared to CurS1, the standout difference is in this core domain. This may suggest that the sequence of these sub-domains is inconsequential in the biosynthesis of (**22**). Comparing Dhc5 and CurS2, the 23% sequence difference is spread out over the entire protein. Of the 6 domains present in these NR PKSs, the least homologous among them is the SAT domain, with 71% sequence identity. The SAT domain of NR PKSs is responsible for transferring the polyketide intermediate from the HR PKS partner to the NR partner, with specific protein-protein interactions between the two enzymes.[34] Thus, it is expected that this protein-protein interaction may differ significantly between different organisms.

We then embarked on specific domain comparisons in hopes of elucidating structural difference between the two sets of proteins. To this end, we prepared homology models of the AT domain of Dhc3 and the PT domain of Dhc5 using I-TASSER.[82, 83] We selected these two domains based on their low sequence identity scores, and the availability of crystal structures to act as reliable threading templates for I-TASSER. Both of these domains are involved in intermediate recognition, and we hoped that homology modeling might illuminate structural similarities key for substrate recognition.

Using the crystal structure of the iterative type I HR PKS domain, DynE8, from *Micromonospora chersina* (PDB ID: 4AMP)[115] as the top threading template, I-TASSER generated a model of $Dhc3_{AT}$, which we then used to map sequence mutations in comparison to $CurS1_{AT}$. We found that the majority of mutations occur on the surface and on one face $Dhc3_{AT}$, as seen in figure 3-7. The substrate cavity, with active site Ser511, is found on the relatively conserved face of the protein.

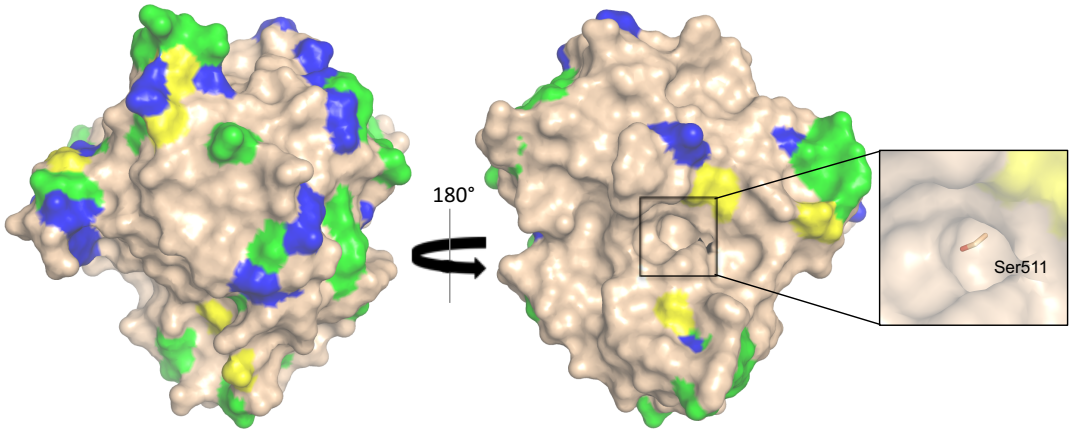

Figure 3-7. Surface representation of Dhc3AT homology model with sequence "mutations" in comparison to CurS1 highlighted (beige, conserved; yellow, homologous; green, less homologous; blue, non-homologous).

Next, we generated a homology model of $Dhc5_{PT}$ and $CurS2_{PT}$, in which I-TASSER selected the crystal structure of the PT domain from the iterative NR PKS PksA, responsible for biosynthesis of aflatoxin B_1 in *Aspergillus parasiticus* (PDB ID: 3HRQ),[29] as its top threading template in both cases. $Dhc5_{PT}$ includes the conserved bulky Trp1583 residue (CurS2 Trp1584), which acts as a "gate-keeper" at the entrance to the substrate cavity. There, it is thought to direct the C2 of the substrate away from the catalytic histidine.[116] Also Phe1454 (CurS2 Phe1455) and Tyr1575 (CurS2 Tyr1576) are conserved in $Dhc3_{PT}$. These residues are located at the back of the substrate binding pocket, where they participate in electrostatic H-bonding, or hydrophobic interactions with the substrate, respectively, thereby directing DAL or RAL formation. Intriguingly however, the active site cavities vary considerably in structure. Although the aforementioned amino acids remain structurally conserved, the substrate cavity of $CurS2_{PT}$ extends beyond the cyclization chamber, figure 3-8. $CurS2_{PT}$ has a long chamber of a hydrophobic nature attached; perhaps indicating relaxed substrate specificity and increased enzyme promiscuity in contrast to $Dhc5_{PT}$.

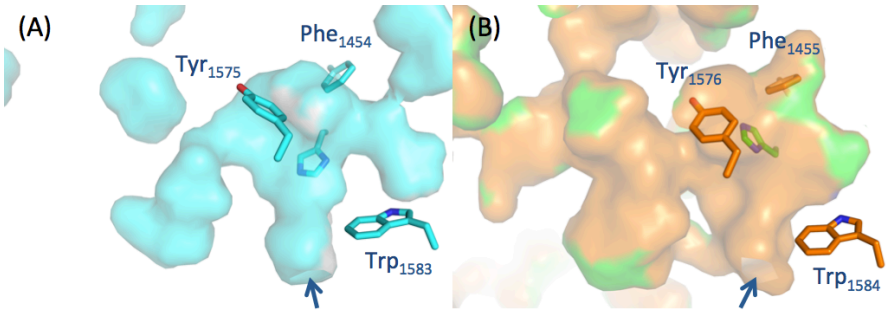

Figure 3-8. (A) Active site cavity of $Dhc5_{PT}$ (cyan) and (B) $CurS2_{PT}$ (green) with conserved tryptophan, phenylalanine, and tyrosine residues highlighted in both. Substrate entrance channels are marked with an arrow.

During the course of these studies, our collaborators at UCLA published the crystal structure of the SAT domain from CazM, the NR PKS involved in the biosynthesis of chaetoviridin A and chaetomugilin A in *Chaetomium globosum*.[117] A key structural motif found in $CazM_{SAT}$, is a parallel αP helix present in the α/β-hydrolase-like subdomain. In the case of $Dhc5_{SAT}$, our homology model (figure 3-9) predicts that the αP helix is in a perpendicular orientation, consistent with all known AT domain crystal structures, the vast majority of which are from modular PKSs.

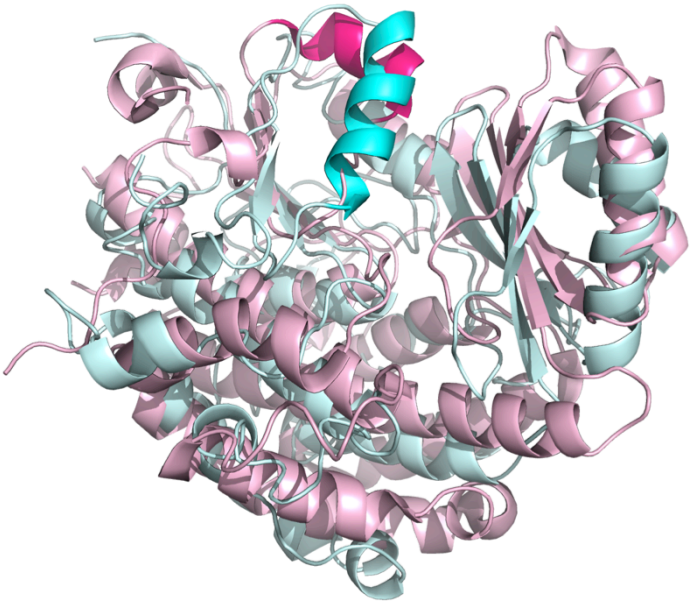

Figure 3-9. Alignment of $Dhc5_{SAT}$ (pale cyan) with $CazM_{SAT}$ (pale pink), with αP helices highlighted in cyan ($Dhc5_{SAT}$) and hot pink ($CazM_{SAT}$).

Moreover, we conducted phylogenetic analysis of NR PKS SAT domains using MEGA6 software and showed that $Dhc5_{SAT}$ and $CurS2_{SAT}$, along with all other DAL and RAL forming PKSs, clade closer to the AT3 domain from the type I modular PKS, 6-

deoxyerythronolide B synthase (DEBS) than that of CazM, figure 3-6. Based on this knowledge, it may be reasonable to suggest that the SAT domains from DAL and RAL forming NR PKSs evolved directly from their AT relatives, which also contain an active site serine.

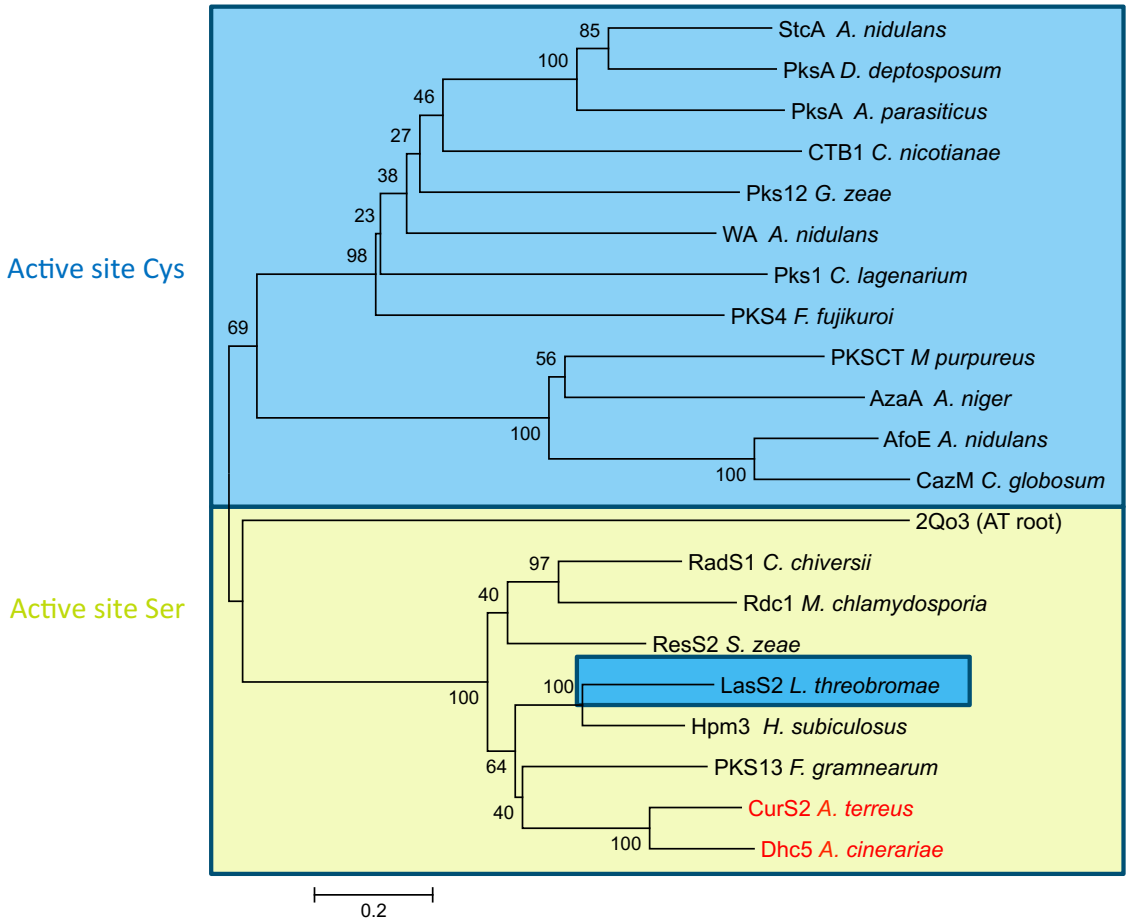

Figure 3-10. Neighbour-joining phylogenetic tree of select NR PKS SAT domains. Those enzymes highlighted in blue contain an active site cysteine, and those in the yellow box contain an active site serine. The tree is rooted with the AT3 domain from DEBS3 (2QO3) and the values at the internal nodes are bootstrap percentages. The scale bar indicates 0.2 changes per amino acid.

3.3 Conclusions and outlook

The present work consists of identification of the DHC gene cluster in *A. cinerariae,* along with complete reconstitution of the PKS biosynthetic machinery in *S. cerevisiae*. Furthermore, addition of NaOAc and cyclopentanone increased DHC production from 500 μg/L to 11 mg/L, highlighting the utility of secondary metabolite production in yeast.

Recent publication of the PKSs responsible for DHC production in *A. terreus*, allowed us to compare metabolite production in two somewhat distantly related organisms. Based on our structural analysis, the sequence differences between the AT domains of Dhc3 and CurS1 are found mainly on the proteins surface. In the case of Dhc5, the SAT domain showed the lowest homology with that of CurS2. This is in line with previous thinking that this domain is highly specific for each organism. Furthermore, $Dhc5_{PT}$ contains conserved residues that had previously been suggested to lead to DAL ring formation over RAL ring formation. Our homology model of $CurS2_{PT}$ shows an extensive substrate-binding pocket, perhaps suggesting enhanced substrate promiscuity, which could aid in the design and synthesis of DHC analogues.

Further experiments in which the HR PKS from one partner is swapped with that from the other organism, could aid in our understanding of cross talk between PKSs and pave the way for further domain swapping experiments.

4 Lovastatin

Perhaps one of the most well known examples of a polyketide therapeutic is lovastatin, first isolated from *Aspergillus terreus* cultures in 1980.[118] Lovastatin belongs to a group of molecules known as statins, some of which have annual revenues in the range of billions of dollars. Members of this group include the natural compactin (Mevastatin, **26**), the semisynthetic simvastatin (Zocor, **27**), and the completely synthetic analogues atorvastatin (Lipitor, **28**) and rosuvastatin (Crestor, **29**), shown in figure 4-1.

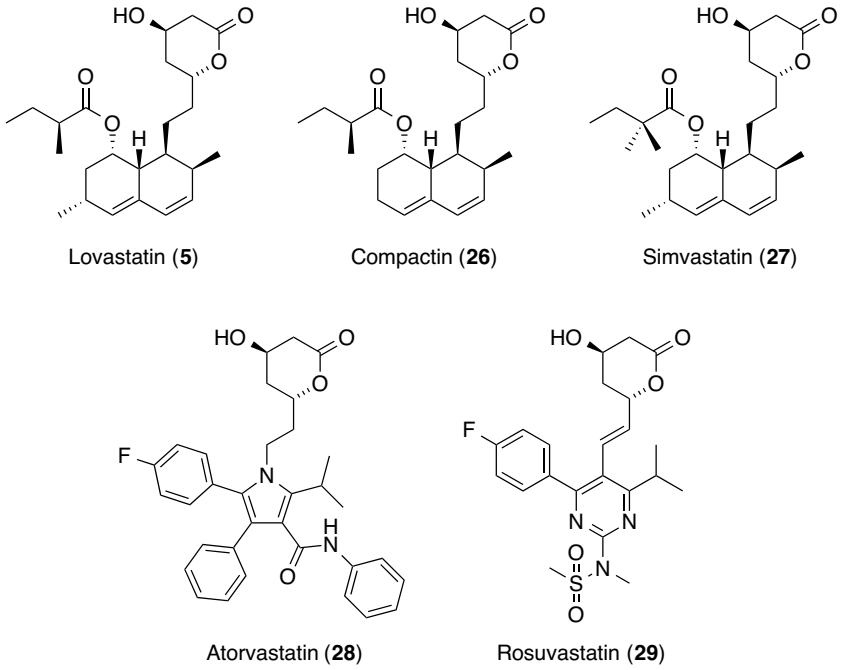

Figure 4-1. Chemical structure of selected statins.

This group of molecules is prescribed to patients with cardiovascular disease, who often exhibit elevated levels of cholesterol. The statins act to lower these cholesterol levels partly by inhibiting 3-hydroxy-3-methylglutaryl-coenzyme A (HMG-CoA) reductase, an NADPH-dependent enzyme that catalyses the reduction of HMG-CoA to produce mevalonic acid, a key intermediate in cholesterol biosynthesis, figure 4-2.

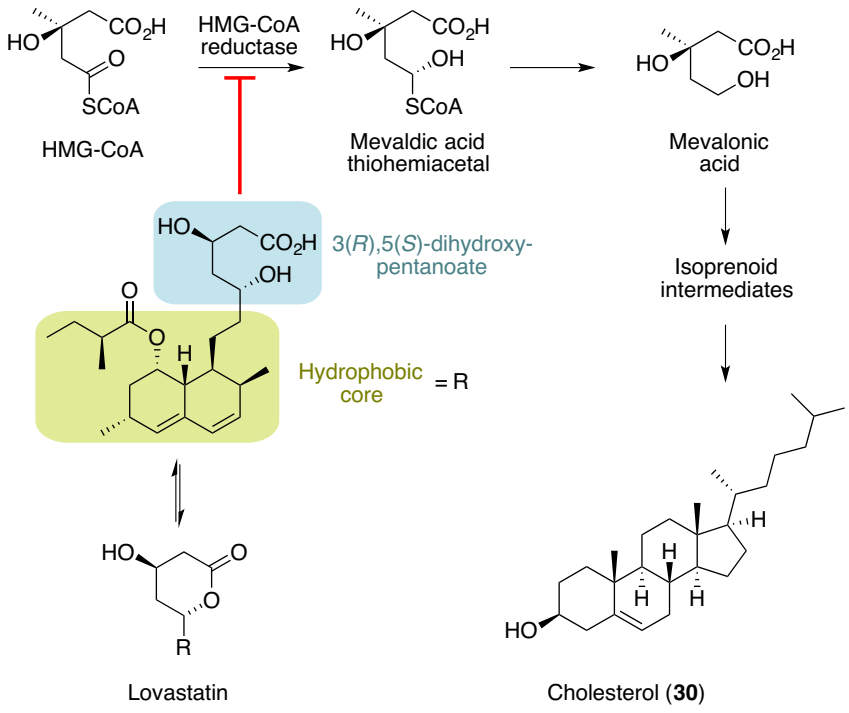

Figure 4-2. Inhibition of HMG-CoA reductase in the mevalonate pathway by lovastatin.

Lovastatin, and other statins, act to mimic the mevaldic acid thiohemiacetal using their 3(*R*),5(*R*)-dihydroxypentanoate moiety, which is in equilibrium with the lactone form of lovastatin. Replacement of this 3(*R*),5(*R*)-dihydroxypentanoate warhead renders analogues inactive. However, modification of the hydrophobic core of (**5**) - which sits in

the hydrophobic binding pocket of HMG-CoA reductase – can significantly increase the efficacy of the overall structure.

4.1 Lovastatin biosynthesis

Dihydromonacolin L (DML, **7**), an intermediate in the biosynthesis of lovastatin, is made by the cooperative action of a HR PKS (LovB) and trans-acting enoyl reductase (LovC) in *Aspergillus terreus*.[27, 28, 119, 120] Together, these two enzymes catalyse the head-to-tail addition of nine acetate units to furnish (**7**).

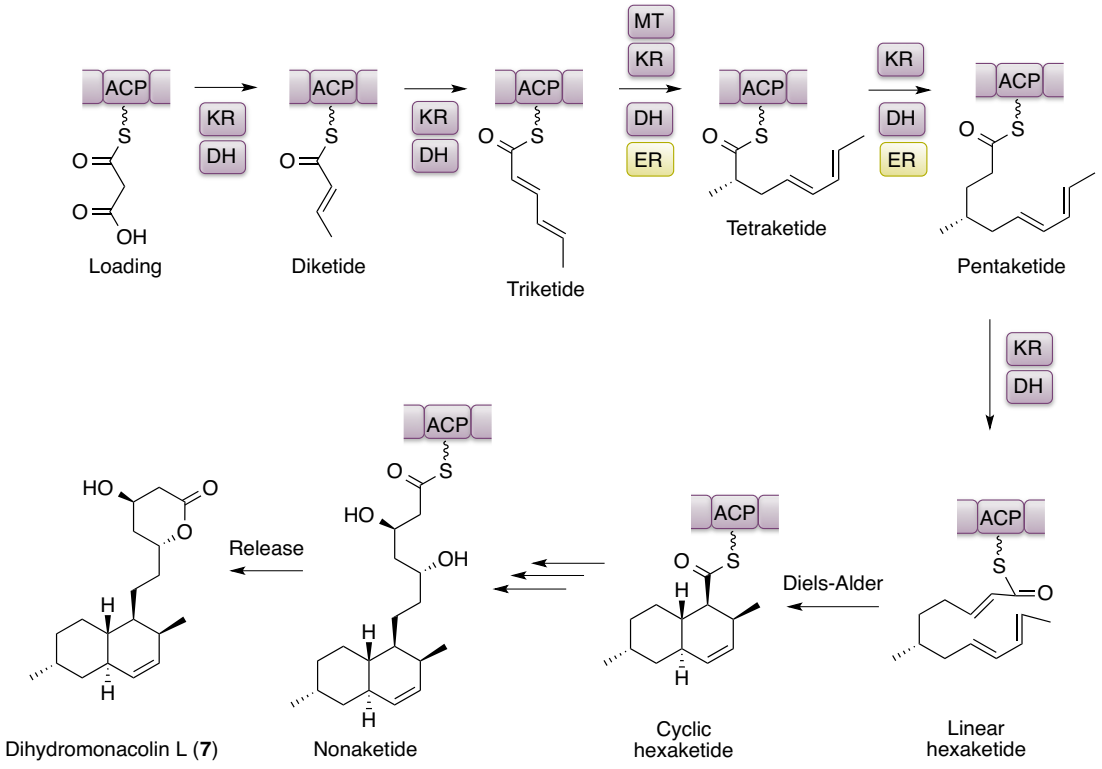

Scheme 4-1. Biosynthesis of DML by LovB and the trans-acting ER, LovC.

Also encoded in the lovastatin gene cluster are several enzymes necessary for production of lovastatin, figure 4-3. Starting from (**7**), the cytochrome P450 monooxygenase LovA first catalyses two successive oxidations to produce monacolin J acid (**32**).[121] The diketide synthase LovF then synthesizes the 2(*S*)-methylbutyrate pendant group, which is transferred to the C8 hydroxy of (**32**) by the acyl transferase, LovD.[25, 26, 119, 122, 123] It has been recently shown that LovG is the thioesterase necessary for release of lovastatin from the enzyme.[124]

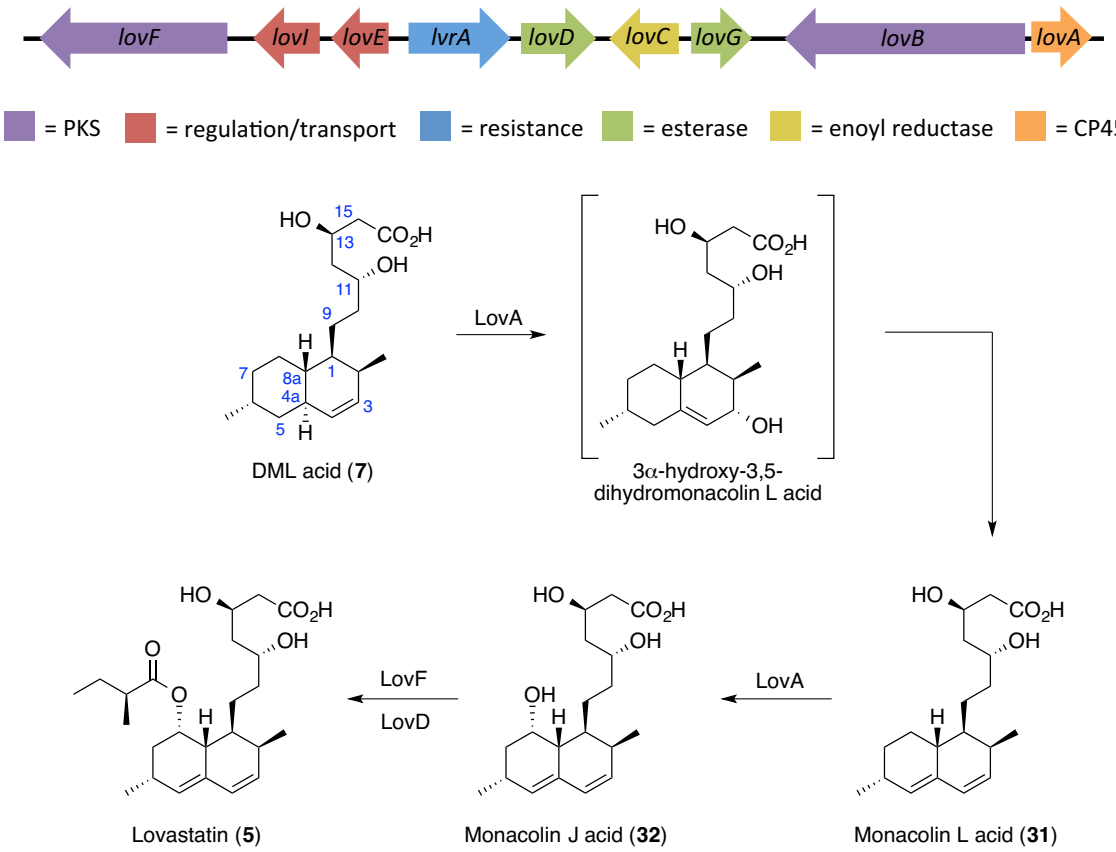

Figure 4-3. Lovastatin gene cluster in *Aspergillus terreus* and conversion of DML to lovastatin by enzymes encoded therein.

4.2 Diels-Alder reaction

During the biosynthesis of lovastatin, an interesting [4+2] cycloaddition must take place.[125-127] Such reactions are well known in synthetic chemistry, and some prospective examples exist in nature, such as in the case of lovastatin, equisetin, cytochalasin E, solanopyrone A, and spinosyn A.[128-132]

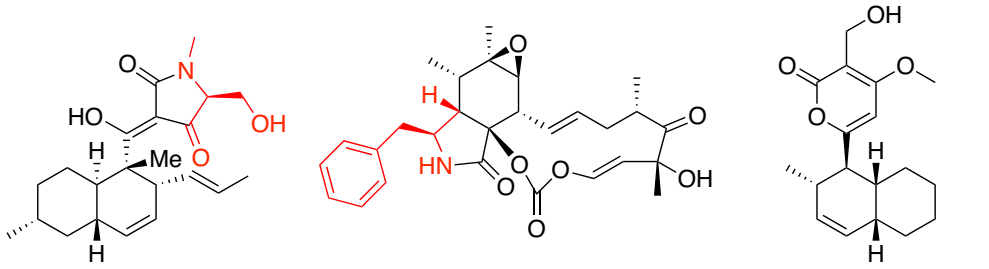

Equisetin (**4**) Cytochalasin E (**3**) Solanopyrone A (**33**)

Figure 4-4. Examples of fungal polyketides that are proposed to be formed via a [4+2] cycloaddition. Those atoms derived from amino acids are shown in red.

In the case of lovastatin, the linear hexaketide must undergo a Diels-Alder reaction with the correct geometry in order to generate the natural product with the correct stereochemistry, figure 4-5. It is interesting to note that the correct stereochemistry of lovastatin includes the methyl groups on the decalin ring system in unfavoured axial orientations. When the synthetic SNAC derivatives of the linear hexaketide triene were synthesized, it was shown that in the absence of LovB, only a 1:1 mixture of the two *exo* products was observed, and the reaction rate was significantly accelerated in aqueous media.[133] However, when LovB was added to the triene in

solution, formation of the correct stereochemistry was observed.[134] These findings suggest the idea that LovB catalyses the Diels-Alder cyclisation in lovastatin biosynthesis.

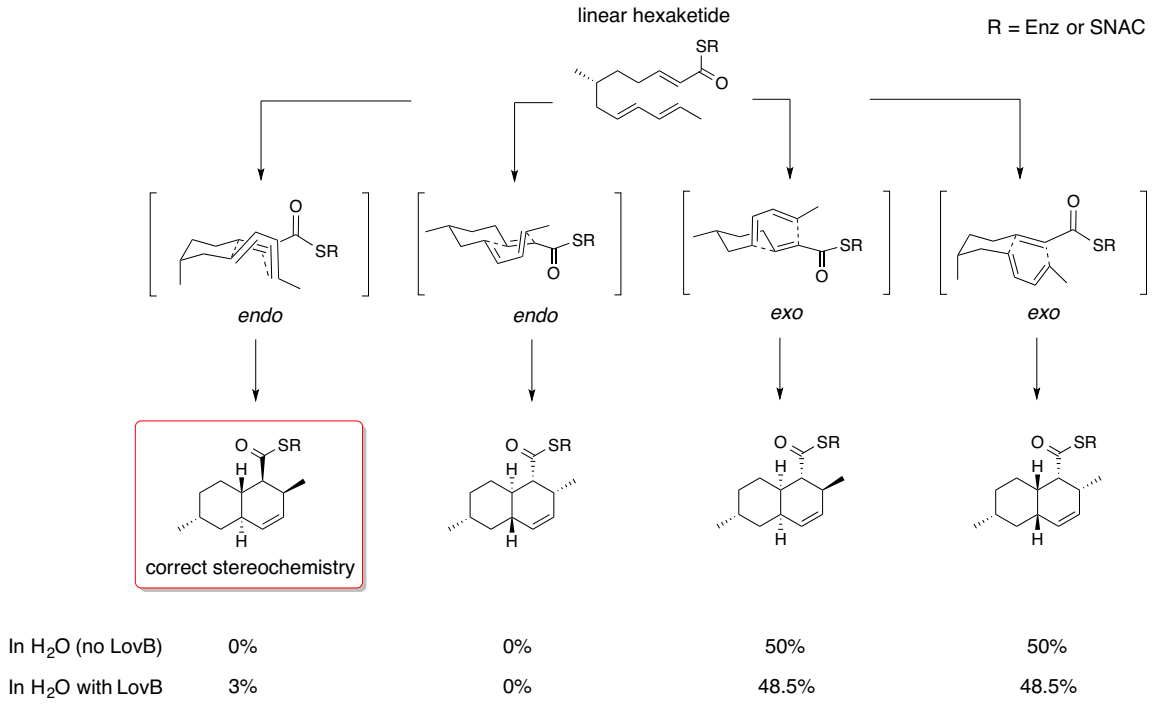

Figure 4-5. Diels-Alder reaction to generate correct stereochemistry in the absence and presence of LovB.

4.2.1 Domain architecture of LovB

Examining the domain architecture of LovB in more detail reveals that LovB does not only contain all the necessary HR PKS domains, but also a non-ribosomal peptide synthetase (NRPS) portion consisting of a condensation (CON) domain, and partially intact adenylation (A) domain, figure 4-6.

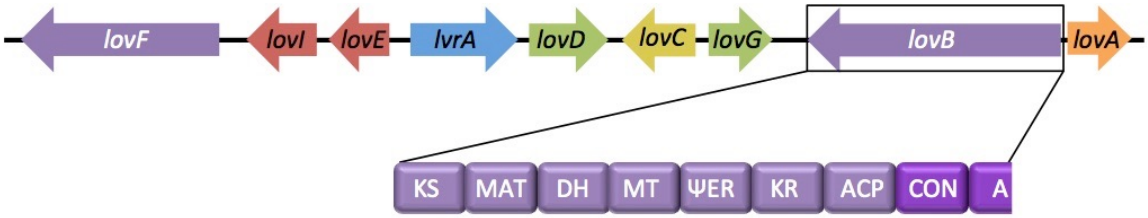

Figure 4-6. Domain architecture of LovB including PKS and NRPS portion.

Interestingly, some other PKS natural products whose biogeneses are proposed to include a [4+2] cycloaddition also contain an NRPS module. For example, the HR PKS (EqiS) responsible for production of the HIV-1 integrase inhibitor, equisetin (**4**) in *Fusarium heterosporum*, contains a fully intact NRPS module.[128] Equisetin also contains a fused decalin ring system, but in contrast to lovastatin, contains atoms derived from serine, added by the NRPS portion.

4.2.2 Condensation domain

One of the NRPS domains that LovB and EquiS have in common is the condensation domain. As the biogenesis of both metabolites is proposed to include a [4+2] cycloaddition, the CON domain is a likely candidate for Diels-Alderase activity. To further investigate the function of this domain, a truncated version of LovB (LovBΔCON), which was missing the entire NRPS portion, was produced by the Tang lab.[28] When LovBΔCON was incubated with LovC, all necessary cofactors, and

Gibberella zeae PKS13 TE to affect hydrolytic off-loading, no detectable amounts of DML were formed. LovBΔCON and malonyl CoA together afforded pyrone (**34**), and when single cofactors were added in, several other pyrones were formed, pyrones (**35**) and (**36**) for example. Interestingly, the CON domain was able to act *in trans* when added to the reconstituted LovBΔCON system, to produce (**7**).

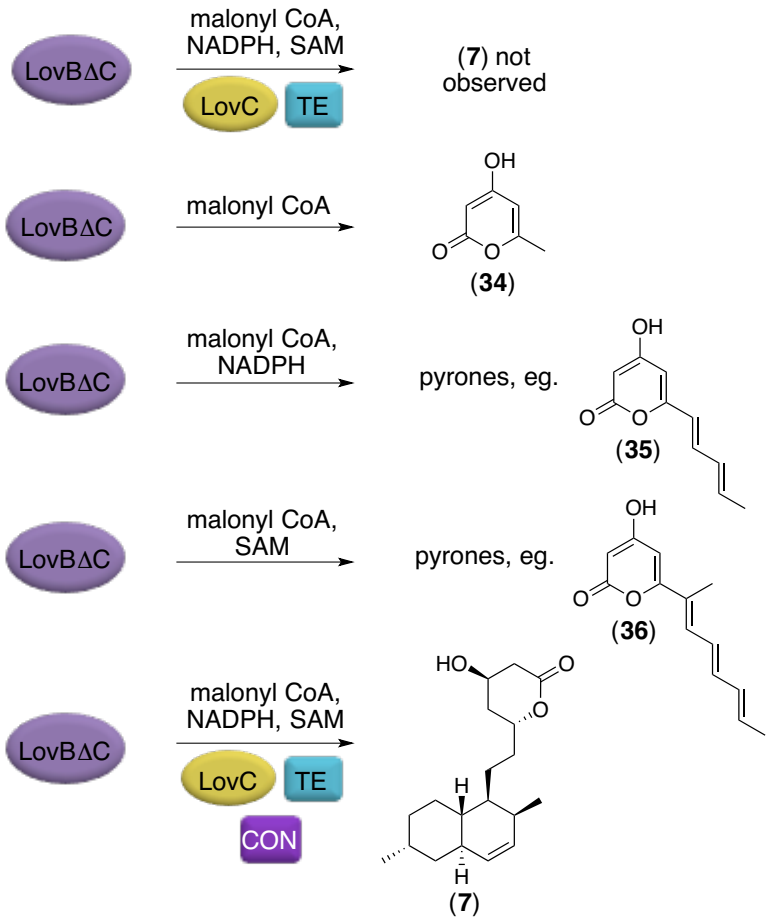

Figure 4-7. Results of LovBΔCON *in vitro* assays.

Recently, our collaborator Dr. Sheryl Tsai at UC Irvine obtained a crystal structure of the LovB condensation domain. In hopes of further elucidating the role of the condensation domain, linear hexaketide analogues that are unable to undergo Diels-Alder cyclisation reaction were synthesized. The hope is to gain a co-crystal structure of the CON domain "frozen" in place with a hexaketide analogue attached. Previous work in our group showed that hexaketide intermediates linked to a SNAC thioester are insoluble and could not be co-crystallized with the enzyme. Therefore phosphopantetheine-coupled hexaketides were synthesized.

4.3 Results and discussion

4.3.1 Phosphopantetheine synthesis

Coenzyme A is one of the most extensively used cofactors in nature, where it is necessary for fatty acid biosynthesis and secondary metabolite biosynthesis. The phosphopantetheine (Ppant) portion of CoA is transferred to the ACP active site serine of the PKS by a phosphopantetheinyl transferase (Pptase). Here, it tethers the acyl intermediate to the enzyme, whilst providing a flexible arm that allows the growing polyketide chain to access domain active sites.

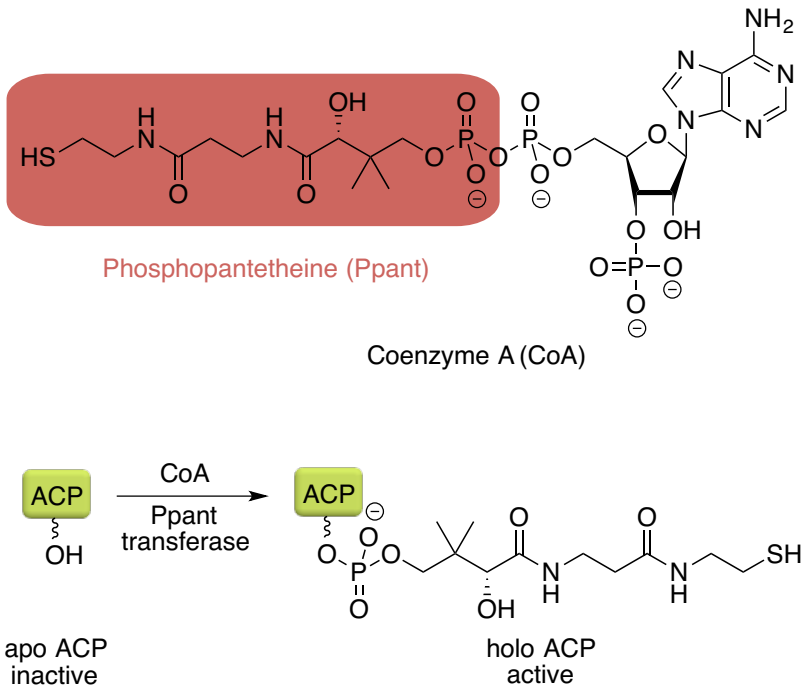

Figure 4-8. Structure of coenzyme A and ACP activation reaction

Mr. Drew Hawranik in our lab showed that when hexaketide analogues were attached to the phosphopantetheine mimic SNAC, they were insoluble in the aqueous media necessary for CON domain solubility. For this reason, the more water soluble Ppant was synthesized via a modified literature procedure[135] with the cooperation of Dr. Jennifer Chaytor of our group.

The eastern half of phosphopantetheine was synthesized starting from commercially available (*R*)-(-)-pantolactone (**37**). Pantolactone is first benzylated to afford **38** followed by reduction to lactol **39** using DIBAL-H. The resulting aldehyde, which is the tautomeric form of **39**, is converted to olefin **40** using Wittig conditions. Compound **40** is then phosphorylated, followed by ozonolysis of the double bond to yield

aldehyde **41**, which is then oxidized under Pinnick type oxidation conditions to furnish acid **42**.

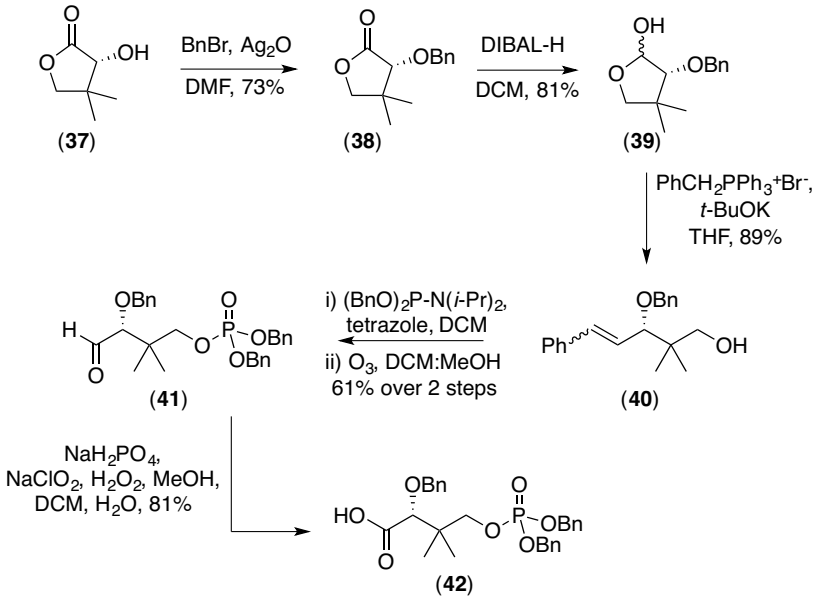

Scheme 4-2. Synthesis of the eastern half of phosphopantetheine.

Synthesis of the western half of phosphopantetheine begins with trityl protection of commercially available cysteamine (**43**), using trityl chloride and trifluoroacetic acid (TFA). Subsequent coupling to Fmoc-β-Ala affords compound **45**, with subsequent removal of the Fmoc protecting group using diethylamine to give free amine **46**. Amine **46** is then coupled to acid **42** to furnish protected phosphopantetheine **47**. Finally, global benzyl deprotection with lithium and naphthalene affords phosphopantetheine (**48**) in excellent yield.

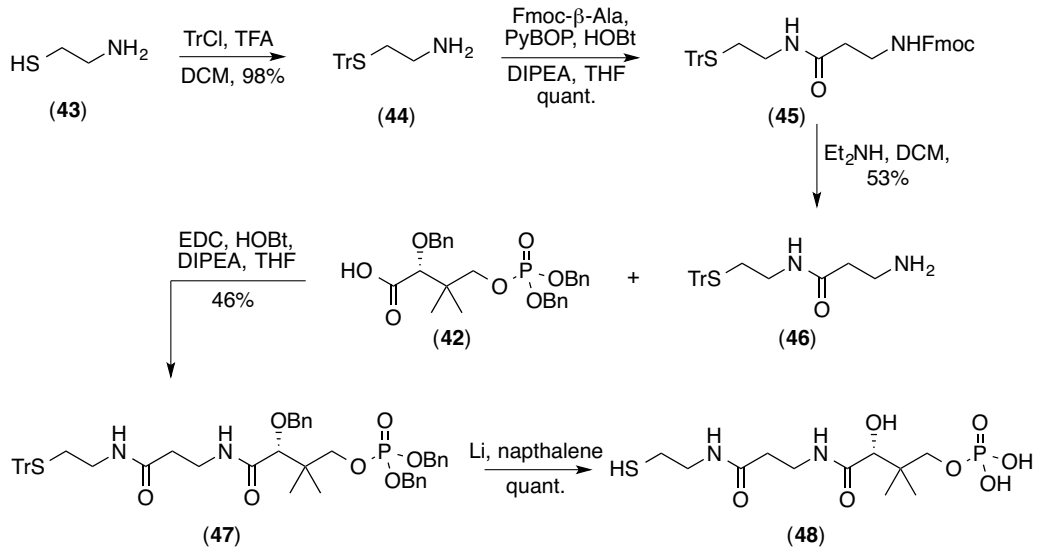

Scheme 4-3. Synthesis of the western portion of phosphopantetheine.

During the initial stages of phosphopantetheine synthesis by Dr. Jennifer Chaytor, several of the steps were quite low yielding. Slight modifications were made to nearly every step of the synthesis in order to improve the efficiency in our hands. Noteworthy changes included substitution of 5-ethylthio-(1H)-tetrazole for tetrazole in the preparation of **41**, and the addition of hydrogen peroxide in the preparation of **42** which increased the yield by approximately 20%. Furthermore, replacement of EDC with PyBOP as the coupling reagent nearly doubled the yield of **45**, and substituting diethylamine for piperidine greatly improved the purity of **46**. Of vital importance was the use of ammonium chloride during the workup of the final Ppant deprotection, which was completely unsuccessful until this was added.

4.3.2 Hexaketide analogues

With Ppant now available, we turned our attention to synthesis of linear hexaketide analogues. Starting from ethyl 6-bromohexanoate (**49**), a DIBAL-H reduction affords aldehyde **50** in 65% yield. The aldehyde is immediately protected as the ethylene acetal using ethylene glycol and alumina as an activator. Compound **51** is converted to the Grignard reagent **52** and used directly in the next step with *trans*-2-hexenyl acetate to afford compound **53**. The acetal is then deprotected using acetic acid and oxidized under Pinnick conditions to furnish acid **55**. The acid is then activated as the *p*-nitrothiophenol thioester under standard coupling conditions, and the activated thioester then coupled to Ppant under reducing, basic conditions to afford compound **57** after HPLC purification.

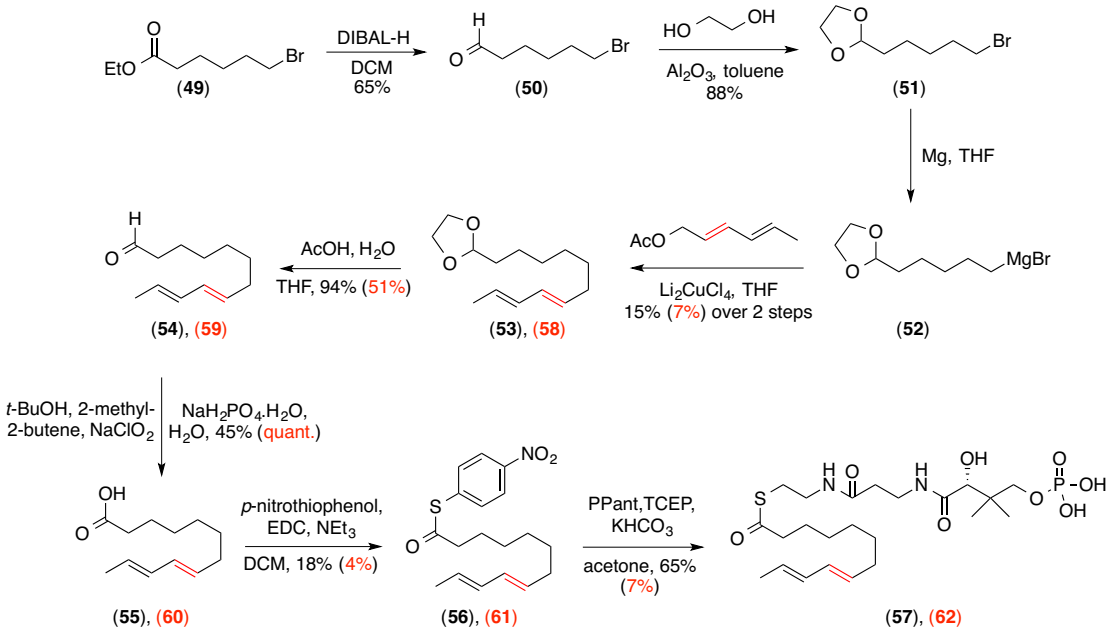

Scheme 4-4. Synthesis of single double bond hexaketide and two double bond hexaketide (red bond is only present in diene).

Several synthetic steps *en route* to **57** proved problematic. For example, the copper-catalysed substitution of the allylic acetate was extremely low yielding. Attempts were made to increase the yield by addition of well known Grignard activators such as iodine and ethylene bromide. Reaction temperature, time, and concentration were also varied. However, the maximum yield observed was a modest 15%, with the Wurtz coupling product as the main side product. Dr. Jennifer Chaytor had previously conducted extensive investigations into the best thioester activator for the penultimate synthetic step. Although activation of the acid went mostly to completion using the designated *p*-nitrothiophenol activating group, the reactions were conducted on relatively low scale (10-30 mg) with subsequent purification by preparatory TLC, resulting in low yield. Further to this, the resulting thioester was extremely acid labile, and would readily decompose during workup and purification, resulting in a maximum 18% yield.

Despite these set backs, the hexaketide analogue **62**, which contains two double bonds, was also synthesized using the same methodology, and both hexaketide-phosphopantetheine-coupled analogues were sent to our collaborators for co-crystallization with LovB condensation domain. Further to this, a hexaketide analogue with no double bonds was also synthesized using the same methodology, but starting from commercially available lauroyl chloride (**63**).

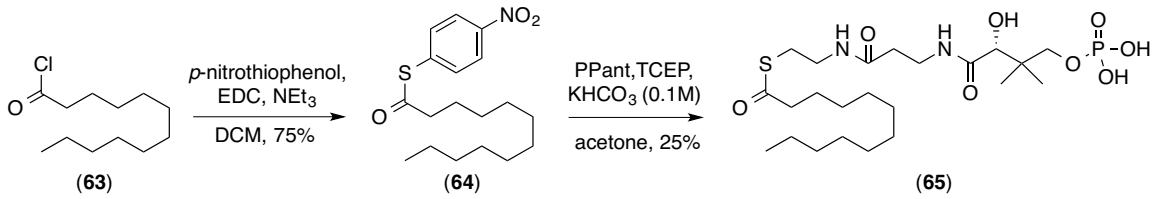

Scheme 4-5. Synthetic route to Ppant-coupled hexaketide analogue with no double bonds.

4.3.3 Synthesis of labeled intermediates

Although the biosynthesis of lovastatin is relatively well understood, incorporation of advanced intermediates would unequivocally confirm each biosynthetic step. To this end, Mr. Drew Hawranik synthesized a ^{13}C labeled triketide intermediate. This triketide was sent to our collaborators, who showed that the ^{13}C label could be located in the correct position of isolated DML, confirming that the triketide was recognized and incorporated by LovB.

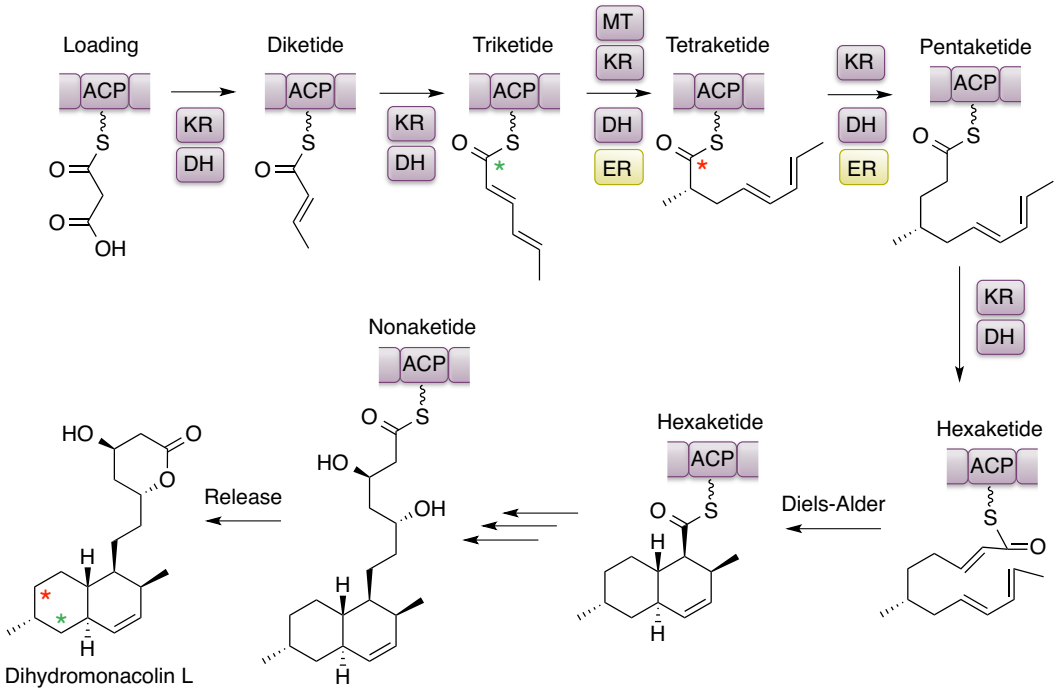

Scheme 4-6. Incorporation of ^{13}C labelled intermediates to DML by LovB. Green asterisk indicates location of ^{13}C label from triketide and red asterisk indicates location of tetraketide ^{13}C label.

Further to this, labeled tetraketide was then synthesized. Starting from ^{13}C labeled sodium propionate (**66**), a chlorination reaction with PCl_5, furnished labeled propionyl chloride (**67**) after reduced pressure distillation. The acyl chloride was then coupled to (*R*)-4-benzyl-1,3-oxazolidin-2-one in relatively low yields. Bromide **71** is prepared by bromination of *trans*,*trans*-2,4-hexadien-1-ol using phosphorus tribromide and used immediately for alkylation of compound **69** using sodium hexamethyldisilazide and the phase transfer catalyst, tetrabutylammonium iodide. Oxidative cleavage of Evans auxiliary from **72**, forms the corresponding acid, which is then directly coupled to SNAC under standard coupling conditions, to afford **73** in good yields.

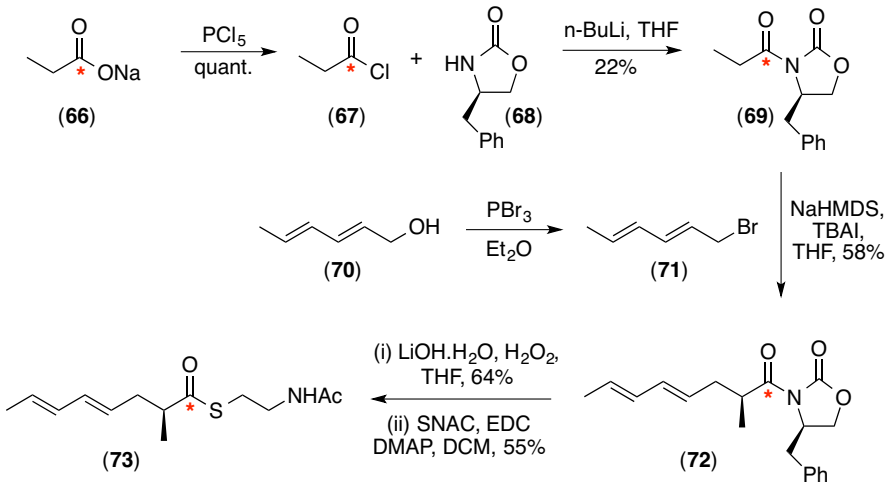

Scheme 4-7. Synthesis of labelled tetraketide intermediate.

This compound was then sent to our collaborators at UCLA for feeding experiments with LovB. Ms. Amy Norquay and Ms. Eva Rodriguez-Lopez have synthesized several other isotopically labeled biosynthetic intermediates *en route* to lovastatin.

4.4 Conclusions and outlook

Phosphopantetheine was first synthesized by a modified literature procedure, in collaboration with Dr. Jennifer Chaytor. Three linear hexaketide analogues were then prepared, and coupled to phosphopantetheine, with hopes of improving aqueous solubility compared the previously prepared SNAC thioesters. The resulting compounds have been sent to our collaborator Dr. Sheryl Tsai for co-crystallization experiments with

the condensation domain of LovB. Once we have crystals in hand, we will be closer to understanding the role of the CON domain in formation of DML.

Additionally, a labeled tetraketide advanced intermediate was also synthesized. This was shipped to our collaborators at UCLA, where feeding studies with LovB are being conducted. Incorporation of advanced intermediates will confirm their intermediacy in the biosynthetic pathway and further our understanding of lovastatin biosynthesis.

5 Cytochalasins

Cytochalasins comprise a diverse group of polyketide secondary metabolites that are produced by several fungal genera, including *Aspergillus*, *Phomopsis*, *Penicillium*, *Zygosporium*, *Rosellinia*, and *Chaetomium*.[136] This group of polyketides also displays a wide variety of interesting biological activities. For example, cytochalasin A, B, D and E, along with chaetoglobosin A are all potent inhibitors of cell proliferation.[9, 137-139] They act by preventing actin filament elongation, efficiently inhibiting cytokinesis, and thus creating giant cells with multiple or no nuclei. Furthermore cytochalasin A and B inhibit glucose transport in human erythrocytes membrane,[140] and cytochalasin D inhibits protein synthesis in HeLa cells.[141]

All members of this group of molecules contain a macrocyclic core fused to a perhydro-isoindolone moiety. This group is partially derived from an amino acid such as phenylalanine, tryptophan or leucine, figure 5-1. As such, cytochalasins are biosynthesized by HR PKS-NRPS hybrid enzymes, where the NRPS portion of the enzyme adds the amino acid to the polyketide product of the PKS system.

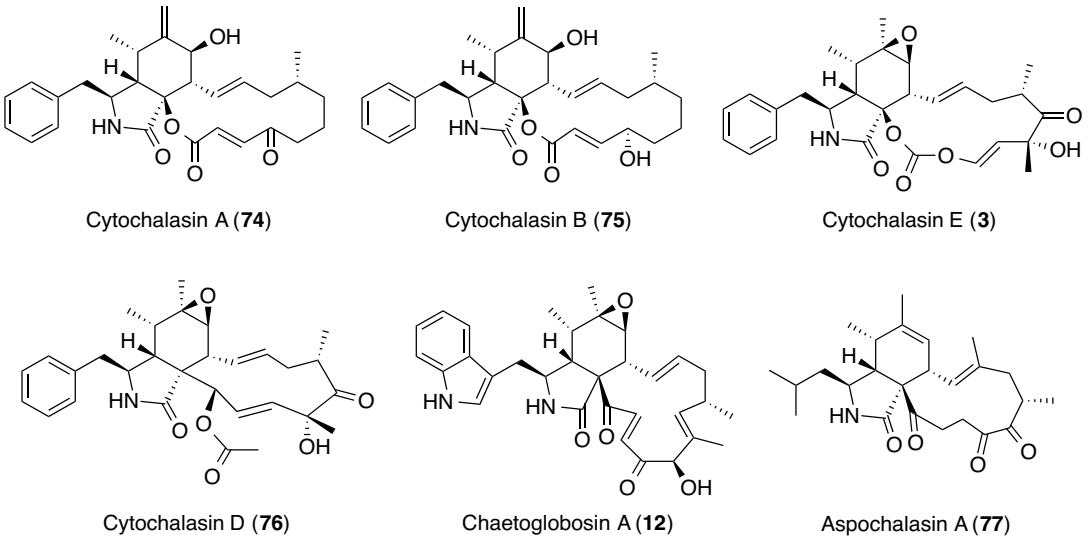

Figure 5-1. Select examples of cytochalasins.

Over a period of several years in the early 1970's, Tamm and co-workers were able to elucidate the origin of all constituent atoms in cytochalasin B (**75**).[142-144] Through a series of elegant incorporation experiments, Tamm and co-workers mapped incorporation of [2-^{13}C] labeled acetate units, and universally ^{14}C-labeled phenylalanine, along with methyl groups from [^{14}C-Me]-*S*-adenosylmethionine, into the structure of **75**. Moreover, the source of oxygen atoms in these molecules has also been identified.[145, 146] These mixed malonate-amino acid origins were the first evidence of a PKS-NRPS involvement in the biosynthesis of cytochalasins, and thus provided a framework for future investigations.

5.1 Chaetoglobosin A

To investigate the biogenesis of chaetoglobosin A (**12**) in *Penicillium expansum*, Hertweck and co-workers generated a cosmid library of genomic DNA and screened this library using a degenerate PCR primers and a dot blot hybridization approach.[147] Sequencing of the appropriate cosmids identified the chaetoglobosin gene cluster that contained a PKS-NRPS (CheA), enoyl reductase (CheB) and three putative oxygenases, CheD, CheE, and CheG. Chaetoglobosin biosynthesis is likely regulated by the two putative transcription factors contained within the cluster, CheC and CheF. The authors then used RNA silencing of CheA to significantly decrease the titer of **12**, thereby confirming correlation of CheA to chaetoglobosin biosynthesis. This also allowed for a plausible biosynthesis to be established.

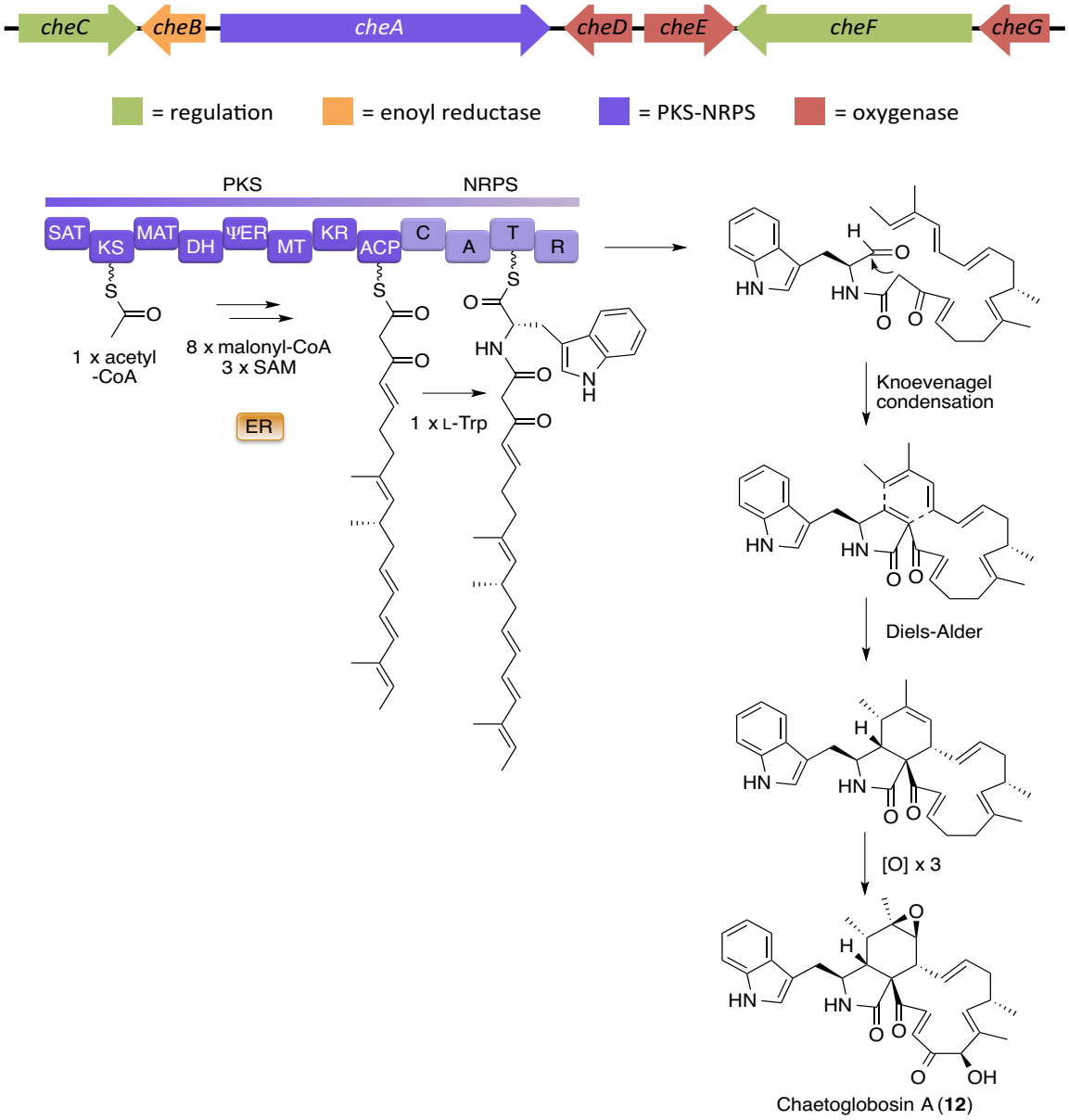

Figure 5-2. Biosynthetic gene cluster and putative biosynthesis of chaetoglobosin A in *Penicillium expansum*.

Chaetoglobosin A is proposed to be derived from a nonaketide chain synthesized by the HR PKS-NRPS CheA in conjunction with the ER CheB, followed by addition of an activated L-tryptophan residue by the NRPS portion of CheA. The reductase domain

would then catalyse reductive offloading using NADPH, and the subsequent aminoaldehyde would undergo a Knoevenagel condensation. This disubstituted 1,5-dihydropyrrol-2-one is perfectly set up to undergo a [4+2] cycloaddition, similar to the previously mentioned biosynthesis of lovastatin. However, in this case cyclization affords the macrocycle, which following three rounds of oxidation, gives **12**.

Confirmation of the latter post-PKS modifications was later reported by Watanabe and co-workers, wherein they deconvoluted the complicated oxidation mechanisms in *Chaetomium globosum*.[148] Through a series of gene deletion studies, heterologous enzyme expression and advanced intermediate feeding studies, the authors were able to establish a complex series of combinatorial oxidation steps catalysed by the three redox enzymes encoded in the chaetoglobosin gene cluster. This ultimately results in production of **12** from **78**, via four intermediate compounds, figure 5-3.

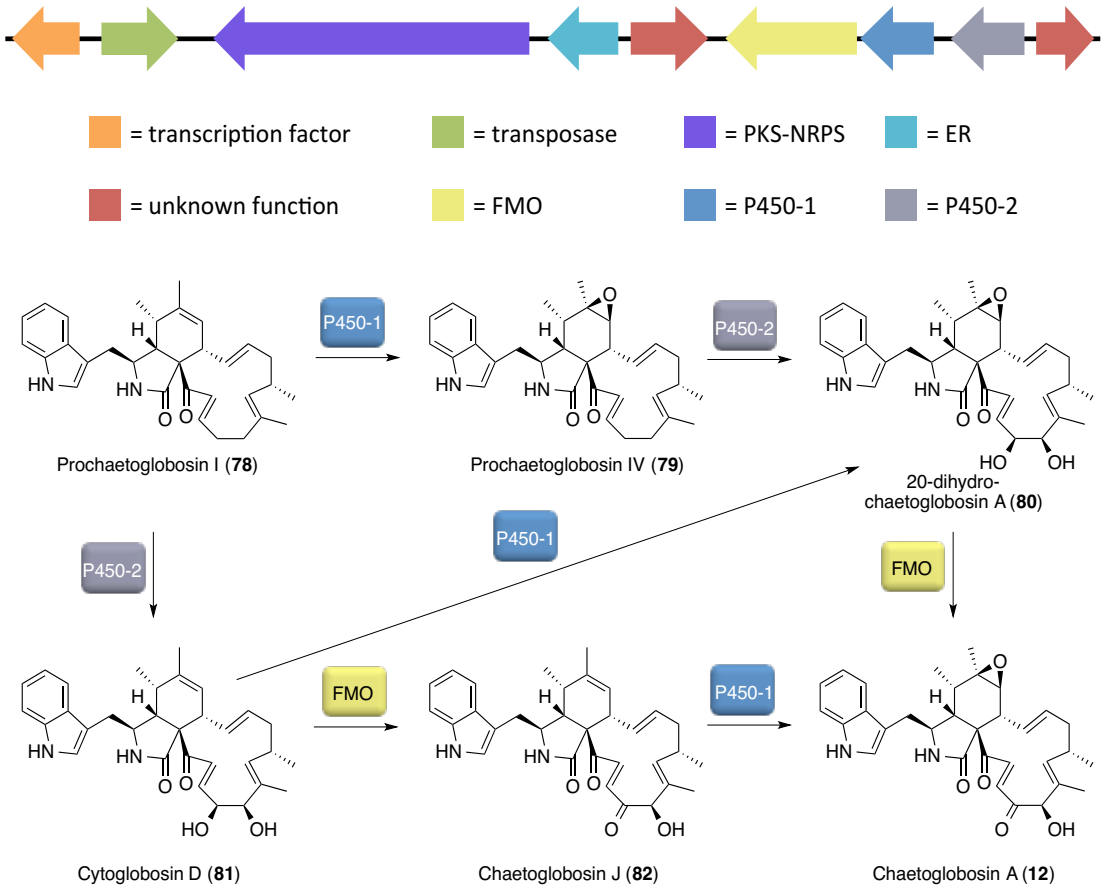

Figure 5-3. Chaetoglobosin A gene cluster in *Chaetomium globosum* and transformation of prochaetoglobosin I to chaetoglobosin A by oxidases encoded therein.

Even though this work and the contributions of many others represents a significant leap in our understanding of the systems that produce PKS-NRPS metabolites, the exact mechanisms by which the mature polyketide-amino acid backbone is formed are still unverified. With the goal of deconvoluting the intermediates involved in this process, we embarked on synthesis of the proposed PKS off loaded product. Recognition and incorporation of this advanced intermediate by the PKS-NRPS, would provide compelling evidence to suggest that it is a true intermediate in the biosynthetic pathway.

Moreover, this intermediate could be used to probe the proposed Knoevenagel condensation and Diels-Alder cycloaddition reactions.

5.1.1 Results and discussion

Because of the sizeable nature of the chaetoglobosin A nonaketide intermediate, the molecule was split into three parts, scheme 5-1. Fragment A and C were synthesized by Dr. Zhizeng Gao and Mr. Justin Thuss, as shown in scheme 5-1.

The middle portion of **83**, fragment B, is synthesized first by acylation of (*R*)-4-benzyl-1,3-oxazolidin-2-one with propionyl chloride followed by alkylation with allyl bromide using sodium hexamethyldisilazide to afford compound **95**. The alkene is subjected to ozonolysis and reductive workup with triphenylphosphine to furnish the aldehyde **96**, which is immediately protected as the ethylene acetal **97** under acidic conditions. Reductive cleavage of Evans auxiliary with lithium borohydride then furnishes the alcohol **98** in good yields, figure 5-2.

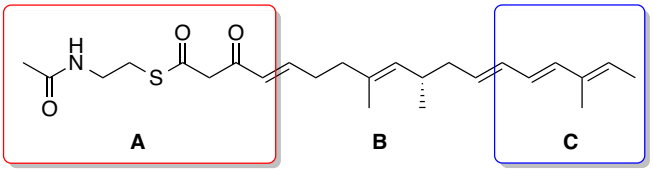

(**83**)

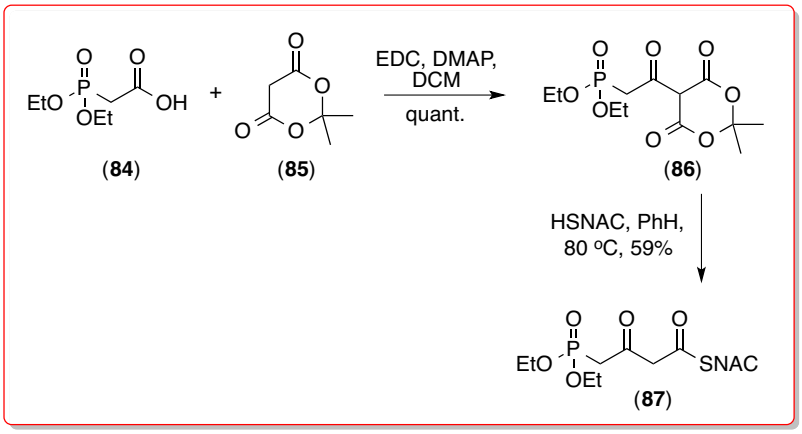

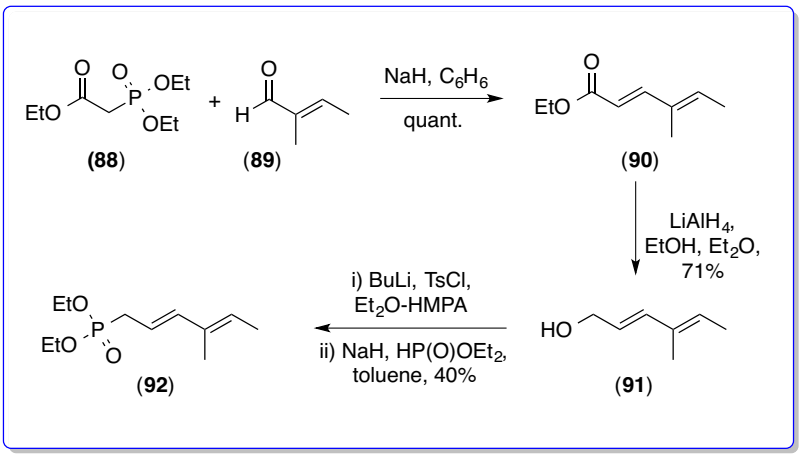

Scheme 5-1. Synthesis of fragments A and C of chaetoglobosin A nonaketide backbone.

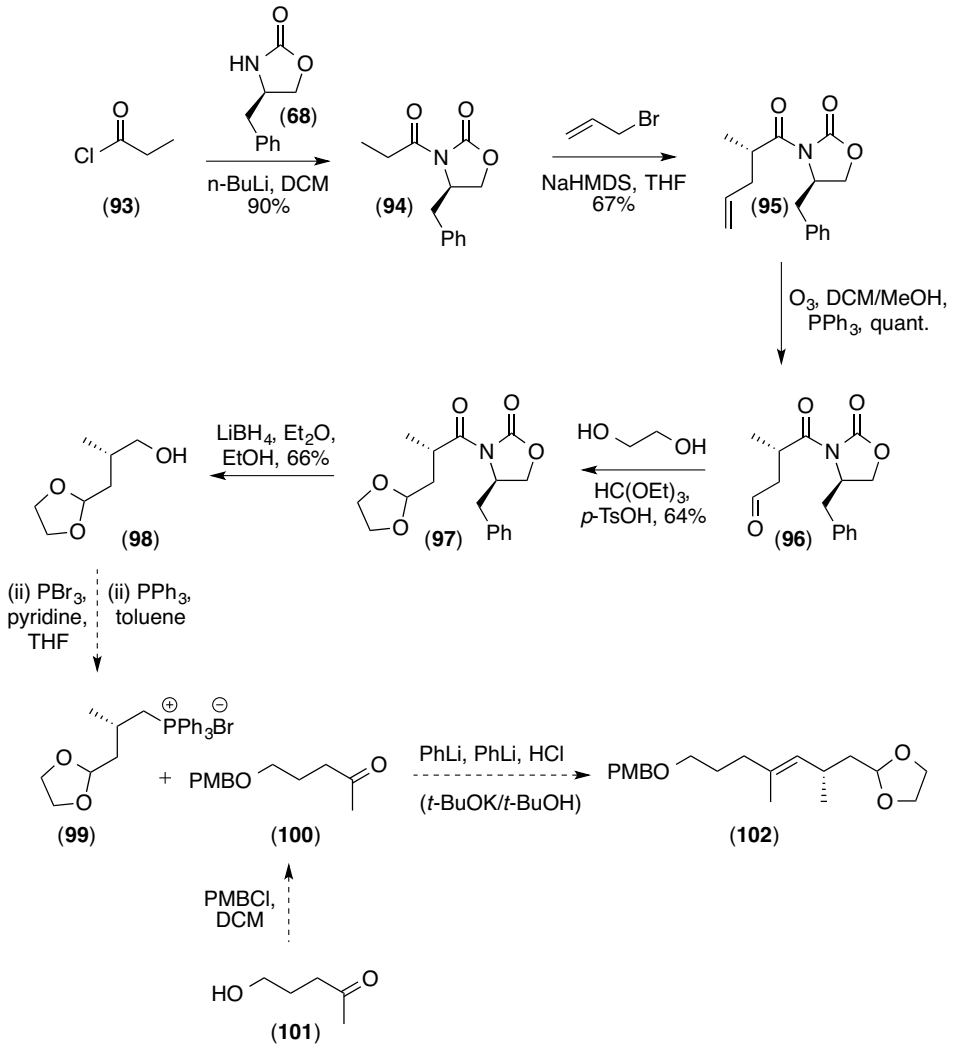

Scheme 5-2. Synthetic route to fragment B of chaetoglobosin A intermediate. Dashed arrows indicate proposed synthetic steps.

Compound **98** would then be converted to the Wittig reagent over two steps, which could then be coupled to the PMB protected ketone **100** via a Wittig-Schlosser reaction. The resulting compound **102** could then be coupled to fragment C by a Horner-Wadsworth-Emmons (HWE) reaction, subject to deprotection of the aldehyde moiety. The western portion of compound **102** would first undergo deprotection of the alcohol,

followed by oxidation to the aldehyde, which could then be coupled to fragment A via another HWE reaction. Due to time constraints, these final steps will be completed by Mr. Sean Larade.

5.2 Cytochalasin E

Cytochalasin E (**3**), is another member of the cytochalasin family which displays potent anti-angiogenic activity. Cytochalasin E contains an epoxide, which was shown to be necessary for bioactivity,[10] as well as a vinyl carbonate moiety that occurs in several cytochalasins (e.g. cytochalasin K, phenochalasin B, scoparasin A), but is otherwise rare in natural products. It is this structural complexity, as well as its potent bioactivity, that make it an interesting target for biochemical study.

Recently, Qiao *et al* published the gene cluster responsible for biosynthesis of **3** in *Aspergillus clavatus*, which was discovered through genome mining, and the identity confirmed through gene deletion and heterologous expression studies.[149] Based on the framework provided by earlier work on cytochalasins, the authors were able to propose a biosynthetic pathway to **3**. They proposed that the PKS-NRPS CcsA first synthesizes an octaketide in conjunction with its ER partner CcsC, followed by addition of an activated L-phenylalanine residue by the NRPS portion. The reductase domain would then catalyse reductive offloading, and the resulting aminoaldehyde would undergo a Knoevenagel condensation. Following a hypothesized [4+2] cycloaddition, five rounds of oxidation afford cytochalasin E.

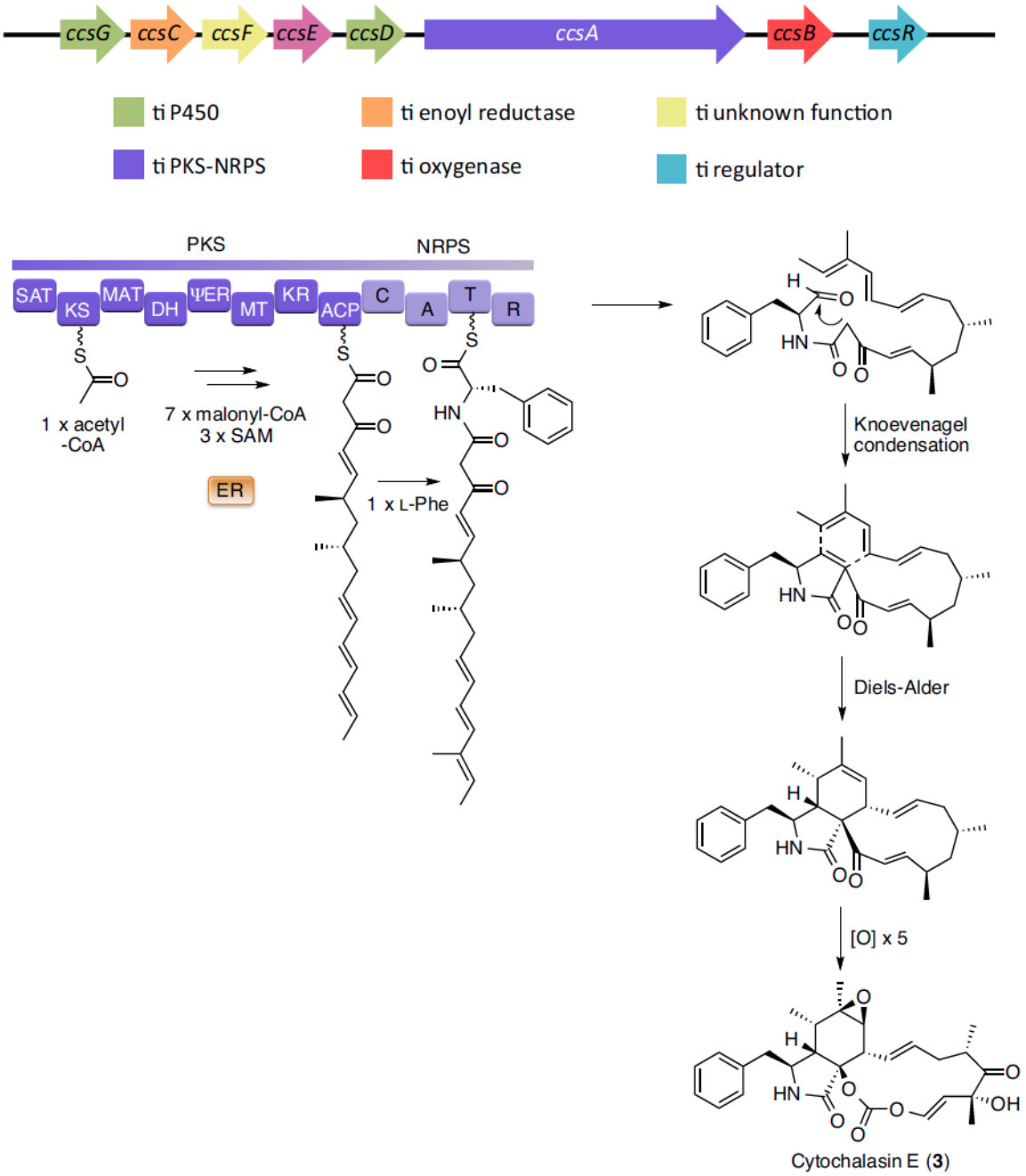

Figure 5-4. Biosynthetic gene cluster and putative biosynthesis of cytochalasin E in *Aspergillus clavatus* NRRL 1.

The authors propose that the P450 monooxygenase CcsG first catalyses two oxidations, with subsequent oxidation by another P450, CcsD. Following this, it is thought that a double Baeyer-Villiger oxidation of the ketone macrocyclic precursor installs the carbonate moiety, catalysed by the Baeyer-Villiger monooxygenase (BVMO), CcsB. It is still unknown in which order these specific oxygenases act, but the most up to date hypothesis is shown in scheme 5-3.

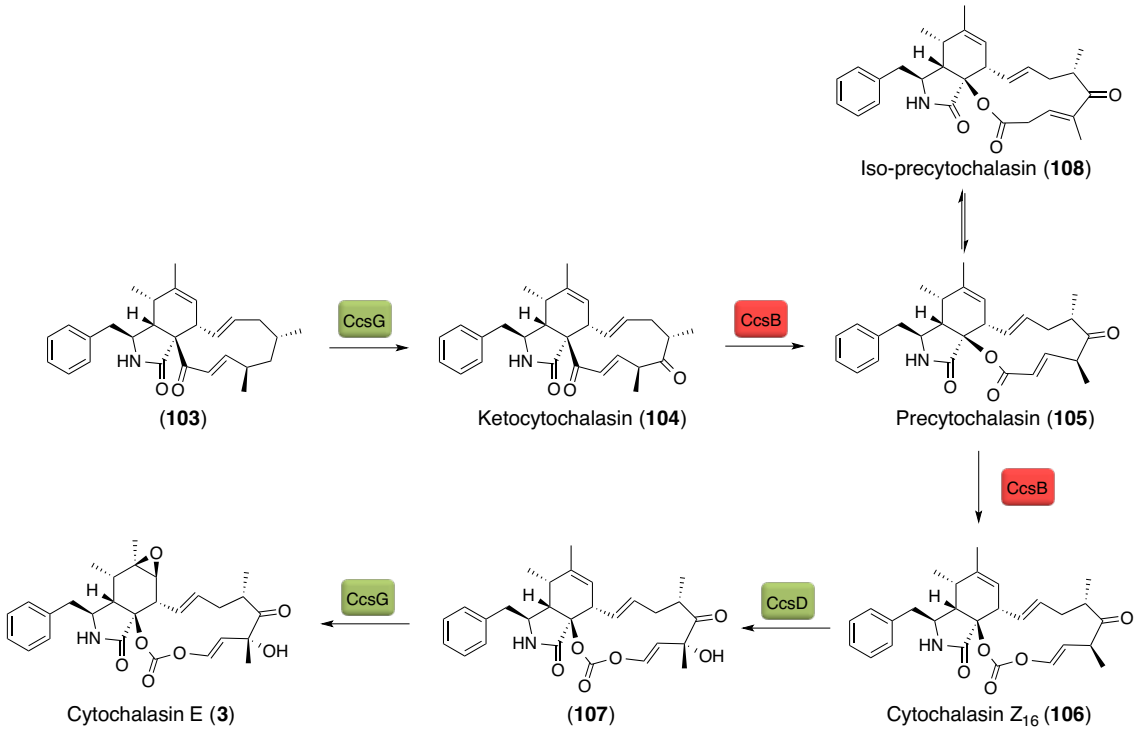

Scheme 5-3. Hypothetical oxidation steps by the cytochrome P450s CcsG and CcsD and by the BVMO CcsB *en route* to cytochalasin E.

To investigate the unusual double Baeyer-Villiger oxidation further, our group, in collaboration with the group of Yi Tang, showed that a partly oxidized macrocyclic ketone **104** could be transformed to a corresponding lactone **105** with double bond shift

(a shunt product, **108**) as well as to the allylic carbonate **106**, figure 5-4.[150] CcsB must reload with oxygen prior to the second oxidation because the singly bonded carbonate oxygens come from different molecules of O_2 (unpublished). As non-enzymatic Baeyer-Villiger oxidations of esters to carbonates is unprecedented, we believe the introduction of the second oxygen requires the particular unsaturated bis carbonyl system, and may proceed via α,β-epoxidation with subsequent rearrangement as indicated in scheme 5-4.

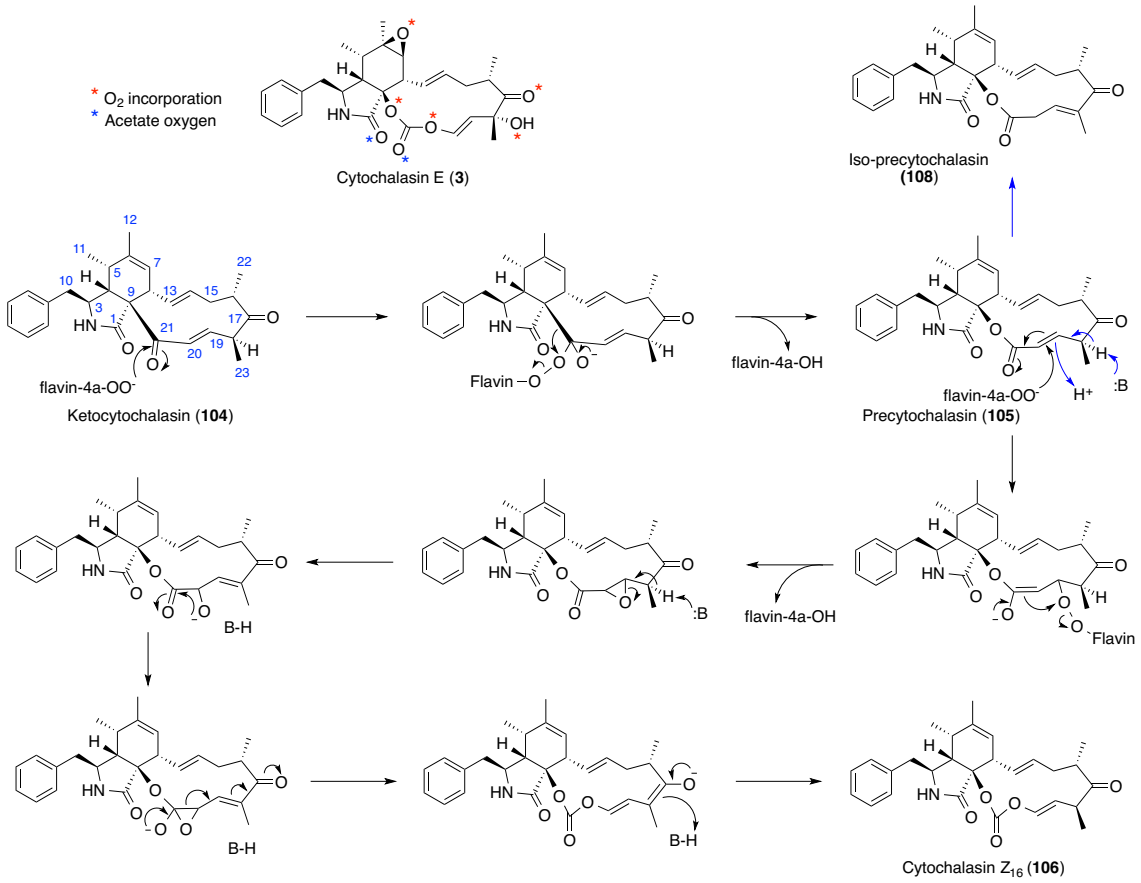

Scheme 5-4. Transformation of a macrocyclic ketone intermediate (104) into a lactone (105) and the corresponding carbonate (106) by CcsB, a flavin monooygenase, during formation of cytochalasin E.

As with chaetoglobosin A, the exact mechanism by which the PKS-NRPS enzyme forms the mature octaketide backbone of cytochalasin E is still unknown. Synthesis of the octaketide chain of **3** and incorporation by the PKS-NRPS, would allow us to determine if it is a true biosynthetic intermediate and could be further used to probe the post-PKS-NRPS reactions.

5.2.1 Results and discussion

Fragments A and C are common to both chaetoglobosin A and cytochalasin E synthesis. Fragment B was synthesized following a similar route. Starting from common intermediate **95**, reductive cleavage of Evans auxiliary affords the free alcohol in excellent yields. Compound **110** is then activated as the triflate using triflic anhydride, which is reacted immediately with sodium hexamethyldisilazide and (*S*)-4-isopropyl-1,3-oxazolidin-2-one to afford **113** in good yields. After reductive cleavage with lithium borohydride, the subsequent alcohol **114** is protected using TBDMS-Cl and imidazole to afford compound **115**. Ozonolysis of the double bond would then afford the aldehyde, which could be coupled to fragment C by a Horner-Wadsworth-Emmons (HWE) reaction. In a similar fashion to chaetoglobosin A, compound **116** would first undergo deprotection of the alcohol, followed by oxidation to the aldehyde that could then be coupled to fragment A via another HWE reaction. This synthesis will be completed by Mr. Sean Larade.

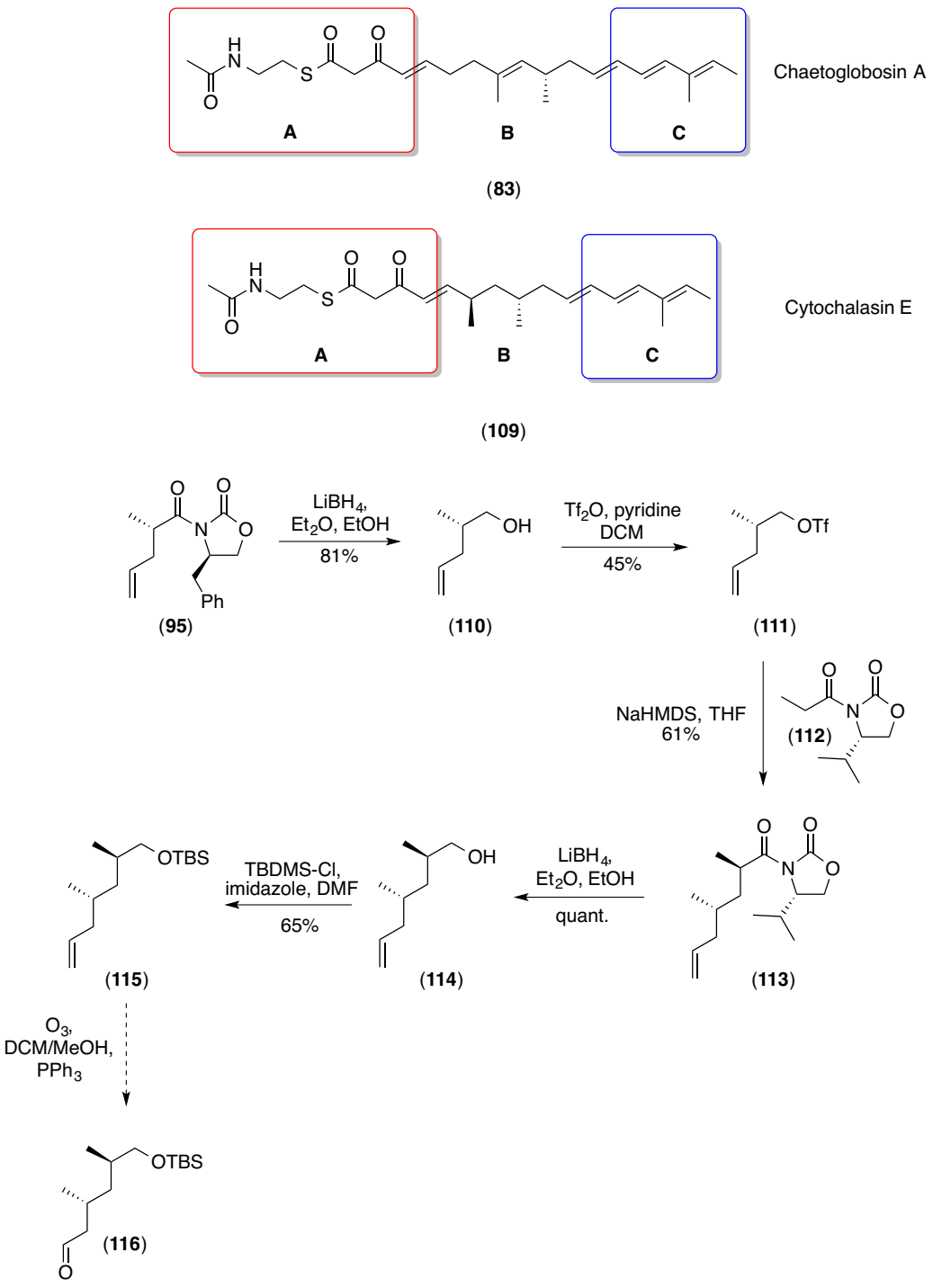

Scheme 5-5. Synthetic route to fragment B of cytochalasin E intermediate, where dashed arrows indicate proposed synthetic steps.

5.3 Conclusions and outlook

Discovery of the chaetoglobosin A gene cluster in *Penicillium expansum*, allowed for a plausible biosynthetic route to be proposed. Subsequently, the highly combinatorial approach to oxidations *en route* to chaetoglobosin A in *Chaetomium globosum* was elaborated. We sought to investigate the PKS-NRPS function in greater detail by first synthesizing the proposed PKS product. To this end, compound **98** was synthesized over 5 steps, which will be elaborated further and coupled to fragments A and C by another graduate student, Mr. Sean Larade. The compound will then be sent to UCLA for feeding studies with CheA.

Previous work in our group and in collaboration with the Tang group at UCLA, allowed for investigation of the oxidation pattern (post-PKS-NRPS) in cytochalasin E biosynthesis. This allowed a plausible series of oxidation reactions to be proposed, along with a mechanism by which the Baeyer-Villiger monooxygenase acts. Further to this, we aimed to synthesize the PKS product of CcsA, the PKS-NRPS responsible for cytochalasin E biosynthesis in *Aspergillus clavatus*. Compound **115** *en route* to fragment B was synthesized in 5 steps. This molecule can then be further elaborated and coupled to fragments A and C. It will then be sent to our collaborators for feeding studies with CcsA.

Further directions for both chaetoglobosin A and cytochalasin E includes investigation of Diels-Alderase activity by enzymes contained within the gene cluster. This could potentially be achieved by co-crystallization studies of the enzymes with

substrate analogues. Also, synthesis of advanced labeled intermediates could be used to probe oxidation mechanisms in the pathways.

6 Experimental

6.1 General information

Root-mean-square deviation (RMSD) relative to the top structural homologue and C-scores (based on the significance of threading template alignments and the convergence parameters of the structure assembly simulations) values were used to assess reliability of homology models generated by I-TASSER. The I-TASSER software consistently gave reliable predictions, with C-scores ranging from -1, 1 (typical range is -5, 2 where a higher value denotes a model with a higher confidence).

Polymerase chain reactions (PCR) were performed on an Eppendorf Mastercycler Nexus Gradient. Yeast cell cultures were pelleted on a Beckman Coulter Avanti J-26XPI High-Performance Centrifuge, using a J-Lite® JLA-9.1000 Fixed Angle Rotor. Protein samples were agitated at 4 °C on a Thermolyne BIGBill Orbital Shaker (Catalog no. M49125) at 50 rpm.

6.2 General synthetic procedures

Reactions involving either air or moisture sensitive reactants were conducted under a stream of dry argon. All solvents and chemicals were reagent grade and used as

supplied from Sigma-Aldrich unless otherwise stated. Anhydrous solvents required were dried according to the procedures outlined in Perrin and Armarego.[151] Removal of solvent was performed under reduced pressure, below 40 °C, using a Büchi rotary evaporator. All reactions and fractions from column chromatography were monitored by thin layer chromatography (TLC). Analytical TLC was done on glass plates (5 × 1.5 cm) pre-coated (0.25 mm) with silica gel (normal SiO_2, Merck 60 F254). Compounds were visualized by exposure to UV light and/ by dipping the plates in $KMnO_4$ solution, followed by heating. Flash chromatography was performed on silica gel (EM Science, 60Å, 230-400 mesh). HPLC grade acetonitrile (ACN) was purchased from Caledon Labs (Georgetown, ON, Canada). Cladosporin was purified on a Gilson preparative high-performance liquid chromatography (HPLC) system equipped with a model 322 HPLC pump, GX-271 liquid handler, 156 UV-vis detector and a 10 mL sample loop.

6.3 Spectroscopic analyses

Nuclear magnetic resonance (NMR) spectra were obtained on Agilent VNMRS 700 MHz and Varian NVMRS 500 MHz, Varian Inova 400 MHz and Varian Inova 300 MHz spectrometers. ^{1}H NMR chemical shifts are reported in parts per million (ppm) using the residual proton resonance of solvents as reference: $CDCl_3$ δ 7.26 and D_2O δ 4.79. ^{13}C NMR chemical shifts are reported relative to $CDCl_3$ δ 77.16. Infrared spectra (IR) were recorded on a Nicolet Magna 750 or a 20SX FT-IR spectrometer. Cast Film refers to the evaporation of a solution on a NaCl plate. Mass spectra were recorded on a

Kratos IMS-50 (high resolution, electron impact ionization (EI)), and a ZabSpec IsoMass VG (high resolution electrospray (ES)). LC-MS analysis was performed on an Agilent Technologies 6220 orthogonal acceleration TOF instrument equipped with +ve and –ve ion ESI ionization, and full-scan MS (high-resolution analysis) with two-point lock mass correction operating mode. The instrument inlet was an Agilent Technologies 1200 SL HPLC system.

6.4 Genome mining

6.4.1 Fosmid library production

After inoculation of a 1 L culture of potato dextrose liquid media with a spore suspension of *C. cladosporioides* UAMH 5063, followed by seven days growth at 250 rpm and 28 °C, the mycelia were collected by filtration through cheesecloth, flash frozen with liquid nitrogen, and ground in a mortar and pestle. DNA from the resulting powder was then extracted using the DNeasy Plant Mini Kit from Qiagen. The DNA was end-repaired to blunt 5'-phosphorylated ends using the end-repair enzyme mix contained within the CopyControl™ kit, followed by purification by pulsed field gel electrophoresis (PFGE) with low melting point agarose. DNA fragments of roughly 40 kb were isolated from the gel using the GELase enzyme preparation. The blunt-ended DNA fragments were ligated into the pCC1FOS vector (figure 2-2), packaged using MaxPlax lambda

packaging extracts, and then used to infect EPI300-T1R *E. coli* cells. The infected cells were grown on LB + chloramphenicol plates overnight at 37 °C.

6.4.2 Dot blot hybridization

Colony lifts followed by hybridization with a heterologous probe were then conducted in order to screen for the presence of PKS-encoding DNA in the clones. First, presterilized circles of Amersham Hybond-XL charged nylon membrane were placed over the plates. After several washing steps, the DNA was cross-linked to the membrane in a Spectrolinker on "optimal cross-linker" setting. Previously, a KS probe containing DNA from PKS13, the NR PKS responsible for biosynthesis of zearalenone in *Gibberella zeae*, had been prepared by PCR amplification with complimentary primers (table 6-1). The probe had been labeled with alkaline phosphatase using the AlkPhos Direct Labelling and Detection System. This labeled probe was then added to the membranes, and incubated with hybridization buffer overnight in a rotisserie incubator at 55 °C. After incubation, the colony lifts were washed to remove any residual KS probe, and detection reagent pipetted over. The membranes were then imaged to check for chemiluminescense, which would indicate the presence of complimentary DNA. Any clones of interest were then cultured from the original plate, in LB + chloramphenicol with autoinduction solution added to induce to high-copy. The DNA was isolated and used in another round of dot

blot hybridization and the "positive hits" were then sequenced by primer walking to confirm the presence of PKS DNA.

Gene name	Primer name	Primer sequence
KS	PKS13-FS3	5'- TTG ATC ACG AGA GAT ATA GAT ATG GC - 3'
	PKS13-RS13	5'- ACA CAC TGG AGA CCG CTC C –3'
AT	PKS13-1F	5'- CCT ACT CTT GGA GCG ATG CGA ATC C -3'
	PKS13-RS10	5'- CTT GGC GTG TCT GCT GAA CC -3'

Table 6-1. Names and sequences of PCR primers used to amplify corresponding probes.

6.5 Genomic DNA extraction and sequencing

Genomic DNA (gDNA) was first isolated from a 7-day culture of *Cladosporium cladosporioides* UAMH 5063 or *Alternaria cinerariae* ATCC 11784. The mycelia were flash frozen in liquid nitrogen and ground in a mortar and pestle. gDNA was then extracted with the DNeasy Plant Mini Kit (Catalog no. 69104, Qiagen) and sent to Ambry Genetics for sequencing using Illumina HiSeq 2000 technology.

6.5.1 Sample preparation

DNA was fragmented and the ends repaired and phosphorylated using Klenow, T4 DNA polymerase and T4 polynucleotide kinase. An 'A' base was then added to the 3' end of the blunted fragments, followed by ligation of Illumina adapters via T-A mediated ligation. The ligated products were size selected by gel purification and PCR amplified using Illumina paired-end primers. The library size and concentration were determined using an Agilent Bioanalyzer.

6.5.2 HiSeq 2000 run conditions

The libraries were seeded onto the flowcell at 9 pM per lane yielding approximately 759 K pass-filter clusters per mm^2 tile area. The libraries were sequenced using 101+7+101 cycles of chemistry and imaging.

6.5.3 HiSeq pipeline analysis

Initial data processing and base calling, including extraction of cluster intensities was done using RTA 1.13.48 (HiSeq Control Software 1.5.15). Sequence quality filtering script was executed in the Illumina CASAVA software (v 1.8.2, Illumina, Hayward, CA).

Number of Reads	186235888
Average Read Length (bp)	100.0
Contig N50 (bp)	305326
Contig Minimum Length (bp)	200
Contig Maximum Length (bp)	1154434

Contig Average Length (bp)	39655
Contig count	764

Table 6-2. Cladosporin sequencing statistics.

Number of Reads	222566064
Average Read Length (bp)	100.0
Contig N50 (bp)	349121
Contig Minimum Length (bp)	200
Contig Maximum Length (bp)	1265344
Contig Average Length (bp)	35661
Contig count	907

Table 6-3. DHC sequencing statistics.

Bioinformatic analysis was conducted using CLC Genomics Workbench, version 5.5.

6.6 Media recipes

Yeast Nitrogen Base (YNB) stock - 6.7 g yeast nitrogen base without amino acids (Catalog no. 291940, BD Biosciences) dissolved in 100 mL Milli-Q water, filtered through a Millex-GV Syringe Filter Unit, 0.22μ, PVDF, 33 mm (Catalog no. SLGV033RS, Millex).

Adenine stock - 40 mg adenine hemisulfate salt (Catalog no. BP395-100, Fisher) dissolved in 20 mL Milli-Q water, filtered through a Millex-GV Syringe Filter Unit, 0.22μ, PVDF, 33 mm (Catalog no. SLGV033RS, Millex).

Tryptophan stock - 40 mg tryptophan (Catalog no. A9126, Sigma) dissolved in 20 mL Milli-Q water, filtered through a Millex-GV Syringe Filter Unit, 0.22μ, PVDF, 33 mm (Catalog no. SLGV033RS, Millex).

Uracil stock - 40 mg uracil (Catalog no. U0750, Sigma) dissolved in 20 mL Milli-Q water, filtered through a Millex-GV Syringe Filter Unit, 0.22μ, PVDF, 33 mm (Catalog no. SLGV033RS, Millex).

SDCt media

0.5 g Bacto Technical Grade Casamino Acids (Catalog no. 223120, BD Biosciences), 2 g dextrose, and 88 mL Milli-Q water (89 mL for SDCt (A)), autoclaved and then supplemented with 10 mL YNB stock, 1 mL adenine stock for SDCt (A), plus 1 mL tryptophan stock for SDCt (A, T) or 1 mL uracil stock for SDCt (A, U). For agar plates, 2 g agar (Catalog no. 214010, BD Biosciences) added before autoclaving.

Yeast Peptone Dextrose (YPD) media

10 g Bacto Yeast extract, 20 g Bacto Peptone and 950 mL Milli-Q water, autoclaved and then supplemented with dextrose to final concentration 1%.

6.7 Molecular cloning of Cla2 and Cla3

Cla2 and Cla3 were cloned into two 2μ-based yeast-*E. coli* shuttle vectors, pKOS518-120A and pXK30. pKOS518-120A contains the *TRP1* auxotrophic marker and an *Nde*I and *Eco*RI restriction site. pXK30 contains a *URA3* auxotrophic marker and *Nde*I and *PmL*I restriction sites. Initially, total RNA was isolated from a 5-day culture of *Cladosporium cladosporioides* UAMH 5063 using the RNeasy Plant Mini Kit (Catalog no. 74903, Qiagen), and reverse transcribed into complementary DNA (cDNA) using AccuScript HighFidelity 1st Strand cDNA Synthesis Kit (Catalog no. 200820, Agilent). Primers (table 6-3) containing a 35 bp overlap with the ADH2 promoter and terminator sequences present in the vectors were ordered from Integrated DNA Technologies and used in PCR reactions (standard conditions for PfuUltra II Fusion HS DNA polymerase Catalog no. 600670, Agilent) to amplify Cla2 and Cla3 from the cDNA library. A 6 × His sequence was also included in primer design so as to introduce a His tag to the C-terminus of the protein for purification purposes. *Saccharomyces cerevisiae* BJ5464-NpgA competent cells were prepared using the *S. c*. EasyComp™ Transformation Kit (Catalog no. K5050-01 Invitrogen), and transformed with the gene and linearized plasmid, where they underwent transformation-associated recombination (TAR). After 48 h growth on selective plates (SDCt (A, T) or SDCt (A, U)), the plasmids were isolated

from the cells using Zymoprep™ Yeast Plasmid Miniprep II kit (Catalog no. D2004, Zymo research). The gene sequences were verified by primer walking and the plasmids harbouring either Cla2 or Cla3 were used for subsequent transformation reactions.

Primer name	Primer sequence
HRPKS-For-pKOS	5- AAT CAA CTA TCA ACT ATT AAC TAT ATC GTA ATA CCA TCA TAT GAC ATC TTC GGG AGA CTC -3
HRPKS-Rev-pKOS	5- GAA GGC ATG TTT AAA CCT AGG ATG CAT GTC GAC TAT GAA TTC CTA ATG ATG ATG ATG ATG ATG GTC TAA GGT AGC AGC AAG ATG -3
NRPKS-For-pXK30-Peni	5- ACA ATC AAC TAT CAA CTA TTA ACT ATA TCG TAA TAC CAT ATG CAC AAC GGA TCA GAA TCA G -3
NRPKS-Rev-pXK30	5- ATA ATG AAA ACT ATA AAT CGT GAA GGC ATC GGT CCG CAC GTG CTA ATG ATG ATG ATG ATG ATG AGC CTC GAT GAG CCT GAA G -3

Table 6-4. Names and sequences of PCR primers used to create genes for TAR.

6.8 Protein purification of Cla2 and Cla3

Plasmids containing either *cla2* or *cla3* genes were transformed separately into *Saccharomyces cerevisiae* strain BJ5464-NpgA. After 72 h growth on the appropriately selective plate, a single colony was used to inoculate a 3 mL selective seed culture, which was incubated at 28 °C and 250 rpm for 72 h. 1 mL of the seed culture was then used to

inoculate a 1 L culture of YPD media and grown at 28 °C and 250 rpm for 72 h. The cells were harvested by centrifugation (5000 g, 15 minutes, 4 °C), resuspended in 25 mL lysis buffer (50 mM NaH_2PO_4, pH = 8.0, 0.15 M NaCl, 10 mM imidazole) and the cells lysed by sonication (sonicate for 1 minute on ice, then let cool for 1 minute. Repeat 9 times). Cellular debris was removed by centrifugation (17000 g, 1 hour, 4 °C). Ni-NTA agarose resin (Catalog no. 30210, Qiagen) was added to the supernatant (typically 1 mL/L of culture) and the solution was agitated for at least 3 hours at 4 °C. The protein/resin slurry was loaded into a gravity flow column (Econo-Pac™ chromatography columns, Catalog no. 732-1010, BIO-RAD) and proteins were purified with increasing concentration of imidazole (10 mM – 250 mM) in Buffer A (50 mM Tris-HCl, pH = 7.9, 2 mM EDTA, 2 mM DTT). Purified proteins were concentrated (Vivaspin 20 100 kDa MWCO, Catalog no. 28-9323-63, GE Healthcare) and resuspended in Buffer A, then concentrated and flash frozen as 20% glycerol stocks.

6.9 Isolation of cladosporin or DHC from double transformations

Plasmids containing either *cla2* or *cla3* were co-transformed into *Saccharomyces cerevisiae* strain BJ5464-NpgA, as were plasmids containing either *Dhc3* or *Dhc5*. After 72 h growth on a selective (SDCt (A)) plate, a single colony was used to inoculate a 3 mL selective seed culture, which was incubated at 28 °C and 250 rpm for 72 h. 1 mL of the seed culture was then used to inoculate a 1 L culture of YPD media and grown at 28 °C

and 250 rpm for 72 h. 2.5 mL of cyclopentanone was added after 24 h and again after 48 h to induce protein expression. Also, 25 mL of 20% NaOAc was added after 24 h and again after 48 h, to increase metabolite production. The cultures were extracted with 2 x 500 mL ethyl acetate, dried and concentrated *in vacuo*. The crude extract was dissolved in 1 mL of 1:1 ACN:H_2O and injected onto a Luna 5µ C18(2) 100Å, AXIA, 250 x 21.2 mm reverse phase column, with detection at 214 nm. Mobile phase composition was as follows: samples were separated on a linear gradient of 40 to 95% ACN (vol/vol) in H_2O supplemented with 0.1% (vol/vol) formic acid at a flow rate of 10 mL/min by HPLC. Initially 40% ACN, ramping up to 75% ACN over 15 min. Eluent was then increased to 95% ACN over 1.5 min, and kept there for 1 min. Concentration of ACN was then decreased to 40% over 1 min and kept there for 2 min. 10 mg of cladosporin or 11 mg of DHC was isolated from a 1L culture. Presence of cladosporin in the sample was confirmed by NMR and LC-ESI-MS using combined retention time matching with accurate mass matching. LC-MS was performed using an Agilent 1200 SL HPLC System with a Kinetex 2.6µ XB-C18 100Å, 100 x 2.1 mm reverse phase column with guard (Phenomenex, Torrance, USA), thermostated at 55 °C and an Agilent 6220 Accurate-Mass TOF HPLC/MS system (Santa Clara, CA, USA) with dual sprayer, the second sprayer delivering a calibrant solution. The buffer gradient system composed 0.1% formic acid in water as mobile phase A and 0.1% formic acid in acetonitrile as mobile phase B. The crude extracts were dissolved in methanol injected onto the column at an initial buffer composition of 20% ACN for 0.5 min, ramping up to 35% ACN over 15 min. Eluent then increased to 95% ACN over 2.5 min, and kept there for 1 min. Eluent ramped

down to 20% ACN over 1 min. Mass spectra were acquired in both positive and negative mode of ionization. Mass spectrometric conditions in positive mode were drying gas 9 L/min at 300 °C, nebulizer 30 psi, mass range 100-1000 Da, acquisition rate of ~1.03 spectra/sec, fragmentor 150V, skimmer 63 V, capillary 3200 V, instrument state 4 GHz High Resolution. Mass correction was performed for every individual spectrum using peaks at m/z 121.0508 and 922.0008 from the reference solution. Data acquisition was performed using the Mass Hunter software package (ver. B.04.00) Analysis of the HPLC-UV-MS data was done using the Find by Formula feature of the Agilent Mass Hunter Qualitative Analysis software (ver. B.07.00).

6.10 Cladosporin advanced intermediate *in vitro* assays

For incorporation of cladosporin precursor assays, purified Cla3 was dissolved in Buffer A (50 mM Tris-HCl, pH = 7.9, 2 mM EDTA, 2 mM DTT, 10% glycerol) to a final concentration of 10 μM. To this (1 mL) solution was added 2 mM malonyl-CoA and 2 mM of each advanced intermediate, and the reaction was incubated overnight at room temperature. In parallel and under the same reaction conditions, two negative controls were performed in either the absence of Cla3, or the absence of pentaketide (**2**). The reactions were quenched and extracted with an equal volume of 99% ethyl acetate 1% acetic acid solution, concentrated, and analyzed by LC-MS using an Agilent 1200 SL HPLC System with a Kinetex 2.6μ XB-C18 100Å, 100 x 2.1 mm reverse phase column with guard (Phenomenex, Torrance, USA), thermostated at 55°C and an Agilent 6220

Accurate-Mass TOF HPLC/MS system (Santa Clara, CA, USA) with dual sprayer. The buffer gradient system composed 0.1% formic acid in water and 0.1% formic acid in acetonitrile as mobile phase A and B, respectively. The crude extracts were dissolved in methanol injected onto the column at an initial buffer composition of 20% mobile phase B. After injection the column was washed at the initial condition for 0.5 minutes followed by elution of the analytes using a linear gradient from 20% to 98% mobile phase B over 15 minutes, kept at 98% for 4 minutes and to 20% mobile phase B over 0.5 minutes. Mass spectra were acquired in negative mode of ionization. Mass spectrometric conditions were drying gas 9 L/min at 300 °C, nebulizer 30 psi, mass range 100-1100 Da, acquisition rate of ~1.03 spectra/sec, fragmentor 140 V, skimmer 63 V, capillary 3200 V, instrument state 4 GHz High Resolution. Mass correction was performed for every individual spectrum using peaks at m/z 112.98559 and 1033.98811 from the reference solution. Data acquisition was performed using the Mass Hunter software package (ver. B.04.00.) Analysis of the HPLC-UV-MS data was done using the Find by Formula feature of the Agilent Mass Hunter Qualitative Analysis software (ver. B.07.00).

6.11 Chemical syntheses

6.11.1 Phosphopantetheine

(*R*)-3-(Benzyloxy)-4,4-dimethyldihydrofuran-2(3*H*)-one (38)

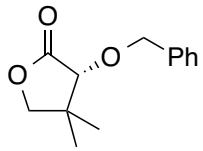

To a solution of pantolactone (4.00 g, 30.8 mmol) in DMF (80 mL) at 0 °C was added Ag_2O (14.1 g, 61.2 mmol) and benzyl bromide (4.00 mL, 33.6 mmol) at stirred at 0 °C for 2 hr. The reaction mixture was diluted with DCM (100 mL) and Ag_2O removed by gravity filtration. After concentration *in vacuo* the reaction mixture was diluted with EtOAc (50 mL) and washed with H_2O (3 x 50 mL), 1 M HCl (2 x 50 mL) and brine (50 mL), dried over Na_2SO_4 and concentrated *in vacuo*. The crude extract was purified by flash column chromatography (SiO_2, 3:1 hexanes:EtOAc) to yield the product **38** as a clear oil (4.97g, 73%). IR ($CHCl_3$ cast) 2965, 2933, 2875, 1787, 1587 cm^{-1}; ^{1}H-NMR (400 MHz; $CDCl_3$): δ 7.41-7.30 (m, 5H, Ph), 5.07-5.03 (m, 1H, C$\underline{H_2}$Ph), 4.78-4.74 (m, 1H, C$\underline{H_2}$Ph), 4.02-3.99 (m, 1H, OC$\underline{H_2}$CCH_3CH_3), 3.90-3.86 (m, 1H, OC$\underline{H_2}$CCH_3CH_3), 3.74 (s, 1H, OC$\underline{H_2}$Ph), 1.14 (s, 3H, C$\underline{H_3}$), 1.11 (s, 3H, C$\underline{H_3}$); ^{13}C NMR ($CDCl_3$, 125 MHz): δ 178.8, 128.4, 128.0, 80.4, 76.4, 72.3, 40.3, 23.2, 19.3.

(*R*)-3-(Benzyloxy)-4,4-dimethyltetrahydrofuran-2-ol (39)

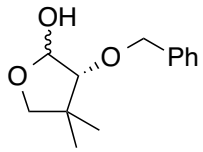

To a solution of **38** (5.00 g, 22.7 mmol) in dry DCM (50 mL) at -78 °C was added 1M DIBAL-H in DCM (27.2 mL, 27.2 mmol) and left to stir at -78 °C for 3 hr. The reaction was quenched with 1:1 Et_2O:1M H_2SO_4 (100 mL) and concentrated *in vacuo* followed by dilution with EtOAc (50 mL). The organic extract was washed with 1M H_2SO_4 (50 mL), $NaHCO_3$ (50 mL), H_2O (50 mL), and brine (50 mL), dried over Na_2SO_4 and concentrated *in vacuo*. The crude extract was purified by flash column chromatography (SiO_2, 6:1 hexanes:EtOAc) to yield the product **39** as a clear oil (4.09 g, 81%). IR ($CHCl_3$ cast) 3406, 3031, 2963, 2873, 1670 cm^{-1}; ^{1}H-NMR (700 MHz; $CDCl_3$): δ 7.37-7.30 (m, 5H), 5.46-5.36 (m, 1H), 4.70-4.57 (m, 2H), 3.96 (d, *J* = 10.0 Hz, 3/5H), 3.80 (d, *J* = 8.5 Hz, 2/5H), 3.71 (d, *J* = 8.2 Hz, 3/5H), 3.63 (d, *J* = 8.1 Hz, 2/5H), 3.51 (d, *J* = 2.9 Hz, 2/5H), 3.45 (d, *J* = 4.3 Hz, 3/5H), 3.41 (d, *J* = 8.2 Hz, 3/5H), 1.11 (s, 9/5H), 1.10 (s, 6/5H), 1.09 (s, 9/5H), 1.05 (s, 6/5H); ^{13}C NMR ($CDCl_3$, 125 MHz): δ 128.6, 128.3, 128.2, 127.9, 127.6, 127.4, 103.0, 97.6, 91.6, 85.4, 78.8, 76.7, 74.5, 72.4, 42.2, 42.2, 25.7, 24.1, 20.4, 19.7. HRMS (EI) Calcd for $C_6H_{11}O_3$ [M-Bn] 131.0708, found 131.0707, Calcd for C_7H_7 $[Bn]^{\cdot}$ 91.0548, found 91.0547.

(*S*)-3-(Benzyloxy)-2,2-dimethyl-5-phenylpent-4-en-ol (40)

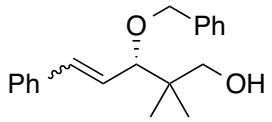

To a suspension of benzyl triphenylphosphonium bromide (8.40 g, 19.4 mmol) in

dry THF (100 mL) at -78 °C was added 1M *t*-BuOK (18.9 mL, 18.9 mmol) and left to stir at -78 °C for 1 h. To this solution via cannula was added **39** (1.44 g, 6.5 mmol) in THF (10 mL). The reaction mixture was left to warm to room temperature over 2 hours, after which time it was heated to 60 °C for an additional 1.5 h. The reaction was quenched with NH_4Cl (100 mL), diluted with Et_2O (50 mL) and the combined organic extracts washed with H_2O (50 mL), and brine (50 mL), dried over Na_2SO_4 and concentrated *in vacuo*. The crude extract was purified by flash column chromatography (SiO_2, 3:1 hexanes:EtOAc) to yield **40** as a yellow oil (1.71 g, 89%). ^{1}H-NMR (300 MHz; $CDCl_3$): δ 7.49-7.18 (m, 10H), 7.18-7.01 (m, 1H), 6.91-6.87 (m, 1H), 6.59-6.54 (m, 1H), 6.21 (dd, *J* = 16.0, 8.5 Hz, 1H), 5.84-5.63 (m, 1H), 4.62 (dd, *J* = 26.2, 11.8 Hz, 2H), 4.38-4.28 (m, 2H), 3.82 (d, *J* = 8.6 Hz, 1H), 1.02-0.89 (m, 6H); ^{13}C NMR ($CDCl_3$, 125 MHz): δ 134.7, 129.0 – 126.5 (multiple signals), 87.7, 80.0, 71.4, 70.5, 70.0, 39.2, 39.3, 22.7, 22.6, 20.0, 19.8.

(*R*)-Dibenzyl-3-(benzyloxy)-2,2-dimethyl-4-oxobutyl phosphate (41)

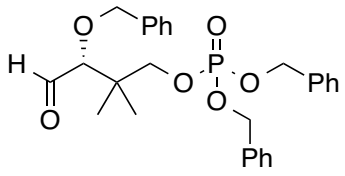

To a solution of 5-ethyl-1H-tetrazole (0.44 g, 3.37 mmol) in dry DCM (40 mL) under argon was added phosphoramidite (1.11 mL, 3.37 mmol). To this solution via

cannula was added **40** (1.00 g, 3.37 mmol) in dry DCM (10 mL). The reaction mixture was left for 16 h at ambient temperature after which time it was diluted with H_2O (50 mL) and DCM (50 mL). The aqueous layer was extracted with DCM (3 x 30 mL) and the combined organic extracts washed with H_2O (50 mL), and brine (50 mL), dried over Na_2SO_4 and concentrated *in vacuo*. To this crude extract was added 9:1 DCM:MeOH (40 mL) and the solution cooled to -78 °C. Oxygen was bubbled through the system for 2 min, followed by ozone for an additional 10 min, by which time the solution had turned pale blue. The system was then purged with oxygen for 10 min, followed by reductive work up with dimethyl sulphide (10 mL) and concentration *in vacuo*. The crude reaction mixture was purified by flash column chromatography (SiO_2, 2:1 hexanes:EtOAc to 1:1 hexanes:EtOAc) to yield the product **41** as a colourless oil (1.00 g, 61%). IR ($CHCl_3$ cast) 3033, 2967, 2876, 1723, 1698 cm^{-1}; ^{1}H-NMR (300 MHz; $CDCl_3$): δ 9.68 (d, J = 3.0 Hz, 1H, C<u>H</u>O), 7.35-7.28 (m, 15H, Ph), 5.02 (d, J = 8.4 Hz, 4H, OPOC<u>H$_2$</u>Ph x 2), 4.51 (dd, J = 47.8, 11.5 Hz, 2H, OC<u>H$_2$</u>Ph), 3.87 (dd, J = 14.4, 4.4 Hz, 2H, CC<u>H$_2$</u>OP), 3.48 (d, J = 3.0 Hz, 1H, CHOC<u>H</u>CCH$_3$CH$_3$), 0.97 (s, 3H, CH$_3$), 0.96 (s, 3H, C<u>H$_3$</u>); ^{13}C NMR ($CDCl_3$, 125 MHz) δ 133.7, 130.1, 128.4-127.4 (multiple signals), 90.9, 78.8, 72.5, 69.9, 42.1, 23.9, 20.5.

(*R*)-2-Benzyloxy-4-(bis(benzyloxy)phosphoryloxy)-3,3-dimethylbutanoic acid (42)

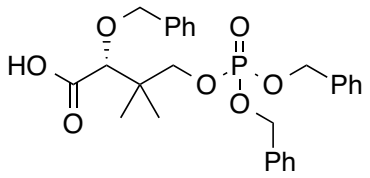

To a solution of **41** (0.50 g, 1.04 mmol) in DCM (9 mL), MeOH (18 mL) and H_2O (6 mL) was added NaH_2PO_4 (0.57 g, 4.15 mmol), $NaClO_2$ (0.188 g, 2.08 mmol) and 30% H_2O_2 (32 μL, 1.04 mmol), and left to stir for 3 h at ambient temperature. The reaction was quenched with 1M HCl (10 mL), concentrated *in vacuo*, and then diluted with H_2O (20 mL) and DCM (20 mL). The aqueous layer was extracted with DCM (3 x 30 mL) and the combined organic extracts were washed with H_2O (50 mL), and dried over Na_2SO_4 and concentrated *in vacuo*. The crude extract was purified by flash column chromatography (SiO_2, 1:2 hexanes:EtOAc) to yield **42** as a colourless oil (0.41 g, 81%). IR ($CHCl_3$ cast) 3034, 2973, 1735 cm^{-1}; ^{1}H-NMR (700 MHz; $CDCl_3$): δ 7.34-7.25 (m, 15H, Ph), 5.05-4.96 (m, 4H, OPOC$\underline{H_2}$Ph x 2), 4.58 (d, *J* = 11.2 Hz, 1H, OC$\underline{H_2}$Ph), 4.36 (d, *J* = 11.2 Hz, 1H, OC$\underline{H_2}$Ph), 3.93 (dd, *J* = 9.8, 4.7 Hz, 1H, CC$\underline{H_2}$OP), 3.82-3.80 (m, 2H, CC$\underline{H_2}$OP, CHOC$\underline{H}$CCH$_3$CH$_3$), 0.99 (s, 3H, C$\underline{H_3}$), 0.95 (s, 3H, C$\underline{H_3}$); ^{13}C NMR ($CDCl_3$, 125 MHz): δ 172.9, 136.8, 135.7, 135.6, 128.6-127.9 (multiple signals), 81.8, 73.3, 72.6, 69.5, 69.4 (multiple signals), 38.9, 38.9, 21.3, 21.3, 20.1. HRMS (ES) Calcd for $C_{27}H_{30}O_7P$ $[M-H]^-$ 497.1735, found 497.1724.

2-(Tritylthio)ethanamine (44)

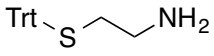

To a solution of cysteamine (1.50 g, 13.2 mmol) and TFA (2.12 mL, 27.7 mmol) in dry DCM (60 mL) was added trityl chloride (3.86 g, 13.9 mmol). After stirring for 1 h at ambient temperature, the reaction was quenched with 1 M NaOH (50 mL) and extracted with DCM (50 mL). The combined organic extracts were washed with brine (50 mL), dried over Na_2SO_4 and concentrated *in vacuo* to yield the product as a yellow solid (4.14 g, 98%). The crude product **44** was used without further purification. IR ($CHCl_3$ cast) 3364, 3056, 2922, 2853, 1595 cm^{-1}; ^{1}H-NMR (700 MHz; $CDCl_3$): δ 7.42-7.18 (m, 15H, Trt), 2.57 (d, J = 6.5 Hz, 2H, SC$\underline{H_2}$), 2.30 (t, J = 6.5 Hz, 2H, C$\underline{H_2}NH_2$), 1.27 (s, 2H, N$\underline{H_2}$); ^{13}C NMR ($CDCl_3$, 125 MHz): δ 129.6, 127.8, 126.6, 41.1, 36.3. HRMS (ES) Calcd for $C_{21}H_{22}NS$ $[M+H]^+$ 320.1467, found 320.1470.

(9*H*-Fluoren-9-yl)methyl-3-oxo-3-(2-tritylthio)ethylamino)propylcarbamate (45)

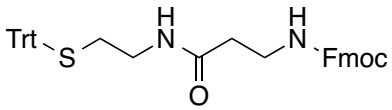

To a suspension of **44** (1 g, 3.13 mmol), Fmoc-β-alanine (1.5 g, 4.70 mmol), PyBOP (4.07 g, 7.83 mmol), and HOBt (1.27 g, 9.39 mmol) in dry THF (100 mL) under argon was added DIPEA (3.27 mL, 18.8 mmol). The reaction mixture was stirred at

ambient temperature for 20 h and then quenched with NH_4Cl (50 mL) and diluted with Et_2O (50 mL). The organic extract was washed with H_2O (50 mL) and brine (50 mL), and dried over Na_2SO_4 and concentrated *in vacuo*. Subsequent purification by flash column chromatography (SiO_2, 1:1 hexanes:EtOAc to 100% EtOAc) to yield the product **45** as a white solid (1.92 g, quant.). ^{1}H-NMR (300 MHz; $CDCl_3$): δ 7.81-7.20 (m, 23H, Trt, Fmoc), 5.56 (d, *J* = 37.9 Hz, 2H, NH), 4.37-4.33 (m, 2H, Fmoc), 4.21-4.18 (m, 1H, Fmoc), 3.47-3.41 (m, 2H, CH_2NHFmoc), 3.11-3.05 (m, 2H, CH_2NHCO), 2.45-2.40 (m, 2H, SCH_2), 2.35-2.31 (m, 2H, COCH_2).

3-Amino-N-(2-(tritylthio)ethyl)propanamide (46)

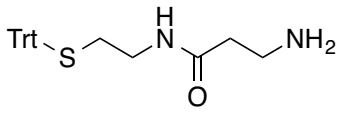

To a solution of **45** (1.00 g, 1.63 mmol) in dry DCM (15 mL) under argon, was added Et_2NH (15 mL). The reaction mixture was left to stir at ambient temperature for 3 h and the volatile solvents removed *in vacuo*. The crude reaction mixture was dissolved in DCM (50 mL) and washed with 10% citric acid (50 mL) and H_2O (50 mL). The aqueous layer was basified with K_2CO_3 until pH 8 and the extracted with DCM (2 x 50 mL). The combined organic layers were washed with H_2O (50 mL), dried over Na_2SO_4 and concentrated *in vacuo* to yield the product as a white solid (0.36 mg, 53%). Compound **46** was used without further purification. IR ($CHCl_3$ cast) 3061, 2926, 2853,

1716, 1649 cm^{-1}; HRMS (ES) Calcd for $C_{24}H_{27}N_2OS$ $[M+H]^+$ 391.1839, found 391.1840.

(*R*)-Dibenzyl-3-(benzyloxy)-2,2-dimethyl-4-oxo-4-(3-oxo-3-(2-(tritylthio)ethylamino)-propylamino)butyl phosphate (47)

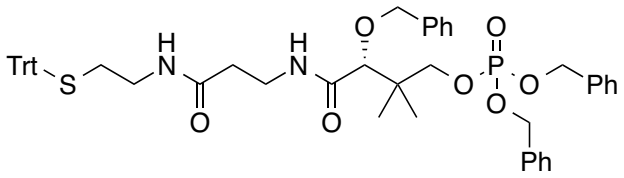

To a suspension of compound **42** (150 mg, 0.30 mmol) in dry THF (30 mL), was added EDC (89 mg, 0.45 mmol) and HOBt (61 mg, 0.45 mmol). Amine **46** (223 mg, 0.57 mmol) was then added, along with DIPEA (263 μL, 1.50 mmol), and left to stir at ambient temperature under argon for 21 h. The reaction was quenched with H_2O (50 mL) and diluted with Et_2O (50 mL). The combined organic extracts were washed with 1M HCl (50 mL), $NaHCO_3$ (50 mL) and brine (50 mL), then dried over Na_2SO_4 and concentrated *in vacuo*. Subsequent purification by flash column chromatography (SiO_2, 100% EtOAc) afforded the product as a colourless oil (124 mg, 46%). IR ($CHCl_3$ cast) 3416, 3299, 3063, 2933, 1666 cm^{-1}; ^{1}H-NMR (300 MHz; $CDCl_3$): δ 7.41-7.17 (m, 30H, Trt, Ph), 7.04 (t, *J* = 6.0 Hz, 1H, NH), 5.79 (t, *J* = 5.4 Hz, 1H, NH), 5.02 (t, *J* = 8.0 Hz, 4H, OPOCH_2Ph x 2), 4.45-4.29 (m, 2H, OCH_2Ph), 3.96 (dd, *J* = 9.5, 4.2 Hz, 1H, CCH_2OP), 3.76 (dd, *J* = 9.4, 4.5 Hz, 1H, CCH_2OP), 3.65 (s, 1H, COCHC), 3.49 (q, *J* = 6.0 Hz, 2H, CH_2NHCOCH), 3.04 (q, *J* = 6.2 Hz, 2H, CH_2NHCOCH_2), 2.38 (t, *J* = 6.5

Hz, 2H, $SC\underline{H_2}CH_2$), 2.30 (t, *J* = 6.0 Hz, 2H, $COC\underline{H_2}CH_2NH$), 0.96 (s, 3H, $C\underline{H_3}$), 0.86 (s, 3H, $C\underline{H_3}$); ^{13}C NMR ($CDCl_3$, 125 MHz): δ 170.7, 170.6, 144.5, 136.9, 129.5-126.9 (multiple signals), 83.3, 73.6, 73.0, 69.2 (multiple signals), 38.9, 38.9, 38.2, 35.6, 34.9, 31.7, 21.2, 20.0. $\alpha_D^{25} = 6.7$ (c = 0.50, $CHCl_3$)

(*R*)-3-Hydroxy-4-(3-(2-mercaptoethylamino)-3-oxopropylamino-2,2-dimethyl-4-oxo-butyl dihydrogen phosphate (phosphopantetheine, 48)

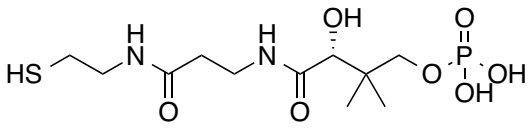

To dry THF (8 mL) under argon was added lithium that had been rinsed with dry hexanes (37 mg, 5.3 mmol) and naphthalene (641 mg, 5.0 mmol), and left to stir for 22 h at ambient temperature. The solution was then cooled to -20 °C and compound **47** (58 mg, 0.067 mmol) in dry THF (8 mL) added via cannula, and left to stir at -20 °C for 6 h. NH_4Cl (879 mg in 6 mL H_2O) was then added and the reaction mixture allowed to warm to room temperature, at which time it was washed with DCM (4 x 10 mL), and extracted with H_2O (2 x 10 mL). The combined aqueous extracts were washed with Et_2O (2 x 10 mL), concentrated *in vacuo* and lyophilized. The brown powder was then dissolved in 5 mL water and passed through acid form Dowex AG-50W-X8 ion exchange 28 resin (50 mL) that had been washed H_2O (3 x 50 mL), 1M NaOH (3 x 50 mL), H_2O (3 x 50 mL), 6 M HCl (3 x 50 mL), and H_2O (3 x 50 mL). The column was run at 2.0 mL/min using

H2O as the eluent and the first 150 mL of eluent were concentrated *in vacuo* and lyophilized to give phosphopantetheine as a pale solid (24 mg, quant.). ^{1}H-NMR (700 MHz; D_2O): δ 4.04-4.02 (3, 1H, C<u>H</u>OH), 3.78 (dd, *J* = 9.8, 4.7 Hz, 1H, CC<u>H$_2$</u>OP), 3.57 (dd, *J* = 9.8, 4.8 Hz, 1H, CC<u>H$_2$</u>OP), 3.50 (td, *J* = 6.4, 2.9 Hz, 4H, C<u>H$_2$</u>NHCOCH, C<u>H$_2$</u>NHCOCH$_2$), 2.83 (t, *J* = 6.4 Hz, 2H, SC<u>H$_2$</u>CH$_2$), 2.49 (t, *J* = 6.5 Hz, 2H, COC<u>H$_2$</u>CH$_2$NH), 0.96 (s, 3H, C<u>H$_3$</u>), 0.88 (s, 3H, C<u>H$_3$</u>); ^{13}C NMR ($CDCl_3$, 125 MHz): δ 175.7, 174.9, 159.7, 148.1, 128.3, 127.1, 75.4, 72.1, 39.2, 37.4, 36.2, 21.6, 19.9.

6.11.2 Two double bonds hexaketide-phosphopantetheine analogue

6-Bromohexanal (50)

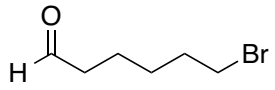

Ethyl 6-bromohexanoate (**49**) (10.0 mL, 56.2 mmol) was dissolved in dry DCM (40 mL) and cooled to -78 ^{o}C under argon. 1M DIBAL-H in DCM (56.2 mL, 56.2 mmol) was added drop wise over 15 min and the reaction mixture stirred for an additional 1 h. The reaction was quenched by the addition of 1M HCl (200 mL) and extracted with CH_2Cl_2 (2 × 50 mL). The combined organic extracts were washed with H_2O (50 mL) and brine (50 mL), dried over anhydrous Na_2SO_4 and concentrated *in vacuo*. The crude oil was purified by flash column chromatography (SiO_2, 3:1 hexanes:EtOAc) to yield the title compound **50** as a colourless oil (6.6 g, 65%). IR ($CHCl_3$, cast film) 2939, 2865,

2722, 1728 cm^{-1}; ^1H NMR ($CDCl_3$, 500 MHz): δ 9.77 (t, *J* = 3.1, 1.5 Hz, 1H, C<u>H</u>O), 3.44-3.40 (m, 2H, C<u>H$_2$</u>Br), 2.48 (tdd, *J* = 7.23, 3.15, 1.62, 2H, CHOC<u>H$_2$</u>), 1.92-1.85 (m, 2H, C<u>H$_2$</u>CH$_2$Br), 1.71-1.63 (m, 2H, CHOCH$_2$C<u>H$_2$</u>), 1.53-1.47 (m, 2H, CH$_2$C<u>H$_2$</u>CH$_2$); ^{13}C NMR ($CDCl_3$, 125 MHz): δ 202.1, 43.6, 33.3, 32.4, 27.6, 24.0; R_f 0.6 (2:1 hexanes:EtOAc). HRMS (EI) Calcd for $C_6H_{10}OBr$ $[M-H]^{\cdot+}$ 176.9915, found 176.9913.

2-(5-Bromopentyl)-1,3-dioxolane (51)

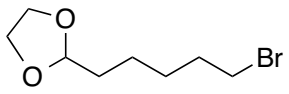

Compound **50** (3.6 g, 20 mmol) was dissolved in dry toluene (100 mL) under argon. Alumina (5 g) was added along with anhydrous ethylene glycol (5.6 mL, 100 mmol) and the reaction mixture heated to reflux for 24 h. After 24 h the alumina was removed by gravity filtration and washed several times with DCM. The combined organic extracts were washed twice with H_2O and concentrated *in vacuo* to yield the product as a colourless oil (3.9 g, 88%). IR ($CHCl_3$, cast film) 2941, 2867 cm^{-1}; ^1H NMR ($CDCl_3$, 500 MHz): δ 4.86 (t, *J* = 4.7 Hz, 1H, OOC<u>H</u>), 4.01-3.81 (m, 4H, C<u>H$_2$</u>O x 2), 3.41 (t, *J* = 6.8 Hz, 2H, C<u>H$_2$</u>Br), 1.88 (q, *J* = 7.1 Hz, 2H, CHC<u>H$_2$</u>), 1.71-1.66 (m, 2H, C<u>H$_2$</u>CH$_2$Br), 1.52-1.41 (m, 4H, CHCH$_2$C<u>H$_2$</u>, CH$_2$C<u>H$_2$</u>CH$_2$); ^{13}C NMR ($CDCl_3$, 125 MHz): δ 104.4, 64.8, 60.3, 34.1, 33.4, 32.4, 27.6, 24.0. R_f 0.65 (2:1 hexanes:EtOAc). HRMS (EI) Calcd for $C_8H_{14}O_2Br$ $[M-H]^{\cdot+}$ 221.0177, found 221.0174.

(*E*)-2-(Undec-7-enyl)-1,3-dioxolane (53)

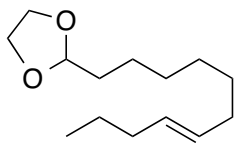

To a 3-neck flask under argon containing magnesium (1.46 g, 60 mmol) and 4.5 mL of dry THF, **51** (2.00 g, 9 mmol) in dry THF (4.5 mL) was slowly added over 1 h. In a 3-neck flask under argon, *trans*-2-hexenyl acetate (2.14 mL, 13.5 mmol) and 0.1M Li_2CuCl_4 (4.5 mL, 0.45 mmol) were dissolved in dry THF (20 mL) and cooled to -30 ^oC. To this activated electrophile solution was added the Grignard reagent via cannula and the reaction mixture was stirred for 18 h. The mixture was then quenched with saturated NH_4Cl (40 mL) and the aqueous layer extracted with Et_2O (4 x 50 mL). The combined organic extracts were washed with brine (100 mL), dried over anhydrous Na_2SO_4 and concentrated *in vacuo*. To the resulting yellow oil was added NaOH (8 g), and 3:1 MeOH:THF (200 mL). After stirring for 2 h at ambient temperature, 1:1 $NaHCO_3$:H_2O (50 mL) was added. The mixture was extracted with Et_2O (3 x 30 mL) and the combined organic extracts washed with brine (100 mL), dried over Na_2SO_4 and concentrated *in vacuo*. The crude oil was purified by flash column chromatography (SiO_2, 3:1 hexanes:EtOAc) to yield **53** as a yellow oil (300 mg, 15% over 2 steps). ^{1}H-NMR (400 MHz; $CDCl_3$): δ 5.56-5.34 (m, 2H, HC=CH), 4.87-4.83 (m, 1H, OOCH), 4.01-3.81 (m,

4H, C$\underline{H_2}$O x 2), 2.01-1.89 (m, 3H, CHC$\underline{H_2}$, C=CHC$\underline{H_2}$, C$\underline{H_2}$C=C), 1.69-1.61 (m, 3H, CHC$\underline{H_2}$, C=CHC$\underline{H_2}$, C$\underline{H_2}$C=C), 1.46-1.17 (m, 10H, CHCH$_2$C$\underline{H_2}$, CHCH$_2$CH$_2$C$\underline{H_2}$, CHCH$_2$CH$_2$CH$_2$C$\underline{H_2}$, C=CCH$_2$C$\underline{H_2}$, CH$_3$C$\underline{H_2}$), 0.94-0.83 (m, 3H, C$\underline{H_3}$); ^{13}C NMR ($CDCl_3$, 125 MHz): δ 130.5, 130.2, 104.7, 64.8, 34.7, 33.9, 32.6, 29.5, 29.4, 29.0, 24.1, 22.8, 13.7; R_f 0.7 (3:1 hexanes:EtOAc). HRMS (ES) Calcd for $C_{14}H_{27}O_2$ $[M+H]^+$ 227.2006, found 227.2005.

(*E*)-Dodec-8-enal (54)

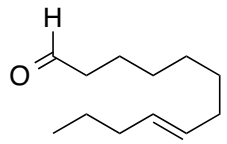

To a solution of **53** (100 mg, 0.44 mmol) in THF (1.24 mL) was added H_2O (1.54 mL) and acetic acid (777 μL) and refluxed for 5 h. To the flask was added $NaHCO_3$ (20 mL) and the mixture was extracted with hexanes (3 x 20 mL). The combined organic extracts were washed with brine (100 mL), dried over Na_2SO_4 and concentrated *in vacuo* to yield the product as a colourless oil (75 mg, 94%). This compound was used without any further purification. ^{1}H-NMR (400 MHz; $CDCl_3$): δ 9.77 (t, *J* = 1.8 Hz, 1H, C$\underline{H}$O), 5.56-5.38 (m, 2H, $\underline{H}$C=C$\underline{H}$), 2.44-2.40 (m, 2H, CHOC$\underline{H_2}$), 2.00-1.93 (m, 2H, H-7, H-10), 1.67-1.59 (m, 2H, C=CHC$\underline{H_2}$, C$\underline{H_2}$C=C), 1.41-1.19 (m, 10H, CHOCH$_2$C$\underline{H_2}$, CHCH$_2$CH$_2$C$\underline{H_2}$, CHCH$_2$CH$_2$CH$_2$C$\underline{H_2}$, C=CCH$_2$C$\underline{H_2}$, CH$_3$C$\underline{H_2}$), 0.89 (t, *J* = 7.4 Hz, 3H,

CH_3). ^{13}C NMR ($CDCl_3$, 125 MHz): δ 202.5, 130.0, 129.9, 43.5, 34.3, 32.1, 29.0, 28.2, 28.4, 22.3, 21.7, 13.2; R_f 0.65 (3:1 hexanes:EtOAc).

(*E*)-Dodec-8-enoic acid (55)

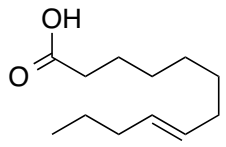

A solution of *t*-BuOH (21.8 mL) and 2-methyl-2-butene (1.44 mL, 13.6 mmol) was combined with a solution of $NaClO_2$ (264 mg, 2.90 mmol), $NaH_2PO_4.H_2O$ (202 mg, 1.5 mmol) and H_2O (6.12 mL) and stirred for 10 min to form a stock solution of reagents. 25% by volume (7.34 mL) of this stock solution was added to **54** (62 mg, 0.34 mmol) and stirred at ambient temperature for 5 h. The reaction mixture was then diluted with H_2O (5 mL) and adjusted to pH 6 with 1M HCl. The aqueous layer was washed with EtOAc (3 x 10 mL) and the combined organic extracts washed with brine (20 mL), dried over anhydrous Na_2SO_4 and concentrated *in vacuo*. The crude reaction mixture was purified by flash column chromatography (SiO_2, 3:1 hexanes:EtOAc) to yield **55** as a colourless liquid (30 mg, 45 %). IR ($CHCl_3$ cast) 2927, 2856, 1711 cm^{-1}; ^1H-NMR (700 MHz; $CDCl_3$): δ 5.37-5.36 (m, 2H, HC=CH), 2.33 (td, *J* = 7.5, 3.7 Hz, 2H, $HOOCCH_2$), 1.97-1.92 (m, 2H, $C=CHCH_2$, $CH_2C=C$), 1.62 (dt, *J* = 14.9, 7.5 Hz, 2H, $C=CHCH_2$, $CH_2C=C$), 1.56-1.51 (m, 1H, COOH), 1.37-1.19 (m, 10H, $COCH_2CH_2$, $CHCH_2CH_2CH_2$,

$CHCH_2CH_2CH_2C\underline{H_2}$, $C{=}CCH_2C\underline{H_2}$, $CH_3C\underline{H_2}$), 0.86 (t, J = 7.4 Hz, 3H, $C\underline{H_3}$); ^{13}C NMR ($CDCl_3$, 125 MHz): δ 130.3, 130.3, 34.1, 33.5, 32.5, 29.7, 29.3, 28.9, 28.7, 24.6, 22.7, 13.6; R_f 0.4 (3:1 hexanes:EtOAc). HRMS (ES) Calcd for $C_{12}H_{21}O_2$ $[M\text{-}H]^-$ 197.1547, found 197.1549.

(*E*)-*S*-4-Nitrophenyldodec-8-enethioate (56)

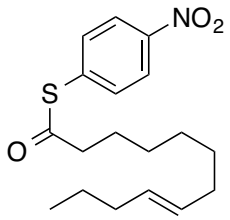

To a solution of **55** (10 mg, 0.051 mmol) in dry DCM (1 mL) was added *p*-nitrothiophenol (5.6 mg, 0.051 mmol), EDC (10.7 mg, 0.0561 mmol) and NEt_3 (5.7 μL, 0.0561 mmol) and stirred at ambient temperature for 20 h. The reaction mixture was then washed with 1M HCl (3 x 1 mL), $NaHCO_3$ (3 x 1 mL) and then brine (2 x 5 mL), dried over Na_2SO_4 and concentrated *in vacuo*. The crude reaction mixture was purified by preparatory TLC (SiO_2, 500 micron, 10:1 hexanes:EtOAc) to yield **56** as a colourless liquid (3 mg, 18 %). IR ($CHCl_3$ cast) 2974, 2933, 1779, 1697 cm^{-1}; ^{1}H-NMR (600 MHz; $CDCl_3$): δ 8.26-8.24 (m, 2H, $ArC\underline{H}NO_2$ x 2), 7.61-7.59 (m, 2H, $SArC\underline{H}$ x 2), 5.53-5.38 (m, 2H, $\underline{H}C{=}C\underline{H}$), 2.72-2.69 (m, 2H, $COC\underline{H_2}$), 1.99-1.95 (m, 4H, $C{=}CHC\underline{H_2}$, $C\underline{H_2}C{=}C$), 1.74 (t, J = 6.8 Hz, 2H, $COCH_2C\underline{H_2}$), 1.38-1.26 (m, 8H, $CHCH_2CH_2C\underline{H_2}$,

$CHCH_2CH_2CH_2C\underline{H_2}$, $C{=}CCH_2C\underline{H_2}$, $CH_3C\underline{H_2}$), 0.91-0.87 (m, 3H, $C\underline{H_3}$); ^{13}C NMR ($CDCl_3$, 125 MHz): δ 180.4, 36.3, 34.3 (2 overlapping signals), 29.6, 26.7, 25.2, 19.3, 11.5; R_f 0.8 (5:1 hexanes:EtOAc).

(*E*)-Dodec-8-enyl-phosphopantetheine thioester (57)

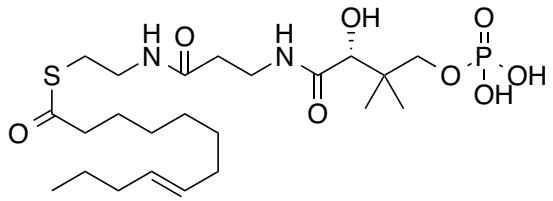

To a solution of **56** (2 mg, 0.006 mmol) in degassed acetone-d_6 (1 mL) was added a solution of phosphopantetheine (4.3 mg, 0.012 mmol) in 0.1M $KHCO_3$ (358 μL, 0.036 mmol), followed by TCEP (3 mg, 0.012 mmol). The reaction was monitored by ^1H-NMR for disappearance of the methylene protons alpha to the starting material thioester and additional 0.1M $KHCO_3$ added (up to a total of 12 eq.) if necessary. The crude reaction mixture was purified using C_8-RP-HPLC: VYDAC C_8 column, flow rate 1 mL/min, detected at 210/254 nm. Gradient: starting from 100% H_2O (0.1% TFA) for 5 min, ramping up to 95% H_2O (0.1% TFA) and 5% ACN (0.05% TFA) over 5 min, then ramping up to 85% H_2O (0.1% TFA) and 15% ACN (0.05% TFA) over 5 min, ramping up again to 30% H_2O (0.1% TFA) and 70% ACN (0.05% TFA) over 5 min, staying there for 10 min and then ramping down to 100% H_2O (0.1% TFA) for 3 min. The product

eluted at 22 min and product containing fractions were lyophilized to yield the hexaketide-phosphopantetheine coupled thioester as a white powder (2 mg, 65%). ^{1}H-NMR (600 MHz; D_2O): δ 5.52-5.46 (m, 2H, HC=CH), 4.07-4.02 (m, 1H, CHOH), 3.81-3.73 (m, 1H, CCH_2OP), 3.58-3.51 (m, 1H, CCH_2OP), 3.51-3.43 (m, 2H, $CH_2NHCOCH$), 3.41-3.30 (m, 2H, $CH_2NHCOCH_2$), 3.06-2.99 (m, 2H, SCH_2), 2.68-2.57 (m, 2H, $SCOCH_2$), 2.50-2.40 (m, 2H, $COCH_2CH_2NH$), 2.02-1.89 (m, 5H, $C=CHCH_2$, $CH_2C=C$), 1.68-1.55 (m, 2H, $SCOCH_2CH_2$), 1.35-1.20 (m, 11H, $CHCH_2CH_2CH_2$, $CHCH_2CH_2CH_2CH_2$, $C=CCH_2CH_2$, CH_3CH_2), 1.02-0.92 (m, 3H, CH_3), 0.90-0.77 (m, 6H, H-21, H-21'). ^{13}C NMR ($CDCl_3$, 125 MHz): δ 75.7, 44.5, 39.6, 39.4, 39.3, 36.4, 36.4, 32.2, 29.7, 29.6, 29.5, 29.4, 29.2, 29.0, 28.9, 26.3, 23.0, 22.1, 19.3, 14.4; HRMS (ES) Calcd for $C_{23}H_{42}N_2O_8PS$ $[M-H]^-$ 537.2405, found 537.2413.

6.11.3 One double bond hexaketide-phosphopantetheine analogue

2-((7*E*,9*E*)-Undeca-7,9-dienyl)-1,3-dioxolane (58)

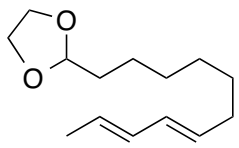

To a 3-neck flask under argon containing magnesium (0.729g, 30 mmol) and 4.5 mL of dry THF, common intermediate **51** (1.00 g, 4.5 mmol) in dry THF (4.5 mL) was slowly added over 1 h. In a 3-neck flask under argon, *trans,trans*-2,4-hexadienylacetate

(1.00 mL, 6.75 mmol) and 0.1M Li_2CuCl_4 (2.25 mL, 0.225 mmol) were dissolved in dry THF (10 mL) and cooled to -30 ^oC. To this activated electrophile solution was added the Grignard reagent via cannula and the reaction mixture was stirred for 18 h. The mixture was then quenched with saturated NH_4Cl (20 mL) and the aqueous layer extracted with Et_2O (4 x 20 mL). The combined organic extracts were washed with brine (100 mL), dried over anhydrous Na_2SO_4 and concentrated *in vacuo*. To the resulting yellow oil was added NaOH (4 g), and 3:1 MeOH:THF (100 mL). After stirring for 2 h at ambient temperature, 1:1 $NaHCO_3$:H_2O (50 mL) was added. The mixture was extracted with Et_2O (3 x 30 mL) and the combined organic extracts washed with brine (50 mL), dried over Na_2SO_4 and concentrated *in vacuo*. The crude oil was purified by flash column chromatography (SiO_2, 3:1 hexanes:EtOAc) to yield the product **58** as a yellow oil (74 mg, 7% over 2 steps). IR ($CHCl_3$, cast film) 2927, 2855, 1690 cm-1; ^{1}H-NMR (700 MHz; $CDCl_3$): δ 6.01-5.94 (m, 2H, $CH_3C\underline{H}$=C$\underline{H}$), 5.57-5.50 (m, 2H, $\underline{H}$C=C$\underline{H}$), 4.82 (dd, J = 6.3, 3.4 Hz, 1H, OOC$\underline{H}$), 3.96-3.80 (m, 4H, C$\underline{H_2}$O x 2), 2.02 (q, J = 7.3 Hz, 2H, CHC$\underline{H_2}$), 1.71-1.70 (m, 3H, CH_3), 1.65-1.61 (m, 2H, HC=CHC$\underline{H_2}$), 1.42-1.24 (m, 8H, CHCHC$\underline{H_2}$, $CHCH_2CH_2C\underline{H_2}$, $CHCH_2CH_2CH_2C\underline{H_2}$, HC=$CHCH_2C\underline{H_2}$); ^{13}C NMR ($CDCl_3$, 125 MHz): δ 132.0, 131.7, 130.2, 126.6, 104.6, 64.8, 33.9, 32.5, 29.4, 29.2, 29.0, 24.0, 18.0; R_f 0.7 (3:1 hexanes:EtOAc). HRMS (ES) Calcd for $C_{14}H_{25}O_2$ $[M+H]^+$ 225.1849, found 225.1850.

(8*E*,10*E*)-Dodeca-8,10-dienal (59)

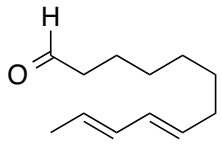

To a solution of **58** (74 mg, 0.33 mmol) in THF (0.93 mL) was added H_2O (1.15 mL) and acetic acid (583 μL) and refluxed for 3 h. To the flask was added $NaHCO_3$ (20 mL) and the mixture was extracted with hexanes (3 x 20 mL). The combined organic extracts were washed with brine (100 mL), dried over Na_2SO_4 and concentrated *in vacuo* to yield the product as a colourless oil (30 mg, 51%). The product was used in the next step without further purification. IR ($CHCl_3$, cast film) 2931, 2858, 1712, 1636 cm^{-1}; ^{1}H-NMR (400 MHz; $CDCl_3$): δ 9.77 (t, *J* = 1.8 Hz, 1H, C<u>H</u>O), 6.06-5.95 (m, 1H, $CH_3C\underline{H}=C\underline{H}$), 5.74-5.28 (m, 2H, $\underline{H}C=C\underline{H}$), 2.42 (ddd, *J* = 8.4, 6.3, 2.0 Hz, 2H, $CHOC\underline{H_2}$), 2.08-2.02 (m, 2H, $HC=CHC\underline{H_2}$), 1.73 (d, *J* = 6.8 Hz, 2H, $CHOCH_2C\underline{H_2}$), 1.68-1.59 (m, 3H, $C\underline{H_3}$), 1.42-1.25 (m, 6H, $CHCH_2CH_2C\underline{H_2}$, $CHCH_2CH_2CH_2C\underline{H_2}$, $HC=CHCH_2C\underline{H_2}$). R_f 0.65 (3:1 hexanes:EtOAc). HRMS (ES) Calcd for $C_{12}H_{21}O$ $[M+H]^+$ 181.1587, found 181.1585.

(8*E*,10*E*)-Dodeca-8,10-dienoic acid (60)

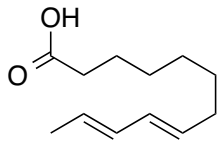

A solution of *t*-BuOH (10.6 mL) and 2-methyl-2-butene (703 μL, 6.64 mmol) was combined with a solution of $NaClO_2$ (129 mg, 1.43 mmol), $NaH_2PO_4.H_2O$ (98 mg, 0.71 mmol) and H_2O (2.99 mL) and stirred for 10 min to form a stock solution of reagents. 25% by volume (3.57 mL) of this stock solution was added to **59** (30 mg, 0.17 mmol) and stirred at ambient temperature for 5 h. The reaction mixture was then diluted with H_2O (5 mL) and adjusted to pH 6 with 1M HCl. The aqueous layer was extracted with EtOAc (3 x 10 mL) and the combined organic extracts washed with brine (20 mL), dried over anhydrous Na_2SO_4 and concentrated *in vacuo*. The crude product **60** was carried through as a colourless liquid (33 mg, quant.), without further purification. ^{1}H-NMR (400 MHz; $CDCl_3$): δ 6.06-5.95 (m, 2H, $CH_3C\underline{H}$=C$\underline{H}$), 5.74-5.28 (m, 2H, $\underline{H}$C=C$\underline{H}$), 2.38-2.32 (m, 2H, HOOCC$\underline{H}_2$), 1.79-1.71 (m, 2H, HC=CHC$\underline{H}_2$), 1.69-1.56 (m, 3H, C$\underline{H}_3$), 1.45-1.29 (m, 8H, $COOCCH_2C\underline{H}_2$, $HOOCCH_2CH_2C\underline{H}_2$, $HOOCCH_2CH_2CH_2C\underline{H}_2$, $HC=CHCH_2C\underline{H}_2$); ^{13}C NMR ($CDCl_3$, 125 MHz): δ 171.2, 131.9, 131.7, 130.4, 126.8, 60.4, 33.5, 32.5, 24.7, 21.2, 18.0, 14.2; R_f 0.4 (3:1 hexanes:EtOAc).

(8*E*,10*E*)-*S*-4-Nitrophenyldodeca-8,10-dienethioate (61)

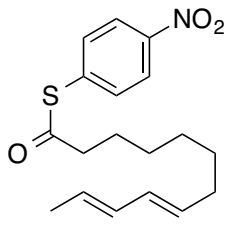

To a solution of **60** (33 mg, 0.17 mmol) in DCM (1 mL) was added *p*-nitrothiophenol (18.7 mg, 0.17 mmol), DCC (35.1 mg, 0.17 mmol) and DMAP (0.2 mg, 0.017 mmol) and left stirring at ambient temperature stirred at ambient temperature for 20 h. The reaction mixture was then washed with 1M HCl (3 x 1 mL), $NaHCO_3$ (3 x 1 mL) and then brine (2 x 5 mL), dried over Na_2SO_4 and concentrated *in vacuo*. The crude reaction mixture was purified by preparatory TLC (SiO_2, 10:1 hexanes:EtOAc) to yield (**61**) as a colourless liquid (2 mg, 4 %). ^{1}H-NMR (400 MHz; $CDCl_3$): δ 8.27-8.23 (m, 2H, $\underline{H}ArNO_2$ x 2), 7.62-7.58 (m, 2H, SAr$\underline{H}$ x 2), 6.03-5.96 (m, 2H, $CH_3C\underline{H}=C\underline{H}$), 5.74-5.28 (m, 2H, $\underline{H}C=C\underline{H}$), 2.73-2.68 (m, 2H, $COC\underline{H}_2$), 2.08-2.03 (m, 2H, $HC=CHC\underline{H}_2$), 1.79-1.72 (m, 3H, $C\underline{H}_3$), 1.70-1.29 (m, 8H, $SCOCH_2C\underline{H}_2$, $SCOCH_2CH_2C\underline{H}_2$, $SCOCH_2CH_2CH_2C\underline{H}_2$, $HC=CHCH_2C\underline{H}_2$); R_f 0.8 (5:1 hexanes:EtOAc).

(8*E*,10*E*)Dodeca-8,10-dienyl-phophopantetheine thioester (62)

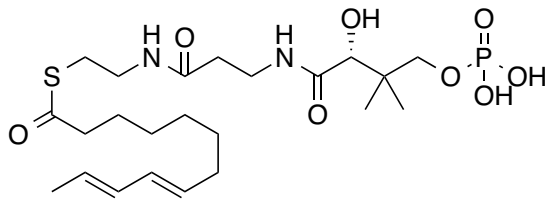

To a solution of **61** (2 mg, 0.006 mmol) in degassed acetone-d_6 (1 mL) was added a solution of phosphopantetheine (4.3 mg, 0.012 mmol) in 0.1M $KHCO_3$ (358 μL, 0.036 mmol), followed by TCEP (3 mg, 0.012 mmol). The reaction was monitored by ^{1}H-NMR

for disappearance of the methylene protons alpha to the starting material thioester and additional 0.1M $KHCO_3$ added (up to a total of 12 eq.) if necessary. The crude reaction mixture was purified using C_8-RP-HPLC: VYDAC C_8 column, flow rate 1 mL/min, detected at 210/254 nm. Gradient: starting from 100% H_2O (0.1% TFA) for 5 min, ramping up to 95% H_2O (0.1% TFA) and 5% ACN (0.05% TFA) over 5 min, then ramping up to 85% H_2O (0.1% TFA) and 15% ACN (0.05% TFA) over 5 min, ramping up again to 30% H_2O (0.1% TFA) and 70% ACN (0.05% TFA) over 5 min, staying there for 10 min and then ramping down to 100% H_2O (0.1% TFA) for 3 min. The product eluted at 22 min and product-containing fractions were lyophilized to yield the title compound **62** as a white powder (0.4 mg, 7%). $[\alpha]_D^{25}$ = -22.0 (*c* = 0.02 g/100 mL, H_2O); IR ($CHCl_3$ cast) 3395, 1686, 1447 cm^{-1}; ^{1}H-NMR (600 MHz; D_2O): δ 6.10-6.06 (m, 2H, $CH_3C\underline{H}=C\underline{H}$), 5.84-5.35 (m, 2H, $\underline{H}C=C\underline{H}$), 4.08-4.02 (m, 1H, $C\underline{H}OH$), 3.84-3.73 (m, 1H, $CC\underline{H_2}OP$), 3.59-3.52 (m, 1H, $CC\underline{H_2}OP$), 3.51-3.46 (m, 2H, $C\underline{H_2}NHCOCH$), 3.40-3.32 (m, 2H, $C\underline{H_2}NHCOCH_2$), 3.07-2.97 (m, 2H, $SC\underline{H_2}$), 2.66-2.59 (m, 2H, $SCOC\underline{H_2}$), 2.49-2.40 (m, 2H, $COC\underline{H_2}CH_2NH$), 2.06-1.97 (m, 2H, $HC=CHC\underline{H_2}$), 1.72-1.59 (m, 5H, $C\underline{H_3}$), 1.40-1.17 (m, 8H, $SCOCH_2C\underline{H_2}$, $SCOCH_2CH_2C\underline{H_2}$, $SCOCH_2CH_2CH_2C\underline{H_2}$, $HC=CHCH_2C\underline{H_2}$), 1.01-0.93 (m, 3H, $C\underline{H_3}$), 0.91-0.84 (m, 3H, $C\underline{H_3}$); HRMS (ES) Calcd for $C_{23}H_{40}N_2O_8PS$ $[M-H]^-$ 535.2248, found 535.2258.

6.11.4 Saturated hexaketide-phosphopantetheine analogue

***S*-4-Nitrophenyldodecanethioate (64)**

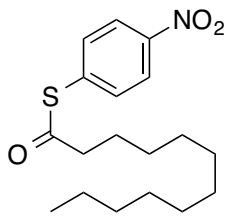

To a solution of lauroyl chloride (1 mL, 4.3 mmol) in dry DCM (20 mL) was added *p*-nitrothiophenol (666 mg, 4.3 mmol), and pyridine (346 μL, 4.3 mmol) The reaction mixture was kept at 0 °C for 2 hours, and then warmed to room temperature over 22 h. The reaction mixture was then washed with H_2O (3 x 10 mL), dried over Na_2SO_4 and concentrated *in vacuo*. The crude reaction mixture was purified by preparatory TLC (SiO_2, 10:1 hexanes:EtOAc) to yield **64** as a colourless liquid (1.09 g, 75 %). IR ($CHCl_3$ cast) 2920, 2851, 1713, 1645 cm^{-1}. ^{1}H-NMR (acetone-d_6, 300 MHz): δ 8.29-8.28 (m, 2H, $\underline{H}ArNO_2$ x 2), 7.75-7.72 (m, 2H, SAr$\underline{H}$), 2.79 (t, J = 7.3 Hz, 2H, COC$\underline{H_2}$), 1.72 (dt, J = 14.6, 7.4 Hz, 2H, $COCH_2C\underline{H_2}$), 1.43-1.25 (m, 15H, aliphatic), 0.88 (t, J = 6.6 Hz, 3H, C$\underline{H_3}$); ^{13}C NMR ($CDCl_3$, 125 MHz): δ 134.6, 123.9, 44.2, 31.9, 29.5, 29.5, 29.4, 29.3, 29.2, 28.9, 25.5, 22.7, 14.1. R_f 0.9 (2:1 hexanes:EtOAc); HRMS (ES) Calcd for $C_{18}H_{27}NNaO_3S$ $[M+Na]^+$ 360.1604, found 360.1603.

Dodecyl phophopantetheine thioester (65)

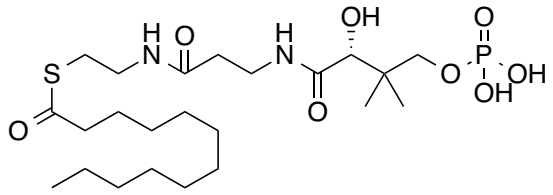

To a solution of **64** (2 mg, 0.006 mmol) in degassed acetone-d_6 (1 mL) was added a solution of phosphopantetheine (4.3 mg, 0.012 mmol) in 0.1M $KHCO_3$ (358 μL, 0.036 mmol), followed by TCEP (3 mg, 0.012 mmol). The reaction was monitored by ^{1}H-NMR for disappearance of the methylene protons alpha to the starting material thioester and additional 0.1M $KHCO_3$ added (up to a total of 12 eq.) if necessary. The crude reaction mixture was purified using C_8-RP-HPLC: VYDAC C_8 column, flow rate 1 mL/min, detected at 210/254 nm. Gradient: starting from 100% H_2O (0.1% TFA) for 5 min, ramping up to 95% H_2O (0.1% TFA) and 5% ACN (0.05% TFA) over 5 min, then ramping up to 85% H_2O (0.1% TFA) and 15% ACN (0.05% TFA) over 5 min, ramping up again to 30% H_2O (0.1% TFA) and 70% ACN (0.05% TFA) over 5 min, staying there for 10 min and then ramping down to 100% H_2O (0.1% TFA) for 3 min. The product eluted at 22 min and product containing fractions were lyophilized to yield the product as a white powder (0.8 mg, 25%). IR ($CHCl_3$ cast) 3283, 2919, 2850, 1686, 1642 cm^{-1}; ^{1}H-NMR (500 MHz; D_2O): δ 4.06 (s, 1H, C<u>H</u>OH), 3.76-3.73 (m, 1H, CC<u>H$_2$</u>OP), 3.49-3.44 (m, 3H, H-22, C<u>H$_2$</u>NHCOCH), 3.36 (t, *J* = 6.0 Hz, 2H, C<u>H$_2$</u>NHCOCH$_2$), 3.02 (t, *J* = 6.7 Hz, 2H, SC<u>H$_2$</u>), 2.62 (t, *J* = 7.4 Hz, 2H, SCOC<u>H$_2$</u>), 2.45 (t, *J* = 6.4 Hz, 2H,

COCH$_2$CH$_2$NH), 1.64-1.59 (m, 2H, SCOCH$_2$CH$_2$), 1.31-1.20 (m, 18H, aliphatic), 0.96 (s, 3H, CH$_3$), 0.86-0.80 (m, 6H, CH$_3$ x 2); ^{13}C NMR ($CDCl_3$, 125 MHz): δ 75.7, 44.5, 39.6, 39.4, 39.3, 36.4, 32.2, 29.7, 29.6, 29.5, 29.4, 29.2, 29.0, 28.9, 26.3, 23.0, 22.1, 19.3, 14.4; HRMS (ES) Calcd for $C_{23}H_{44}N_2O_8PS$ $[M-H]^-$ 539.2561, found 539.2570.

6.11.5 ^{13}C-labelled lovastatin tetraketide synthesis

* denotes position of ^{13}C label

Propionyl chloride (67)

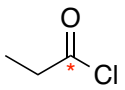

To a 3-neck 50 mL RBF at 0 °C and under argon was added **66** (1 g, 10.3 mmol) and PCl_5 (3.22g, 15.5 mmol). The reaction mixture was heated to 80 °C for 5 min to form a slurry, after which time the reaction mixture was distilled under vacuum. The title compound **67** distilled between 60-75 °C, under house vacuum to afford a clear colourless oil (0.96 g, quant.) The product was used without any further purification.

(*R*)-4-Benzyl-3-propionyloxazolidin-2-one (69)

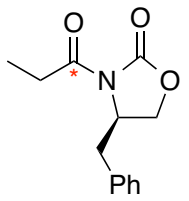

To a solution of (*R*)-4-benzyl-1,3-oxazolidin-2-one (2.22 g, 12.5 mmol) in dry THF (20 mL) at -78 °C, was added n-BuLi (5.52 mL, 13.8 mmol) and stirred for 20 min at -78 °C. To the above solution was added compound **67** (1.29 g, 13.8 mmol) in dry THF (1 mL) at -78 °C, and left to warm to ambient temperature over 45 min. After an additional 30 min at ambient temperature, the reaction was quenched with NH_4Cl (50 mL), extracted with DCM (2 x 40 mL) and the combined organic extracts washed with $NaHCO_3$ (50 mL) and brine (50 mL), dried over Na_2SO_4 and concentrated *in vacuo*. The mixture was purified by flash column chromatography (SiO_2, 3:1 hexanes:EtOAc) to yield the product (**69**) as a clear oil (635 mg, 22%). $[\alpha]_D^{25}$ = -24.3 (*c* = 0.35 g/100 mL, DCM); IR ($CHCl_3$ cast) 3029, 2981, 1782, 1662, 1604 cm^{-1}; ^{1}H-NMR (400 MHz; $CDCl_3$): δ 7.36-7.27 (m, 3H, Ph), 7.22-7.19 (m, 2H, Ph), 4.68 (ddtd, *J* = 9.6, 7.4, 3.3, 0.9 Hz, 1H, NC<u>H</u>CH_2), 4.23-4.15 (m, 2H, C<u>H</u>$_2$Ph), 3.31 (dd, *J* = 13.4, 3.4 Hz, 1H, C<u>H</u>$_2$O), 3.03-2.89 (m, 2H, CH_3C<u>H</u>$_2$CO), 2.77 (dd, *J* = 13.4, 9.6 Hz, 1H, C<u>H</u>$_2$O), 1.21 (td, *J* = 7.4, 5.5 Hz, 3H, C<u>H</u>$_3$); ^{13}C NMR ($CDCl_3$, 125 MHz): δ 174.1, 135.3, 129.4, 129.0, 127.3, 74.5, 66.2, 55.2, 37.9, 29.4, 28.9, 8.3; R_f 0.7 (2:1 hexanes:EtOAc). α_D^{25} = -24.3 (c = 0.35, DCM); HRMS (ES) Calcd for $C_{12}{}^{13}CH_{16}NO_3$ $[M+H]^+$ 235.1158, found 235.1157.

(*R*)-4-Benzyl-3-((*S*,4*E*,6*E*)-2-methylocta-4,6-dienoyl)oxazolidin-2-one (72)

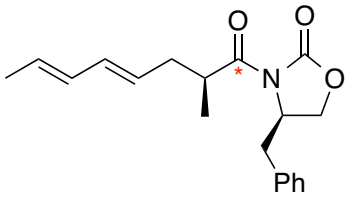

To compound **70** (1.00 g, 10.2 mmol) dissolved in dry Et_2O (50 mL) at -20 °C, was added PBr_3 (441 μL, 4.7 mmol), and left to stir at -20 °C for 1 h. The solution was quenched with an ice/brine slurry (50 mL), extracted with DCM (2 x 40 mL) and the combined organic extracts dried over Na_2SO_4 and concentrated *in vacuo*. The crude oil was carried forward without further purification. To a solution of compound (**69**) (250 mg, 1.07 mmol) dissolved in dry THF (20 mL) at -78 °C, was added 1 M NaHMDS in THF (1.17 mL, 1.17 mmol), and stirred for 15 min. To this solution at -78 °C was then added compound (**71**) (343 mg, 2.13 mmol), followed by TBAI (39 mg, 0.11 mmol), and left to stir at -78 °C for 2.5 h. The reaction was quenched with NH_4Cl (30 mL) and extracted with EtOAc (3 x 20 mL). The combined organic extracts were dried over Na_2SO_4 and concentrated *in vacuo,* followed by purification by flash column chromatography (SiO_2, 6:1 hexanes:EtOAc) to yield (**72**) as a clear oil (196 mg, 58%). $[\alpha]_D^{25}$ = -59.0 (*c* = 0.40 g/100 mL, DCM); IR ($CHCl_3$ cast) 3018, 2974, 2932, 1780, 1657, 1605 cm^{-1}; ^{1}H-NMR (400 MHz; $CDCl_3$): δ 7.35-7.27 (m, 3H, Ph), 7.20 (dd, *J* = 5.3, 3.1 Hz, 2H, Ph), 6.10-5.98 (m, 2H, HC=CH), 5.64-5.51 (m, 2H, H_3CCH=CH), 4.68 (ddtd, *J* = 9.8, 7.6, 3.3, 1.0 Hz, 1H, NCHCH$_2$), 4.20-4.12 (m, 2H, CH$_2$Ph), 3.89-3.82 (m, 1H,

C<u>H</u>CH_3), 3.27 (dd, *J* = 13.4, 3.4 Hz, 1H, CHC<u>H_2</u>O), 2.68 (dd, *J* = 13.4, 9.8 Hz, 1H, CHC<u>H_2</u>O), 2.53-2.47 (m, 1H, C<u>H_2</u>$CHCH_3$), 2.27-2.21 (m, 1H, C<u>H_2</u>$CHCH_3$), 1.72 (d, *J* = 6.7 Hz, 3H, C<u>H_3</u>CH=C), 1.18 (dd, *J* = 6.8, 5.0 Hz, 3H, CHC<u>H_3</u>); ^{13}C NMR ($CDCl_3$, 125 MHz): δ 176.6 (multiple signals), 143.7, 136.5, 135.4, 133.0, 131.3, 129.4, 128.9, 128.1, 127.7, 127.6, 127.3, 66.0, 66.0, 55.3, 38.1, 37.9, 37.4, 37.0, 37.0, 18.0, 16.5, 16.5; R_f 0.45 (5:1 hexanes:EtOAc). HRMS (ES) Calcd for $C_{18}{}^{13}CH_{23}NO_3$ $[M+H]^+$ 315.1784, found 315.1790.

(*S*,4*E*,6*E*)-2-Methylocta-4,6-dienoic acid (72')

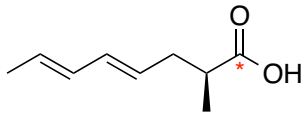

To compound **72** (34 mg, 0.11 mmol) dissolved in a 1:1 mixture of H_2O/THF at 0 °C, was added 30% H_2O_2 (48.7 μL, 0.43 mmol) and $LiOH.H_2O$ (9 mg, 0.22 mmol) and left to stir at 0 °C for 2 h. The solution was concentrated, acidified with 1M HCl to pH 1, extracted with EtOAc (2 x 10 mL) and the combined organic extracts dried over Na_2SO_4 and concentrated *in vacuo*. The crude extract was purified by flash column chromatography (SiO_2, 2:1 hexanes:EtOAc) to yield the product **72'** as a clear oil (11 mg, 64%). ^{1}H-NMR (400 MHz; $CDCl_3$): δ 8.10 (s, 1H, COO<u>H</u>), 6.09-5.98 (m, 2H, <u>H</u>C=C<u>H</u>), 5.66-5.59 (m, 1H, H_3CC<u>H</u>=C<u>H</u>), 5.52-5.45 (m, 1H, H_3CC<u>H</u>=C<u>H</u>), 2.55-2.42 (m, 2H, C<u>H</u>CH_3, C<u>H_2</u>$CHCH_3$), 2.23-2.18 (m, 1H, C<u>H_2</u>$CHCH_3$), 1.73 (d, *J* = 6.6 Hz, 3H,

$C\underline{H_3}CH=C$), 1.18 (dd, J = 6.9, 5.0 Hz, 3H, $C\underline{H_3}CH$); ^{13}C NMR ($CDCl_3$, 125 MHz): δ 181.8, 132.9, 131.3, 128.1, 127.5, 60.4, 36.3, 31.6, 29.0, 22.6, 21.0, 18.7, 18.0, 14.2, 14.1; R_f 0.4 (2:1 hexanes:EtOAc).

(*S*,4*E*,6*E*)-*S*-2-Acetamidoethyl 2-methylocta-4,6-dienethioate (73)

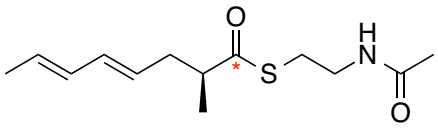

To compound **72'** (11 mg, 0.07 mmol) dissolved in dry DCM (2 mL), was added EDC (12 mg, 0.08 mmol) DMAP (catalytic) and SNAC (8 μL, 0.07 mmol). The reaction mixture was left to stir at ambient temperature for 17 h. The solution was quenched with NH_4Cl and extracted with DCM (3 x 10 mL). Combined organic extracts were washed with 1M HCl (3 x 10 mL), $NaHCO_3$ (3 x 10 mL), brine (10 mL), and dried over Na_2SO_4 and concentrated *in vacuo*. The crude extract was purified by flash column chromatography (SiO_2, 100% EtOAc) to yield the product (**73**) as a clear oil (10 mg, 55%) $[\alpha]_D^{25}$ = 9.46 (c = 0.37 g/100 mL, $CHCl_3$); IR ($CHCl_3$ cast) 2972, 2927, 2852, 1721, 1652 cm^{-1}, ^{1}H-NMR (400 MHz; $CDCl_3$): δ 6.06-5.97 (m, 2H, $\underline{H}C=C\underline{H}$), 5.81-5.76 (m, 1H, $N\underline{H}$), 5.66-5.57 (m, 1H, $H_3CC\underline{H}=C\underline{H}$), 5.48-5.40 (m, 1H, $H_3CC\underline{H}=C\underline{H}$), 3.44-3.39 (m, 2H, $SC\underline{H_2}$), 3.07-2.96 (m, 2H, $C\underline{H_2}NH$), 2.75-2.69 (m, 1H, $C\underline{H}CH_3$), 2.48-2.40 (m, 1H, $C\underline{H_2}CHCH_3$), 2.24-2.15 (m, 1H, $C\underline{H_2}CHCH_3$), 1.96-1.93 (m, 3H, $COC\underline{H_3}$), 1.73 (d, J

= 6.1 Hz, 3H, C$\underline{H_3}$CH=C), 1.17 (dd, 3H, *J* = 6.9, 5.4 Hz, CHC$\underline{H_3}$); ^{13}C NMR ($CDCl_3$, 125 MHz): δ 202.6, 170.2, 132.9, 131.1, 128.4, 127.2, 48.9, 48.4, 39.7, 37.0, 28.3, 23.2, 18.0, 17.1 R_f 0.5 (5:1 100% EtOAc). α_D^{25} = 9.46 (c = 0.37, $CHCl_3$); HRMS (ES) Calcd for $C_{12}{}^{13}CH_{21}NNaO_2S$ $[M+Na]^+$ 279.1219, found 279.1215.

6.11.6 Chaetoglobosin A

(*R*)-4-Benzyl-3-propionyloxazolidin-2-one (94)

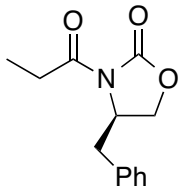

To a solution of (*R*)-4-benzyl-1,3-oxazolidin-2-one (5 g, 28.2 mmol) in dry THF (50 mL) at -78 °C, was added 2.5 M in THF n-BuLi (12.4 mL, 31.1 mmol) and left to stir for 15 min. Propionyl chloride (2.71 mL, 31.1 mmol) was then added, and the reaction mixture allowed to warm from -78 °C to room temperature over 2 h. The reaction was quenched with NH_4Cl (50 mL), extracted with DCM (2 x 50 mL) and the combined organic extracts washed with $NaHCO_3$ and then dried over Na_2SO_4 and concentrated *in vacuo*. Subsequent purification by flash column chromatography (SiO_2, 3:1 hexanes:EtOAc) afforded the product **94** as a colourless oil (5.9, 90%). IR ($CHCl_3$ cast) 3029, 2981, 2941, 1780, 1702 cm^{-1}; ^{1}H-NMR (700 MHz; $CDCl_3$): δ 7.33-7.25 (m, 3H,

Ph), 7.20-7.19 (m, 2H, Ph), 4.66 (ddt, *J* = 9.6, 7.7, 3.1 Hz, 1H, NC<u>H</u>), 4.20-4.14 (m, 2H, C<u>H</u>$_2$Ph), 3.29 (dd, *J* = 13.4, 3.3 Hz, 1H, C<u>H</u>$_2$O), 2.99-2.90 (m, 2H, C<u>H</u>$_2$CO), 2.76 (dd, *J* = 13.4, 9.6 Hz, 1H, C<u>H</u>$_2$O), 1.19 (t, *J* = 7.4 Hz, 3H, C<u>H</u>$_3$); ^{13}C NMR ($CDCl_3$, 125 MHz): δ 174.0, 153.5, 135.3, 129.4, 128.9, 127.3, 66.2, 55.1, 37.9, 29.2, 8.3. R_f 0.5 (2:1 hexanes:EtOAc). HRMS (ES) Calcd for $C_{13}H_{16}NO_3$ $[M+H]^+$ 234.1125, found 234.1125.

(*R*)-4-Benzyl-3-((*S*)-2-methylpent-4-enoyl)oxazolidin-2-one (95)

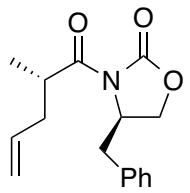

To a solution of **94** (2.50 g, 10.7 mmol) in dry THF (50 mL) at -78 °C, was added 1 M in THF NaHMDS (12.9 mL, 12.9 mmol) and left to stir for 30 min. Allyl bromide (1.11 mL, 1.2 mmol) was then added, and the reaction mixture allowed to warm from -78 °C to room temperature over 2 h. The reaction was quenched with H_2O (50 mL), concentrated *in vacuo* and then extracted with DCM (3 x 50 mL), dried over Na_2SO_4 and concentrated *in vacuo*. Subsequent purification by flash column chromatography (SiO_2, 5:1 hexanes:EtOAc) afforded the product **95** as a colourless oil (1.96, 67%). IR ($CHCl_3$ cast) 2981, 2941, 1780, 1702, 1604 cm^{-1}; ^{1}H-NMR (400 MHz; $CDCl_3$): δ 7.37-7.29 (m, 3H, Ph), 7.25-7.22 (m, 2H, Ph), 5.84 (ddt, *J* = 17.1, 10.1, 7.0 Hz, 1H, CH_2=C<u>H</u>), 5.14-5.06 (m, 2H, C<u>H</u>$_2$=CH), 4.70 (dd, *J* = 9.9, 7.4 Hz, 1H, NC<u>H</u>), 4.23-4.16 (m, 2H, C<u>H</u>$_2$Ph),

3.88 (sextet, J = 6.8 Hz, 1H, C<u>H</u>CH$_3$), 3.31 (dd, J = 13.3, 3.3 Hz, 1H, C<u>H$_2$</u>O), 2.71 (dd, J = 13.3, 9.9 Hz, 1H, C<u>H$_2$</u>O), 2.58-2.51 (m, 1H, C<u>H$_2$</u>CHCH$_3$), 2.29-2.22 (m, 1H, C<u>H$_2$</u>CHCH$_3$), 1.21 (d, J = 6.8 Hz, 3H, C<u>H$_3$</u>); ^{13}C NMR ($CDCl_3$, 125 MHz): δ 176.5, 153.1, 135.4, 135.3, 129.4, 128.9, 127.3, 117.2, 66.0, 55.4, 38.1, 38.0, 37.2, 16.4. R_f 0.65 (2:1 hexanes:EtOAc).

(*S*)-4-((*R*)-4-Benzyl-2-oxooxazolidin-3-yl)-3-methyl-4-oxobutanal (96)

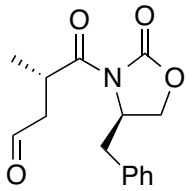

Compound **95** (5.00 g, 18.3 mmol) was dissolved in 9:1 DCM:MeOH (200 mL) and the solution cooled to -78 °C. Oxygen was bubbled through the system for 2 min, followed my ozone for an additional 20 min, by which time the solution had turned pale blue. The system was then purged with oxygen for 15 min, followed by reductive work up with PPh_3 (4.8 g, 18.3 mmol) at ambient temperature for 1 h. The crude reaction mixture was concentrated *in vacuo* purified by flash column chromatography (SiO_2, 2:1 hexanes:EtOAc) to yield the product **96** as a colourless oil (5.00 g, 99%). IR ($CHCl_3$ cast) 2974, 2933, 1779, 1722, 1697 cm^{-1}; ^{1}H-NMR (400 MHz; $CDCl_3$): δ 9.78 (s, 1H, C<u>H</u>O), 7.38-7.24 (m, 5H, Ph), 4.71-4.65 (m, 1H, NC<u>H</u>), 4.25-4.18 (m, 3H, C<u>H$_2$</u>Ph), 3.30 (dd, J = 13.5, 3.2 Hz, 1H, C<u>H$_2$</u>O), 3.13 (dd, J = 18.4, 9.4 Hz, 1H, CHOC<u>H$_2$</u>), 2.82 (dd, J = 13.6,

9.6 Hz, 1H, C$\underline{H_2}$O), 2.62 (ddd, *J* = 18.4, 4.6, 0.8 Hz, 1H, CHOC$\underline{H_2}$), 1.25 (d, *J* = 7.0 Hz, 3H, C$\underline{H_3}$); ^{13}C NMR ($CDCl_3$, 125 MHz): δ 199.9, 175.9, 153.0, 135.4, 129.4, 128.9, 127.3, 66.1, 55.3, 47.6, 37.6, 32.4, 17.0; R_f 0.4 (2:1 hexanes:EtOAc). α_D^{25} = -245.8 (c = 0.15, $CHCl_3$) HRMS (ES) Calcd for $C_{15}H_{18}NO_4$ $[M+H]^+$ 276.1230, found 276.1232.

(*R*)-3-((*S*)-3-(1,3-Dioxolan-2-yl)-2-methylpropanoyl)-4-benzyloxazolidin-2-one (97)

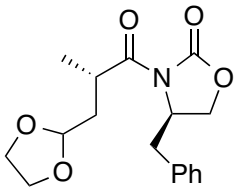

To a solution of compound **96** dissolved in ethylene glycol (7.09 mL, 127 mmol) and triethyl orthoformate (9.07 mL, 54.5 mmol), was added *p*-TsOH (cat.), and the mixture was refluxed at 55 °C for 17 h. The reaction was quenched with H_2O (50 mL), and diluted with DCM (3 x 50 mL). The aqueous layer was extracted with DCM (2 x 50 mL) and the combined organic extracts washed with H_2O (2 x 50 mL), $NaHCO_3$ (50 mL), brine (50 mL), and then dried over Na_2SO_4 and concentrated *in vacuo*. Subsequent purification by flash column chromatography (SiO_2, 2:1 hexanes:EtOAc) afforded (**97**) as a colourless oil (3.68 g, 64%). IR ($CHCl_3$ cast) 2925, 2852, 1779, 1735, 1698 cm^{-1}; ^{1}H-NMR (400 MHz; $CDCl_3$): δ 7.37-7.25 (m, 5H, Ph), 5.01 (dd, *J* = 5.1, 3.8 Hz, 1H, OOC$\underline{H}$), 4.68 (ddt, *J* = 10.1, 6.8, 3.4 Hz, 1H, NC$\underline{H}$), 4.20-4.05 (m, 3H, C$\underline{H_2}$Ph, C$\underline{H}$CH$_3$), 4.00-3.80 (m, 4H, OC$\underline{H_2}$C$\underline{H_2}$O), 3.40 (dd, *J* = 13.4, 3.2 Hz, 1H, C$\underline{H_2}$O), 2.67 (dd, *J* =

13.4, 10.1 Hz, 1H, C$\underline{H_2}$O), 2.35 (ddd, *J* = 14.2, 9.1, 5.1 Hz, 1H, CHC$\underline{H_2}$CH), 1.84 (dt, *J* = 14.1, 4.0 Hz, 1H, CHC$\underline{H_2}$CH), 1.25 (d, *J* = 7.0 Hz, 3H, C$\underline{H_3}$); ^{13}C NMR ($CDCl_3$, 125 MHz): δ 135.7, 135.4, 128.9, 102.8, 65.1, 55.6, 37.6, 31.9, 18.3; R_f 0.5 (2:1 hexanes:EtOAc); α_D^{25} = -18.1 (c = 0.42, DCM), HRMS (ES) Calcd for $C_{17}H_{22}NO_5$ $[M+H]^+$ 320.1492, found 320.1497.

(*S*)-3-(1,3-Dioxolan-2-yl)-2-methylpropan-1-ol (98)

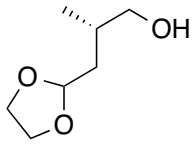

To a solution of compound **97** (3.68 g, 11.5 mmol) dissolved in Et_2O (100 mL) was added EtOH (1 mL) and $LiBH_4$ (754 mg, 34.6 mmol) at 0 °C. After 1 h, the reaction was quenched with NH_4Cl (50 mL), and the aqueous extracted with Et_2O (2 x 50 mL). The combined organic extracts were dried over Na_2SO_4 and concentrated *in vacuo* followed by flash column chromatography purification (SiO_2, 1:1 DCM:EtOAc), which afforded the product **98** as a colourless oil (1.11 g, 66%). IR ($CHCl_3$ cast) 3434, 2956, 2882, 1748, 1671 cm^{-1}; ^{1}H-NMR (400 MHz; $CDCl_3$): δ 4.97 (t, *J* = 4.8 Hz, 1H, OOC$\underline{H}$), 4.03-3.85 (m, 4H, OC$\underline{H_2}$C$\underline{H_2}$O), 3.58-3.45 (m, 2H, C$\underline{H_2}$OH), 2.34 (dd, *J* = 6.8, 5.7 Hz, 1H, O$\underline{H}$), 1.97-1.89 (m, 1H, C$\underline{H}$CH$_3$), 1.73 (ddd, *J* = 6.5, 4.7, 1.8 Hz, 2H, CHC$\underline{H_2}$CH), 0.99 (d, *J* = 6.9 Hz, 3H, C$\underline{H_3}$); ^{13}C NMR ($CDCl_3$, 125 MHz): δ 103.6, 64.8, 65.0, 38.1,

32.2, 17.9. R_f 0.3 (1:1 DCM:MeOH). α_D^{25} = -2.64 (c = 0.50, $CHCl_3$) HRMS (EI) Calcd for $C_9H_{17}O_2$ $[M-H]^{+\cdot}$ 145.0865, found 145.0862.

6.11.7 Cytochalasin E

(*S*)-2-Methylpent-4-en-1-ol (110)

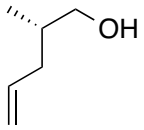

To a solution of common intermediate **95** (7.1 g, 26 mmol) dissolved in Et_2O (100 mL) was added EtOH (1 mL) and $LiBH_4$ (1.7 g, 78 mmol) at 0 °C. After 20 h, the reaction was quenched with NH_4Cl (50 mL), and the aqueous extracted with Et_2O (2 x 50 mL). The combined organic extracts were dried over Na_2SO_4 and concentrated *in vacuo* followed by flash column chromatography purification (SiO_2, 1:1 Et_2O:pentane), which afforded the product as a colourless oil (2.1 g, 81%). IR ($CHCl_3$ cast) 3316, 3077, 2958, 2930, 1644 cm^{-1}; ^{1}H-NMR (400 MHz; $CDCl_3$): δ 5.83 (ddt, *J* = 17.1, 10.1, 7.1 Hz, 1H, CH_2=C<u>H</u>), 5.09-5.02 (m, 2H, C<u>H$_2$</u>=CH), 3.49 (q, *J* = 7.0 Hz, 2H, C<u>H$_2$</u>OH), 2.23-2.15 (m, 1H, H-3), 1.96 (dtt, *J* = 13.8, 7.4, 1.2 Hz, 1H, CHC<u>H$_2$</u>CH), 1.76 (tq, *J* = 13.3, 6.6 Hz, 1H, C<u>H</u>CH_3), 1.36 (s, 1H, O<u>H</u>), 0.94 (d, *J* = 6.8 Hz, 3H, C<u>H$_3$</u>); R_f 0.6 (2:1 hexanes:EtOAc). $[\alpha]_D^{25}$ = 0.6 (*c* = 5.1 g/100 mL, $CHCl_3$).

(*S*)-3-((2*R*,4*S*)-2,4-Dimethylhept-6-enoyl)-4-isopropyloxazolidin-2-one (113)

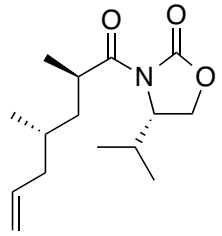

To a solution of compound **110** (693 mg, 6.93 mmol) in dry DCM (50 mL) and under argon, was added dry pyridine (1 mL, 12.4 mmol) and Tf_2O (2.12 mL, 12.6 mmol) at -78 °C. After 1 h, the reaction was quenched with NH_4Cl (50 mL), and the aqueous extracted with DCM (50 mL). The combined organic extracts were dried over Na_2SO_4 and concentrated *in vacuo.* The crude extract was immediately loaded onto a SiO_2 plug (roughly 6 cm of SiO_2 in a 6 cm column) and flushed through using 4:1 hexanes:EtOAc and the product eluted in the first 75 mL fraction, yielding the triflate (**111**) as a colourless oil (725 mg, 45%) after concentration *in vacuo*, R_f 0.9 (2:1 hexanes:EtOAc). To a solution of (S)-4-isopropyl-1,3-oxazolidin-2-one in dry THF (25 mL) at -78 °C, was added 1M in THF NaHMDS (6.56 mL, 6.56 mmol) and stirred for 45 min. To this solution was added compound **111** (725 mg, 232.2 mmol) in dry THF (10 mL), and left to stir at -78 °C for 2 h followed by an additional 2 h at 0 °C. The reaction was quenched with NH_4Cl (50 mL), the aqueous extracted with EtOAc (2 x 50 mL), and the combined organic extracts dried over Na_2SO_4 and concentrated *in vacuo* followed by flash column chromatography purification (SiO_2, 10:1 hexanes:EtOAc), to afford the product **113** as a

colourless oil (505 mg, 61%). IR ($CHCl_3$ cast) 2965, 2930, 1782, 1701, 1640 cm^{-1}; ^{1}H-NMR (600 MHz; $CDCl_3$): δ 5.78-5.72 (m, 1H, CH_2=C<u>H</u>), 5.01-4.97 (m, 2H, C<u>H$_2$</u>=CH), 4.46 (ddd, *J* = 8.4, 3.8, 3.1 Hz, 1H, NC<u>H</u>), 4.27-4.18 (m, 2H, C<u>H$_2$</u>O), 3.94-3.88 (m, 1H, C<u>H</u>CH$_3$), 2.34 (quintetd, *J* = 7.0, 3.9 Hz, 1H, CH$_3$C<u>H</u>CH$_3$), 2.08 (dddt, *J* = 13.8, 6.8, 5.5, 1.4 Hz, 1H, CH_2=CHC<u>H$_2$</u>), 1.92 (dtt, *J* = 14.0, 7.1, 1.2 Hz, 1H, CH_2=CHC<u>H$_2$</u>), 1.63-1.57 (m, 2H, CH_2=CHCH$_2$C<u>H</u>, CHC<u>H$_2$</u>CH), 1.41-1.37 (m, 1H, CHC<u>H$_2$</u>CH), 1.12 (d, *J* = 6.7 Hz, 3H, C<u>H$_3$</u>CHCO), 0.92 (dd, *J* = 6.7, 5.0 Hz, 6H, C<u>H$_3$</u>CHC<u>H$_3$</u>), 0.87 (d, *J* = 6.9 Hz, 3H, C<u>H$_3$</u>CHCH$_2$); ^{13}C NMR ($CDCl_3$, 125 MHz): δ 177.6, 137.0, 116.0, 63.0, 58.4, 41.6, 40.6, 35.3, 30.6, 28.4, 18.9, 18.0, 16.6, 14.6. R_f 0.6 (2:1 hexanes:EtOAc). α_D^{25} = 54.1 (c = 2.1 g/100 mL, $CHCl_3$)

(2*R*,4*S*)-2,4-Dimethylhept-6-en-1-ol (114)

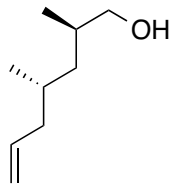

To a solution of compound **113** (485 mg, 1.8 mmol) dissolved in Et_2O (20 mL) was added EtOH (200 μL) and $LiBH_4$ (119 mg, 5.4 mmol) at 0 °C and the reaction mixture allowed to warm to room temperature over 6 h. The reaction was quenched with NH_4Cl (30 mL), and the aqueous fraction extracted with Et_2O (2 x 50 mL). The combined organic extracts were dried over Na_2SO_4 and concentrated *in vacuo* followed by flash

column chromatography purification (SiO_2, 6:1 hexanes:EtOAc), which afforded the product as a colourless oil (255 mg, quant.). IR ($CHCl_3$ cast) 3354, 2960, 2926, 1725, 1641 cm^{-1}; ^{1}H-NMR (600 MHz; $CDCl_3$): δ 5.80 (ddt, *J* = 17.0, 10.2, 7.0 Hz, 1H, CH_2=C<u>H</u>), 5.05-5.00 (m, 2H, C<u>H$_2$</u>=CH), 3.47 (ddd, *J* = 42.1, 10.4, 6.2 Hz, 2H, C<u>H$_2$</u>OH), 2.08-2.03 (m, 1H, CH_2=CHCH_2), 1.98-1.93 (m, 1H, CH_2=CHCH_2), 1.78-1.70 (m, 1H, C<u>H</u>CH_2OH), 1.66-1.60 (m, 1H, C<u>H</u>CH_2CH), 1.21-1.11 (m, 2H, CHC<u>H$_2$</u>CH), 0.91 (d, *J* = 6.7 Hz, 3H, C<u>H$_3$</u>CHCH_2OH), 0.89 (d, *J* = 6.6 Hz, 3H, C<u>H$_3$</u>CHCH_2); ^{13}C NMR ($CDCl_3$, 125 MHz): δ 137.5, 115.7, 69.0, 42.3, 40.1, 33.2, 29.9, 19.1, 16.3. R_f 0.5 (2:1 hexanes:EtOAc). $[\alpha]_D^{25}$ = 18.1 (*c* = 0.4 g/100 mL, $CHCl_3$)

***tert*-Butyl((2*R*,4*S*)-2,4-dimethylhept-6-enyloxy)dimethylsilane (115)**

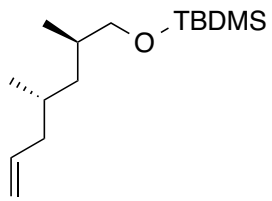

To a solution of **114** (100 mg, 0.7 mmol) dissolved in dry DMF (2 mL) was added imidazole (72 mg, 1.1 mmol) and TBDMS-Cl (133 mg, 0.88 mmol) and the reaction allowed to proceed at ambient temperature. After 3 h, the reaction mixture was diluted with hexanes (20 mL), and the aqueous fraction extracted with hexanes (2 x 20 mL). The combined organic extracts were washed with H_2O (3 x 50 mL), dried over Na_2SO_4 and concentrated *in vacuo* followed by flash column chromatography purification (SiO_2, 2:1

hexanes:EtOAc) to yield the product **115** as a pale yellow oil (117 mg, 65%). IR ($CHCl_3$ cast) 2958, 2929, 2858, 1726, 1641 cm^{-1}; ^{1}H-NMR (498 MHz; $CDCl_3$): δ 5.82-5.74 (m, 1H, CH_2=C<u>H</u>), 5.01-4.96 (m, 2H, C<u>H$_2$</u>=CH), 3.42 (dd, *J* = 9.7, 5.8 Hz, 1H, C<u>H$_2$</u>OTBDMS), 3.34 (dd, *J* = 9.7, 6.8 Hz, 1H, C<u>H$_2$</u>OTBDMS), 2.06-2.00 (m, 1H, CH_2=CHC<u>H$_2$</u>), 1.94-1.88 (m, 1H, CH_2=CHC<u>H$_2$</u>), 1.70-1.66 (m, 1H, C<u>H</u>CH_2OTBDMS), 1.63-1.56 (m, 1H, C<u>H</u>CH_2CH), 1.15 (ddd, *J* = 13.6, 9.3, 4.5 Hz, 1H, CHC<u>H$_2$</u>CH), 1.05 (ddd, *J* = 13.7, 9.2, 4.7 Hz, 1H, CHC<u>H$_2$</u>CH), 0.90 (s, 9H, TBDMS <u>*t*-Bu</u>), 0.85 (d, *J* = 2.5 Hz, 3H, C<u>H$_3$</u>$CHCH_2$O), 0.84 (d, *J* = 2.5 Hz, 3H, C<u>H$_3$</u>$CHCH_2$), 0.04 (s, 6H, TBDMS C<u>H$_3$</u>); ^{13}C NMR ($CDCl_3$, 125 MHz): δ 137.7, 115.5, 69.0, 42.3, 40.3, 33.3, 30.0, 26.0, 19.2, 16.5, -5.3. R_f 0.8 (2:1 hexanes:EtOAc)

7 References

1. Rawlings, B. J. Type I polyketide biosynthesis in bacteria (Part A--erythromycin biosynthesis). *Nat. Prod. Rep.*, **2001**, *18*, 190-227.
2. Rawlings, B. J. Type I polyketide biosynthesis in bacteria (part B). *Nat. Prod. Rep.*, **2001**, *18*, 231-281.
3. Staunton, J., and Weissman, K. J. Polyketide biosynthesis: a millennium review. *Nat. Prod. Rep.*, **2001**, *18*, 380-416.
4. Weissman, K. J., and Leadlay, P. F. Combinatorial biosynthesis of reduced polyketides. *Nat. Rev. Microbiol.*, **2005**, *3*, 925-936.
5. Li, J. W.-H., and Vederas, J. C. Drug discovery and natural products: end of an era or an endless frontier. *Science*, **2009**, *325*, 161-165.
6. Hertweck, C. The biosynthetic logic of polyketide diversity. *Angew. Chem. Int. Ed. Engl.*, **2009**, *48*, 4688-4716.
7. Endo, A. The discovery and development of HMG-CoA reductase inhibitors. *J. Lipid. Res.*, **1992**, *33*, 1569-1582.
8. Endo, A., and Hasumi, K. HMG-CoA reductase inhibitors. *Nat. Prod. Rep.*, **1993**, *10*, 541-550.
9. Brenner, S. L., and Korn, E. D. The effects of cytochalasins on actin polymerization and actin ATPase provide insights into the mechanism of polymerization. *J. Biol.*

Chem., **1980**, *255*, 841-844.

10. Udagawa, T., Yuan, J., Panigrahy, D., Chang, Y.-H., Shah, J., and D'Amato, R. J. Cytochalasin E, an Epoxide Containing *Aspergillus*-Derived Fungal Metabolite, Inhibits Angiogenesis and Tumor Growth. *J. Pharmacol. Exp. Ther.*, **2000**, *294*, 421-427.
11. Washington, J. A., and Wilson, W. R. Erythromycin: a microbial and clinical perspective after 30 years of clinical use (1). *Mayo Clin. Proc.*, **1985**, *60*, 189-203.
12. Hazuda, D., Blau, C. U., Felock, P., Hastings, J., Pramanik, B., Wolfe, A., Bushman, F., Farnet, C., Goetz, M., Williams, M., Silverman, K., Lingham, R., and Singh, S. Isolation and characterization of novel human immunodeficiency virus integrase inhibitors from fungal metabolites. *Antivir. Chem. Chemother.*, **1999**, *10*, 63-70.
13. Smith, S., and Tsai, S. C. The type I fatty acid and polyketide synthases: a tale of two megasynthases. *Nat. Prod. Rep.*, **2007**, *24*, 1041-1072.
14. Elovson, J., and Vagelos, P. R. Acyl carrier protein. X. Acyl carrier protein synthetase. *J. Biol. Chem.*, **1968**, *243*, 3603-3611.
15. Keatinge-Clay, A. T. The structures of type I polyketide synthases. *Nat. Prod. Rep.*, **2012**, *29*, 1050-1073.
16. Weissman, K. J. The structural biology of biosynthetic megaenzymes. *Nat. Chem. Biol.*, **2015**, *11*, 660-670.
17. Caffrey, P., Bevitt, D. J., Staunton, J., and Leadlay, P. F. Identification of DEBS 1, DEBS 2 and DEBS 3, the multienzyme polypeptides of the erythromycin-producing

polyketide synthase from *Saccharopolyspora erythraea*. *FEBS Lett.*, **1992**, *304*, 225-228.

18. Wiesmann, K. E., Cortés, J., Brown, M. J., Cutter, A. L., Staunton, J., and Leadlay, P. F. Polyketide synthesis in vitro on a modular polyketide synthase. *Chem. Biol.*, **1995**, *2*, 583-589.
19. Bycroft, M., Weissman, K. J., Staunton, J., and Leadlay, P. F. Efficient purification and kinetic characterization of a bimodular derivative of the erythromycin polyketide synthase. *Eur. J. Biochem.*, **2000**, *267*, 520-526.
20. Lowry, B., Robbins, T., Weng, C. H., O'Brien, R. V., Cane, D. E., and Khosla, C. In vitro reconstitution and analysis of the 6-deoxyerythronolide B synthase. *J. Am. Chem. Soc.*, **2013**, *135*, 16809-16812.
21. Edwards, A. L., Matsui, T., Weiss, T. M., and Khosla, C. Architectures of whole-module and bimodular proteins from the 6-deoxyerythronolide B synthase. *J. Mol. Biol.*, **2014**, *426*, 2229-2245.
22. Townsend, C. A. Aflatoxin and deconstruction of type I, iterative polyketide synthase function. *Nat. Prod. Rep.*, **2014**, *31*, 1260-1265.
23. Chooi, Y. H., and Tang, Y. Navigating the fungal polyketide chemical space: from genes to molecules. *J. Org. Chem.*, **2012**, *77*, 9933-9953.
24. Cox, R. J., and Simpson, T. J. Fungal type I polyketide synthases. *Methods Enzymol.*, **2009**, *459*, 49-78.
25. Auclair, K., Kennedy, J., Hutchinson, C. R., and Vederas, J. C. Conversion of cyclic nonaketides to lovastatin and compactin by a lovC deficient mutant of *Aspergillus*

terreus. *Bioorg. Med. Chem. Lett.*, **2001**, *11*, 1527-1531.

26. Hutchinson, C. R., Kennedy, J., Park, C., Kendrew, S., Auclair, K., and Vederas, J. Aspects of the biosynthesis of non-aromatic fungal polyketides by iterative polyketide synthases. *Antonie Van Leeuwenhoek*, **2000**, *78*, 287-295.
27. Ma, S. M., and Tang, Y. Biochemical characterization of the minimal polyketide synthase domains in the lovastatin nonaketide synthase LovB. *FEBS J.*, **2007**, *274*, 2854-2864.
28. Ma, S. M., Li, J. W., Choi, J. W., Zhou, H., Lee, K. K., Moorthie, V. A., Xie, X., Kealey, J. T., Da Silva, N. A., Vederas, J. C., and Tang, Y. Complete reconstitution of a highly reducing iterative polyketide synthase. *Science*, **2009**, *326*, 589-592.
29. Crawford, J. M., Korman, T. P., Labonte, J. W., Vagstad, A. L., Hill, E. A., Kamari-Bidkorpeh, O., Tsai, S. C., and Townsend, C. A. Structural basis for biosynthetic programming of fungal aromatic polyketide cyclization. *Nature*, **2009**, *461*, 1139-1143.
30. Dimroth, P., Walter, H., and Lynen, F. Biosynthesis of 6-methylsalicylic acid. *Eur. J. Biochem.*, **1970**, *13*, 98-110.
31. Beck, J., Ripka, S., Siegner, A., Schiltz, E., and Schweizer, E. The multifunctional 6-methylsalicylic acid synthase gene of *Penicillium patulum*. Its gene structure relative to that of other polyketide synthases. *Eur. J. Biochem.*, **1990**, *192*, 487-498.
32. Spencer, J. B., and Jordan, P. M. Purification and properties of 6-methylsalicylic acid synthase from *Penicillium patulum*. *Biochem. J.*, **1992**, *288*, 839-846.
33. Moriguchi, T., Kezuka, Y., Nonaka, T., Ebizuka, Y., and Fujii, I. Hidden function

of catalytic domain in 6-methylsalicylic acid synthase for product release. *J. Biol. Chem.*, **2010**, *285*, 15637-15643.

34. Zhou, H., Qiao, K., Gao, Z., Meehan, M. J., Li, J. W., Zhao, X., Dorrestein, P. C., Vederas, J. C., and Tang, Y. Enzymatic synthesis of resorcylic acid lactones by cooperation of fungal iterative polyketide synthases involved in hypothemycin biosynthesis. *J. Am. Chem. Soc.*, **2010**, *132*, 4530-4531.
35. Zhou, H., Gao, Z., Qiao, K., Wang, J., Vederas, J. C., and Tang, Y. A fungal ketoreductase domain that displays substrate-dependent stereospecificity. *Nat. Chem. Biol.*, **2012**, *8*, 331-333.
36. Gao, Z., Wang, J., Norquay, A. K., Qiao, K., Tang, Y., and Vederas, J. C. Investigation of fungal iterative polyketide synthase functions using partially assembled intermediates. *J. Am. Chem. Soc.*, **2013**, *135*, 1735-1738.
37. Strieker, M., Tanović, A., and Marahiel, M. A. Nonribosomal peptide synthetases: structures and dynamics. *Curr. Opin. Struct. Biol.*, **2010**, *20*, 234-240.
38. Du, L., and Lou, L. PKS and NRPS release mechanisms. *Nat Prod Rep*, **2010**, *27*, 255-278.
39. Bailey, A. M., Cox, R. J., Harley, K., Lazarus, C. M., Simpson, T. J., and Skellam, E. Characterisation of 3-methylorcinaldehyde synthase (MOS) in *Acremonium strictum*: first observation of a reductive release mechanism during polyketide biosynthesis. *Chem. Commun.*, **2007**, 4053-4055.
40. Gaitatzis, N., Kunze, B., and Müller, R. In vitro reconstitution of the myxochelin biosynthetic machinery of Stigmatella aurantiaca Sg a15: Biochemical

characterization of a reductive release mechanism from nonribosomal peptide synthetases. *Proc. Natl. Acad. Sci. U. S. A.*, **2001**, *98*, 11136-11141.

41. Li, Y., Weissman, K. J., and Müller, R. Myxochelin biosynthesis: direct evidence for two- and four-electron reduction of a carrier protein-bound thioester. *J. Am. Chem. Soc.*, **2008**, *130*, 7554-7555.

42. Read, J. A., and Walsh, C. T. The lyngbyatoxin biosynthetic assembly line: chain release by four-electron reduction of a dipeptidyl thioester to the corresponding alcohol. *J. Am. Chem. Soc.*, **2007**, *129*, 15762-15763.

43. Halo, L. M., Marshall, J. W., Yakasai, A. A., Song, Z., Butts, C. P., Crump, M. P., Heneghan, M., Bailey, A. M., Simpson, T. J., Lazarus, C. M., and Cox, R. J. Authentic heterologous expression of the tenellin iterative polyketide synthase nonribosomal peptide synthetase requires coexpression with an enoyl reductase. *ChemBioChem*, **2008**, *9*, 585-594.

44. Bergmann, S., Schümann, J., Scherlach, K., Lange, C., Brakhage, A. A., and Hertweck, C. Genomics-driven discovery of PKS-NRPS hybrid metabolites from Aspergillus nidulans. *Nat. Chem. Biol.*, **2007**, *3*, 213-217.

45. Sims, J. W., and Schmidt, E. W. Thioesterase-like role for fungal PKS-NRPS hybrid reductive domains. *J. Am. Chem. Soc.*, **2008**, *130*, 11149-11155.

46. Hertweck, C., Luzhetskyy, A., Rebets, Y., and Bechthold, A. Type II polyketide synthases: gaining a deeper insight into enzymatic teamwork. *Nat. Prod. Rep.*, **2007**, *24*, 162-190.

47. Shen, B. Biosynthesis of aromatic polyketides. *Top. Curr. Chem.*, **2000**, *209*, 1-51.

48. Austin, M. B., and Noel, J. P. The chalcone synthase superfamily of type III polyketide synthases. *Nat. Prod. Rep.*, **2003**, *20*, 79-110.

49. Katsuyama, Y., and Ohnishi, Y. Type III polyketide synthases in microorganisms. *Methods Enzymol.*, **2012**, *515*, 359-377.

50. Hashimoto, M., Nonaka, T., and Fujii, I. Fungal type III polyketide synthases. *Nat. Prod. Rep.*, **2014**, *31*, 1306-1317.

51. Scott, P. M., Van Walbeek, W., and MacLean, W. M. Cladosporin, a new antifungal metabolite from *Cladosporium cladosporioides*. *J. Antibiot. (Tokyo)*, **1971**, *24*, 747-755.

52. Grove, J. F. New metabolic products of *Aspergillus flavus*. I. Asperentin, its methyl ethers, and 5'-hydroxyasperentin. *J. Chem. Soc. Perkin 1*, **1972**, *19*, 2400-2406.

53. Wang, S., Li, X. M., Teuscher, F., Li, D. L., Diesel, A., Ebel, R., Proksch, P., and Wang, B. G. Chaetopyranin, a benzaldehyde derivative, and other related metabolites from *Chaetomium globosum*, an endophytic fungus derived from the marine red alga *Polysiphonia urceolata*. *J. Nat. Prod.*, **2006**, *69*, 1622-1625.

54. Flewelling, A. J., Johnson, J. A., and Gray, C. A. Antimicrobials from the marine algal endophyte *Penicillium* sp. *Nat. Prod. Commun.*, **2013**, *8*, 373-374.

55. Anke, H., and Zähner, H. Metabolic products of microorganisms. 170. On the antibiotic activity of cladosporin. *Arch. Microbiol.*, **1978**, *116*, 253-257.

56. Slack, G. J., Puniani, E., Frisvad, J. C., Samson, R. A., and Miller, J. D. Secondary metabolites from *Eurotium* species, *Aspergillus calidoustus* and *A. insuetus* common in Canadian homes with a review of their chemistry and biological

activities. *Mycol. Res.*, **2009**, *113*, 480-490.

57. Wang, X., Radwan, M. M., Tarawneh, A. H., Gao, J., Wedge, D. E., Rosa, L. H., Cutler, H. G., and Cutler, S. J. Antifungal activity against plant pathogens of metabolites from the endophytic fungus *Cladosporium cladosporioides*. *J. Agric. Food Chem.*, **2013**, *61*, 4551.

58. Anke, H. Metabolic products of microorganisms. 184. On the mode of action of cladosporin. *J. Antibiot.*, **1979**, *32*, 952.

59. Kimura, Y., Shimomura, N., Tanigawa, F., Fujioka, S., and Shimada, A. Plant growth activities of aspyran, asperentin, and its analogues produced by the fungus *Aspergillus* sp. *Z. Naturforsch. C Bio. Sci.*, **2012**, *67*, 587-593.

60. Miller, J. D., Sun, M., Gilyan, A., Roy, J., and Rand, T. G. Inflammation-associated gene transcription and expression in mouse lungs induced by low molecular weight compounds from fungi from the built environment. *Chem. Biol. Interact.*, **2010**, *183*, 113-124.

61. Hoepfner, D., McNamara, C. W., Lim, C. S., Studer, C., Riedl, R., Aust, T., McCormack, S. L., Plouffe, D. M., Meister, S., Schuierer, S., Plikat, U., Hartmann, N., Staedtler, F., Cotesta, S., Schmitt, E. K., Petersen, F., Supek, F., Glynne, R. J., Tallarico, J. A., Porter, J. A., Fishman, M. C., Bodenreider, C., Diagana, T. T., Movva, N. R., and Winzeler, E. A. Selective and specific inhibition of the *Plasmodium falciparum* lysyl-tRNA synthetase by the fungal secondary metabolite cladosporin. *Cell Host Microbe*, **2012**, *11*, 654-663.

62. Khan, S., Garg, A., Camacho, N., Van Rooyen, J., Kumar Pole, A., Belrhali, H.,

Ribas de Pouplana, L., Sharma, V., and Sharma, A. Structural analysis of malaria-parasite lysyl-tRNA synthetase provides a platform for drug development. *Acta Crystallogr. D Biol. Crystallogr.*, **2013**, *69*, 785-795.

63. Khan, S., Sharma, A., Belrhali, H., Yogavel, M., and Sharma, A. Structural basis of malaria parasite lysyl-tRNA synthetase inhibition by cladosporin. *J. Struct. Funct. Genomics*, **2014**, *15*, 63-71.

64. Guiguemde, W. A., and Guy, R. K. An all-purpose antimalarial drug target. *Cell Host Microbe*, **2012**, *11*, 555-557.

65. Reese, P. B., Rawlings, B. J., Ramer, S. E., and Vederas, J. C. Comparison of stereochemistry of fatty acid and cladosporin biosynthesis in *Cladosporium cladosporioides* using deuterium-decoupled proton, carbon-13 NMR shift correlation. *J. Am. Chem. Soc.*, **1988**, *110*, 316-318.

66. Rawlings, B. J., Reese, P. B., Ramer, S. E., and Vederas, J. C. Comparison of fatty acid and polyketide biosynthesis: stereochemistry of cladosporin and oleic acid formation in *Cladosporium cladosporioides*. *J. Am. Chem. Soc.*, **1989**, *111*, 3382-3390.

67. Jacyno, J. M., Harwood, J. S., Cutler, H. G., and Lee, M. K. Isocladosporin, a biologically active isomer of cladosporin from *Cladosporium cladosporioides*. *J. Nat. Prod.*, **1993**, *56*, 1397-1401.

68. Zheng, H., Zhao, C., Fang, B., Jing, P., Yang, J., Xie, X., and She, X. Asymmetric total synthesis of cladosporin and isocladosporin. *J. Org. Chem.*, **2012**, *77*, 5656-5663.

69. Mohapatra, D. K., Maity, S., Rao, T. S., Yadav, J. S., and Sridhar, B. An efficient formal total synthesis of cladosporin. *Eur. J. Org. Chem.*, **2013**, *2013*, 2859-2863.

70. Zhou, H., Qiao, K., Gao, Z., Vederas, J. C., and Tang, Y. Insights into radicicol biosynthesis via heterologous synthesis of intermediates and analogs. *J. Biol. Chem.*, **2010**, *285*, 41412-41421.

71. Arai, K., Rawlings, B. J., Yoshizawa, Y., and Vederas, J. C. Biosyntheses of antibiotic A26771B by *Penicillium turbatum* and dehydrocurvularin by *Alternaria cinerariae*: comparison of stereochemistry of polyketide and fatty acid enoyl thiol ester reductases. *J. Am. Chem. Soc.*, **1989**, *111*, 3391 - 3399.

72. Yoshizawa, Y., Li, Z., Reese, P. B., and Vederas, J. C. Intact incorporation of acetate-derived di-and tetraketides during biosynthesis of dehydrocurvularin, a macrolide phytotoxin from *Alternaria cinerariae*. *J. Am. Chem. Soc.*, **1990**, *112*, 3212-3213.

73. Li, Z., Martin, F. M., and Vederas, J. C. Biosynthetic incorporation of labeled tetraketide intermediates into dehydrocurvularin, a phytotoxin from *Alternaria cinerariae*, with assistance of. β-oxidation inhibitors. *J. Am. Chem. Soc.*, **1992**, *114*, 1531-1533.

74. Liu, Y., Li, Z., and Vederas, J. C. Biosynthetic incorporation of advanced precursors into dehydrocurvularin, a polyketide phytotoxin from *Alternaria cinerariae*. *Tetrahedron*, **1998**, *54*, 15937-15958.

75. Medema, M. H., Blin, K., Cimermancic, P., de Jager, V., Zakrzewski, P., Fischbach, M. A., Weber, T., Takano, E., and Breitling, R. antiSMASH: rapid

identification, annotation and analysis of secondary metabolite biosynthesis gene clusters in bacterial and fungal genome sequences. *Nucleic Acids Res.*, **2011**, *39*, W339 - W346.

76. Salamov, A. A., and Solovyev, V. V. Ab initio gene finding in *Drosophila* genomic DNA. *Genome Res.*, **2000**, *10*, 516-522.

77. Larionov, V., Kouprina, N., Eldarov, M., Perkins, E., Porter, G., and Resnick, M. A. Transformation-associated recombination between diverged and homologous DNA repeats is induced by strand breaks. *Yeast*, **1994**, *10*, 93-104.

78. Waring, R. B., May, G. S., and Morris, N. R. Characterization of an inducible expression system in *Aspergillus nidulans* using alcA and tubulin-coding genes. *Gene*, **1989**, *79*, 119-130.

79. Zhou, H., Zhan, J., Watanabe, K., Xie, X., and Tang, Y. A polyketide macrolactone synthase from the filamentous fungus *Gibberella zeae*. *Proc. Natl. Acad. Sci. U. S. A.*, **2008**, *105*, 6249-6254.

80. Wang, S., Xu, Y., Maine, E. A., Wijeratne, E. M., Espinosa-Artiles, P., Gunatilaka, A. A., and Molnar, I. Functional characterization of the biosynthesis of radicicol, an Hsp90 inhibitor resorcylic acid lactone from *Chaetomium chiversii*. *Chem. Biol.*, **2008**, *15*, 1328-1338.

81. Li, Y., Image, I. I., Xu, W., Image, I., Tang, Y., and Image, I. Classification, prediction, and verification of the regioselectivity of fungal polyketide synthase product template domains. *J. Biol. Chem.*, **2010**, *285*, 22764-22773.

82. Zhang, Y. I-TASSER server for protein 3D structure prediction. *BMC*

Bioinformatics, **2008**, *9*, 40.

83. Zhang, Y. I-TASSER: fully automated protein structure prediction in CASP8. *Proteins*, **2009**, *77 Suppl 9*, 100-113.

84. Roy, A., Kucukural, A., and Zhang, Y. I-TASSER: a unified platform for automated protein structure and function prediction. *Nat. Protoc.*, **2010**, *5*, 725-738.

85. Hanwell, M. D., Curtis, D. E., Lonie, D. C., Vandermeersch, T., Zurek, E., and Hutchison, G. R. Avogadro: an advanced semantic chemical editor, visualization, and analysis platform. *J. Cheminform.*, **2012**, *4*, 17.

86. Trott, O., and Olson, A. J. AutoDock Vina: improving the speed and accuracy of docking with a new scoring function, efficient optimization, and multithreading. *J. Comput. Chem.*, **2010**, *31*, 455-461.

87. Guo, M., Ignatov, M., Musier-Forsyth, K., Schimmel, P., and Yang, X. L. Crystal structure of tetrameric form of human lysyl-tRNA synthetase: Implications for multisynthetase complex formation. *Proc. Natl. Acad. Sci. U. S. A.*, **2008**, *105*, 2331-2336.

88. Robeson, D. J., Strobel, G. A., and Strange, R. N. The identification of a major phytotoxic component from *Alternaria macrospora* as αβ-dehydrocurvularin. *J. Nat. Prod.*, **1985**, *48*, 139-141.

89. Jeon, Y.-T., Ryu, K.-H., Kang, M.-K., Park, S.-H., Yun, H., Pham, Q. T., and Kim, S.-U. Alternariol monomethyl ether and α, β-dehydrocurvularin from endophytic fungi *Alternaria* spp. inhibit appressorium formation of *Magnaporthe grisea*. *J. Korean Soc. Appl. Bi.*, **2010**, *53*, 39-42.

90. Hyeon, S.-B., Ozaki, A., Suzuki, A., and Tamura, S. Isolation of αβ-dehydrocurvularin and β-hydroxycurvularin from *Alternaria* tomato as sporulation-suppressing factors. *Agric. Biol. Chem.*, **1976**, *40*, 1663-1664.

91. Cimmino, A., Andolfi, A., Abouzeid, M., and Evidente, A. Polyphenols as fungal phytotoxins, seed germination stimulants and phytoalexins. *Phytochem. Rev.*, **2013**, *12*, 653-672.

92. Jiang, S., Qiang, S., Zhu, Y., and Dong, Y. Isolation and phytotoxicity of a metabolite from *Curvularia eragrostidis* and characterisation of its modes of action. *Ann. Appl. Biol.*, **2008**, *152*, 103-111.

93. Greve, H., Schupp, P. J., Eguereva, E., Kehraus, S., Kelter, G., Maier, A., Fiebig, H. H., and Konig, G. M. Apralactone A and a new stereochemical class of curvularins from the marine-derived fungus sp. *Eur. J. Org. Chem.*, **2008**, *2008*, 5085-5092.

94. Yao, Y., Hausding, M., Erkel, G., Anke, T., Forstermann, U., and Kleinert, H. Sporogen, S14-95, and *S*-curvularin, three inhibitors of human inducible nitric-oxide synthase expression isolated from fungi. *Mol. Pharmacol.*, **2003**, *63*, 383-391.

95. Kusano, M., Nakagami, K., Fujioka, S., Kawano, T., Shimada, A., and Kimura, Y. βγ-Dehydrocurvularin and related compounds as nematicides of *Pratylenchus penetrans* from the fungus *Aspergillus* sp. *Biosci., Biotechnol., Biochem.*, **2003**, *67*, 1413-1416.

96. He, J., Wijeratne, E. M., Bashyal, B. P., Zhan, J., Seliga, C. J., Liu, M. X., Pierson, E. E., Pierson, L. S., VanEtten, H. D., and Gunatilaka, A. A. Cytotoxic and other metabolites of *Aspergillus* inhabiting the rhizosphere of Sonoran desert plants. *J.*

Nat. Prod., **2004**, *67*, 1985-1991.

97. Xie, L. W., Ouyang, Y. C., Zou, K., Wang, G. H., Chen, M. J., Sun, H. M., Dai, S. K., and Li, X. Isolation and difference in anti-*Staphylococcus aureus* bioactivity of curvularin derivates from fungus *Eupenicillium* sp. *Appl. Biochem. Biotechnol.*, **2009**, *159*, 284-293.
98. Santagata, S., Xu, Y. M., Wijeratne, E. M., Kontnik, R., Rooney, C., Perley, C. C., Kwon, H., Clardy, J., Kesari, S., Whitesell, L., Lindquist, S., and Gunatilaka, A. A. Using the heat-shock response to discover anticancer compounds that target protein homeostasis. *ACS Chem. Biol.*, **2012**, *7*, 340-349.
99. Rudolph, K., Serwe, A., and Erkel, G. Inhibition of TGF-beta signaling by the fungal lactones (*S*)-curvularin, dehydrocurvularin, oxacyclododecindione and galiellalactone. *Cytokine*, **2013**, *61*, 285-296.
100. Almassi, F., Ghisalberti, E. L., Skelton, B. W., and White, A. H. Structural study of dehydrocurvularin, an inhibitor of microtubule assembly. *Aust. J. Chem.*, **1994**, *47*, 1193-1197.
101. Liang, Q., Sun, Y., Yu, B., She, X., and Pan, X. First total syntheses and spectral data corrections of 11-α-methoxycurvularin and 11-β-methoxycurvularin. *J. Org. Chem.*, **2007**, *72*, 9846-9849.
102. Miyagi, T., and Kuwahara, S. A concise synthetic approach to β,γ-dehydrocurvularin: synthesis of (+/-)-di-O-methyl-β,γ-dehydrocurvularin. *Biosci., Biotechnol., Biochem.,* **2007**, *71*, W339-W346.
103. Reddy, G. V., Kumar, R. S. C., Babu, K. S., and Rao, J. M. Stereoselective

syntheses of 11-α-methoxycurvularin and 11-β-methoxycurvularin. *Tetrahedron Lett.*, **2009**, *50*, 4117-4120.

104. Rajesh, K., Suresh, V., Selvam, J. J. P., Babu, D. C., and Venkateswarlu, Y. Stereoselective total synthesis of (11β)-11-methoxycurvularin. *Helv. Chim. Acta.*, **2010**, *93*, 147-152.
105. Tadross, P. M., Virgil, S. C., and Stoltz, B. M. Aryne acyl-alkylation in the general and convergent synthesis of benzannulated macrolactone natural products: an enantioselective synthesis of (-)-curvularin. *Org. Lett.*, **2010**, *12*, 1612-1614.
106. Yadav, J. S., Raju, A., Ravindar, K., and Subba Reddy, B. V. Stereoseletive total synthesis of 11-α-and 11-β-methoxycurvularins. *Synthesis*, **2010**, *2010*, 797-802.
107. Xu, J., Jiang, C. S., Zhang, Z. L., Ma, W. Q., and Guo, Y. W. Recent progress regarding the bioactivities, biosynthesis and synthesis of naturally occurring resorcinolic macrolides. *Acta. Pharm. Sin.*, **2014**, *35*, 316-330.
108. Birch, A. J., Musgrave, O. C., Rickards, R. W., and Smith, H. 638. Studies in relation to biosynthesis. Part XX. The structure and biosynthesis of curvularin. *J. Chem. Soc.*, **1959**, 3391-3399.
109. Xu, Y., Espinosa-Artiles, P., Schubert, V., Xu, Y. M., Zhang, W., Lin, M., Gunatilaka, A. A., Sussmuth, R., and Molnar, I. Characterization of the biosynthetic genes for 10,11-dehydrocurvularin, a heat shock response-modulating anticancer fungal polyketide from *Aspergillus terreus*. *Appl. Environ. Microbiol.*, **2013**, *79*, 2038-2047.
110. Simpson, T. J. Fungal polyketide biosynthesis - a personal perspective. *Nat. Prod.*

Rep., **2014**, *31*, 1247-1252.

111. Xu, Y., Zhou, T., Espinosa-Artiles, P., Tang, Y., Zhan, J., and Molnar, I. Insights into the biosynthesis of 12-membered resorcylic acid lactones from heterologous production in *Saccharomyces cerevisiae*. *ACS Chem. Biol.*, **2014**, *9*, 1119-1127.
112. Gaffoor, I., and Trail, F. Characterization of two polyketide synthase genes involved in zearalenone biosynthesis in *Gibberella zeae*. *Appl. Environ. Microbiol.*, **2006**, *72*, 1793-1799.
113. Kim, Y. T., Lee, Y. R., Jin, J., Han, K. H., Kim, H., Kim, J. C., Lee, T., Yun, S. H., and Lee, Y. W. Two different polyketide synthase genes are required for synthesis of zearalenone in *Gibberella zeae*. *Mol. Microbiol.*, **2005**, *58*, 1102-1113.
114. Solovyev, V., Kosarev, P., Seledsov, I., and Vorobyev, D. Automatic annotation of eukaryotic genes, pseudogenes and promoters. *Genome Biol.*, **2006**, *7 Suppl 1*, S10. 1 - 12.
115. Liew, C. W., Nilsson, M., Chen, M. W., Sun, H., Cornvik, T., Liang, Z. X., and Lescar, J. Crystal structure of the acyltransferase domain of the iterative polyketide synthase in enediyne biosynthesis. *J. Biol. Chem.*, **2012**, *287*, 23203-23215.
116. Xu, Y., Zhou, T., Zhou, Z., Su, S., Roberts, S. A., Montfort, W. R., Zeng, J., Chen, M., Zhang, W., Lin, M., Zhan, J., and Molnar, I. Rational reprogramming of fungal polyketide first-ring cyclization. *Proc. Natl. Acad. Sci. U. S. A.*, **2013**, *110*, 5398-5403.
117. Winter, J. M., Cascio, D., Dietrich, D., Sato, M., Watanabe, K., Sawaya, M. R., Vederas, J. C., and Tang, Y. Biochemical and structural basis for controlling

chemical modularity in fungal polyketide biosynthesis. *J. Am. Chem. Soc.*, **2015**, *137*, 9885-9893.

118. Alberts, A. W., Chen, J., Kuron, G., Hunt, V., Huff, J., Hoffman, C., Rothrock, J., Lopez, M., Joshua, H., Harris, E., Patchett, A., Monaghan, R., Currie, S., Stapley, E., Albers-Schonberg, G., Hensens, O., Hirshfield, J., Hoogsteen, K., Liesch, J., and Springer, J. Mevinolin: a highly potent competitive inhibitor of hydroxymethylglutaryl-coenzyme A reductase and a cholesterol-lowering agent. *Proc. Natl. Acad. Sci. U. S. A.*, **1980**, *77*, 3957-3961.
119. Kennedy, J., Auclair, K., Kendrew, S. G., Park, C., Vederas, J. C., and Hutchinson, C. R. Modulation of polyketide synthase activity by accessory proteins during lovastatin biosynthesis. *Science*, **1999**, *284*, 1368-1372.
120. Campbell, C. D., and Vederas, J. C. Biosynthesis of lovastatin and related metabolites formed by fungal iterative PKS enzymes. *Biopolymers*, **2010**, *93*, 755-763.
121. Barriuso, J., Nguyen, D. T., Li, J. W., Roberts, J. N., MacNevin, G., Chaytor, J. L., Marcus, S. L., Vederas, J. C., and Ro, D. K. Double oxidation of the cyclic nonaketide dihydromonacolin L to monacolin J by a single cytochrome P450 monooxygenase, LovA. *J. Am. Chem. Soc.*, **2011**, *133*, 8078-8081.
122. Xie, X., Watanabe, K., Wojcicki, W. A., Wang, C. C., and Tang, Y. Biosynthesis of lovastatin analogs with a broadly specific acyltransferase. *Chem. Biol.*, **2006**, *13*, 1161-1169.
123. Xie, X., and Tang, Y. Efficient synthesis of simvastatin by use of whole-cell

biocatalysis. *Appl. Environ. Microbiol.*, **2007**, *73*, 2054-2060.

124. Xu, W., Chooi, Y. H., Choi, J. W., Li, S., Vederas, J. C., Da Silva, N. A., and Tang, Y. LovG: the thioesterase required for dihydromonacolin L release and lovastatin nonaketide synthase turnover in lovastatin biosynthesis. *Angew. Chem. Int. Ed. Engl.*, **2013**, *52*, 6472-6475.
125. Oikawa, H., and Tokiwano, T. Enzymatic catalysis of the Diels-Alder reaction in the biosynthesis of natural products. *Nat. Prod. Rep.*, **2004**, *21*, 321-352.
126. Kelly, W. L. Intramolecular cyclizations of polyketide biosynthesis: mining for a "Diels-Alderase". *Org. Biomol. Chem.*, **2008**, *6*, 4483-4493.
127. Kim, H. J., Ruszczycky, M. W., and Liu, H. W. Current developments and challenges in the search for a naturally selected Diels-Alderase. *Curr. Opin. Chem. Biol.*, **2012**, *16*, 124-131.
128. Kato, N., Nogawa, T., Hirota, H., Jang, J. H., Takahashi, S., Ahn, J. S., and Osada, H. A new enzyme involved in the control of the stereochemistry in the decalin formation during equisetin biosynthesis. *Biochem. Biophys. Res. Commun.*, **2015**, *460*, 210-215.
129. Tamm, C. (1980). The biosynthesis of the cytochalasins. In The Biosynthesis of Mycotoxins: a Study in Secondary Metabolism (Steyn, P.S., Ed.), Academic Press, New York), pp. 269-299. Academic Press, New York.
130. Oikawa, H., Yokota, T., Abe, T., Ichihara, A., Sakamura, S., Yoshizawa, Y., and Vederas, J. C. Biosynthesis of solanapyrone A, a phytotoxin of *Alternaria solani*. *J. Chem. Soc., Chem. Commun.*, **1989**, 1282-1284.

131. Kasahara, K., Miyamoto, T., Fujimoto, T., Oguri, H., Tokiwano, T., Oikawa, H., Ebizuka, Y., and Fujii, I. Solanapyrone synthase, a possible Diels-Alderase and iterative type I polyketide synthase encoded in a biosynthetic gene cluster from *Alternaria solani*. *ChemBioChem*, **2010**, *11*, 1245-1252.

132. Kim, H. J., Ruszczycky, M. W., Choi, S. H., Liu, Y. N., and Liu, H. W. Enzyme-catalysed [4+2] cycloaddition is a key step in the biosynthesis of spinosyn A. *Nature*, **2011**, *473*, 109-112.

133. Witter, D. J., and Vederas, J. C. Putative Diels-Alder-catalyzed cyclization during the biosynthesis of lovastatin. *J. Org. Chem.*, **1996**, *61*, 2613-2623.

134. Auclair, K., Sutherland, A., Kennedy, J., Witter, D. J., Van den Heever, J. P., Hutchinson, C. R., and Vederas, J. C. Lovastatin nonaketide synthase catalyzes an intramolecular Diels-Alder reaction of a substrate analogue. *J. Am. Chem. Soc.*, **2000**, *122*, 11519-11520.

135. Mandel, A. L., La Clair, J. J., and Burkart, M. D. Modular synthesis of pantetheine and phosphopantetheine. *Org Lett*, **2004**, *6*, 4801-4803.

136. Scherlach, K., Boettger, D., Remme, N., and Hertweck, C. The chemistry and biology of cytochalasans. *Nat. Prod. Rep.*, **2010**, *27*, 869-886.

137. Löw, I., Jahn, W., Wieland, T., Sekita, S., Yoshihira, K., and Natori, S. Interaction between rabbit muscle actin and several chaetoglobosins or cytochalasins. *Anal. Biochem.*, **1979**, *95*, 14-18.

138. Brown, S. S., and Spudich, J. A. Cytochalasin inhibits the rate of elongation of actin filament fragments. *J. Cell Biol.*, **1979**, *83*, 657-662.

139. Flanagan, M. D., and Lin, S. Cytochalasins block actin filament elongation by binding to high affinity sites associated with F-actin. *J. Biol. Chem.*, **1980**, *255*, 835-838.

140. Rampal, A. L., Pinkofsky, H. B., and Jung, C. Y. Structure of cytochalasins and cytochalasin B binding sites in human erythrocyte membranes. *Biochemistry*, **1980**, *19*, 679-683.

141. Ornelles, D. A., Fey, E. G., and Penman, S. Cytochalasin releases mRNA from the cytoskeletal framework and inhibits protein synthesis. *Mol. Cell. Biol.*, **1986**, *6*, 1650-1662.

142. Binder, M., Kiechel, J. R., and Tamm, C. Zur biogenese des antibioticums phomin. 1. Teil: die grundbausteine. *Helv. Chim. Acta*, **1970**, *53*, 1797-1812.

143. Binder, M., and Tamm, C. The cytochalasans: a new class of biologically active microbial metabolites. *Angew. Chem. Int. Ed. Engl.*, **1973**, *12*, 370-380.

144. Graf, W., Robert, J. L., Vederas, J. C., Tamm, C., Solomon, P. H., Miura, I., and Nakanishi, N. Biosynthesis of the cytochalasans. Part III. C-NMR of cytochalasin B (phomin) and cytochalasin D. Incorporation of [1-13C]- and [2-13C]-sodium acetate. *Helv. Chim. Acta*, **1974**, *57*, 1801-1815.

145. Oikawa, H., Murakami, Y., and Ichihara, A. Biosynthetic study of chaetoglobosin A: origins of the oxygen and hydrogen atoms, and indirect evidence for biological Diels Alder reaction. *J. Chem. Soc., Perkin Trans. 1*, **1992**, 2955-2959.

146. Vederas, J. C., Nakashima, T. T., and Diakur, J. Detection of O-18-label in cytochalasin B by C-13 NMR. *J. Med. Plants Res.*, **1980**, *39*, 201-202.

147. Schümann, J., and Hertweck, C. Molecular basis of cytochalasan biosynthesis in fungi: gene cluster analysis and evidence for the involvement of a PKS-NRPS hybrid synthase by RNA silencing. *J. Am. Chem. Soc.*, **2007**, *129*, 9564-9565.

148. Ishiuchi, K., Nakazawa, T., Yagishita, F., Mino, T., Noguchi, H., Hotta, K., and Watanabe, K. Combinatorial generation of complexity by redox enzymes in the chaetoglobosin A biosynthesis. *J. Am. Chem. Soc.*, **2013**, *135*, 7371-7377.

149. Qiao, K., Chooi, Y. H., and Tang, Y. Identification and engineering of the cytochalasin gene cluster from *Aspergillus clavatus* NRRL 1. *Metab. Eng.*, **2011**, *13*, 723-732.

150. Hu, Y., Dietrich, D., Xu, W., Patel, A., Thuss, J. A., Wang, J., Yin, W. B., Qiao, K., Houk, K. N., Vederas, J. C., and Tang, Y. A carbonate-forming Baeyer-Villiger monooxygenase. *Nat Chem Biol*, **2014**, *10*, 552-554.

151. Kieboom, A. P. G. Purification of Laboratory Chemicals, DD Perrin and WLF Armarego. Pergamon Press, Oxford, 1988. *Recl. Trav. Chim. Pays-Bas*, **1988**, *107*, 685.